

University of South Bohemia

Faculty of Science



The Role of Dco in *Drosophila* Haematopoiesis

Master thesis

Bc. Lucie Jonátová

Supervised by Mgr. Tomáš Doležal, Ph.D.

České Budějovice 2012

Jonátová, L. (2012): The Role of Dco in *Drosophila* Haematopoiesis. Mgr. Thesis, in English, 106 pp. Faculty of Science, University of South Bohemia, České Budějovice, Czech Republic.

ANNOTATION:

Point mutations found in human breast cancer samples introduced into the *Drosophila dco* gene affect the *Drosophila* haematopoiesis. I described different haematopoietic phenotypes in such mutants and tested their connection with the Toll and the JAK/STAT signalling pathways.

Prohlašuji, že svoji diplomovou práci jsem vypracovala samostatně, pouze s použitím pramenů a literatury uvedených v seznamu citované literatury.

Prohlašuji, že v souladu s § 47b zákona č. 111/1998 Sb. v platném znění souhlasím se zveřejněním své diplomové práce, a to v nezkrácené podobě elektronickou cestou ve veřejně přístupné části databáze STAG provozované Jihočeskou univerzitou v Českých Budějovicích na jejích internetových stránkách, a to se zachováním mého autorského práva k odevzdanému textu této kvalifikační práce. Souhlasím dále s tím, aby toutéž elektronickou cestou byly v souladu s uvedeným ustanovením zákona č. 111/1998 Sb. zveřejněny posudky školitele a oponentů práce i záznam o průběhu a výsledku obhajoby kvalifikační práce. Rovněž souhlasím s porovnáním textu mé kvalifikační práce s databází kvalifikačních prací Theses.cz provozovanou Národním registrem vysokoškolských kvalifikačních prací a systémem na odhalování plagiátů.

V Českých Budějovicích, 14.12.2012

.....

ACKNOWLEDGEMENTS

My deep gratitude goes to my supervisor Tomáš Doležal, who expertly guided me through my master's degree study, for his inexhaustible patience, great enthusiasm and never-ending optimism. I am thankful to all my lab colleagues, especially Katka Kučerová and Adam Bajgar, for their great support and affable environment with tons of hilarious moments. My special thanks go to Honza Provazník for rescue of my data after my fatal typing error. I am indebted to Miša Fencková for useful hints and creation of the fly with the FlyFos:Dco construct. I also acknowledge Raquel Perez Gomez for valuable discussion of immunostaining procedure and Matěj Horváth for incessant cheering me up. And last but not least, I would like to thank to my outside-lab friends, and especially my family for their support.

ABBREVIATIONS

AEL	after egg laying
AMP	antimicrobial peptides
CKIε	casein kinase Iε
CZ	cortical zone
DBT	Double-time
dco	discs overgrown
FB	fat body
FF	FlyFos
GFP	green fluorescent protein
Hml	hemolymph
LG	lymph gland
MZ	medullary zone
PL	primary lobes
PSC	posterior signalling centre
RG	ring gland
SL	secondary gland
<i>w</i>	<i>white</i>
WP	wasp parasitization
WT	wild type

CONTENT

1.INTRODUCTION.....	1
1.1 DISCOVERY OF DCO	1
1.2 HAEMATOPOIESIS IN <i>DROSOPHILA</i>	2
1.3 TOLL SIGNALLING PATHWAY IN HAEMATOPOIESIS.....	7
1.4 JAK/STAT SIGNALLING PATHWAY IN HAEMATOPOIESIS	9
1.5 CKI ϵ IN HAEMATOPOIESIS	11
1.6 AIMS OF THIS THESIS.....	12
2.MATERIAL AND METHODS	13
2.1 <i>DROSOPHILA</i> STOCKS.....	13
2.2 TERMINOLOGY.....	14
2.3 CROSSES	15
2.3.1 HEMOLECTIN EXPRESSION	15
2.3.2 TOLL MUTANTS.....	17
2.3.3 COLLIER EXPRESSION	18
2.3.4 DOMELESS EXPRESSION.....	19
2.4 TISSUE IMAGING	20
2.5 HAEMOCYTES COUNTING.....	20
2.6 EVALUATING THE HAEMOCYTE COUNTS.....	21
2.7 WASP TREATMENT.....	21
2.8 APOPTOSIS.....	21
2.9 CRYSTAL CELLS.....	21
2.10 FLYFOS CONSTRUCT.....	22
RECOMBINATION OF FLYFOS:DCO CONSTRUCT TO DCO ^{LE} ALLELE.....	23
2.11 IMMUNOSTAINING.....	25
2.12 RNA ISOLATION AND cDNA SYNTHESIS	26
3.RESULTS.....	28
3.1 CHARACTERISATION OF PHENOTYPES.....	28
3.1.1 LYMPH GLAND	28
3.1.2 CHANGES IN HAEMOCYTE PROLIFERATION AND DIFFERENTIATION	31
3.1.3 MELANOTIC CAPSULES FORMING	48
3.2 <i>DCO/TOLL</i> DOUBLE MUTANTS	51
3.2.1 HAEMATOPOIESIS IN <i>DCO DORSAL</i> DOUBLE MUTANTS	52
3.2.2 IMAGINAL WING DISCS	56
3.2.3 MELANOTIC CAPSULES FORMING	59
3.3 MARKERS FOR HAEMATOPOIESIS.....	61
3.3.1 HEMOLECTIN MARKER	62

3.3.2	COLLIER EXPRESSION	69
3.3.3	DOMELESS EXPRESSION	73
3.4	EXPRESSION OF DCO	81
	EXPRESSION OF THE FLYFOS:DCO CONSTRUCT	82
	CONFOCAL MICROSCOPY	85
	RT-PCR.....	91
4.	DISCUSSION	92
5.	CONCLUSIONS.....	98
	REFERENCES	100

1. INTRODUCTION

1.1. DISCOVERY OF DCO

Disc overgrown (Dco) was originally described to play a role in imaginal disc overgrowth in *Drosophila melanogaster* through a defective gap-junctional communication, described as a disc-autonomous effect (Jursnich et al., 1990). Zilian et al. (1999) showed that *dco* is identical to *double-time* (DBT) gene, an essential component of *Drosophila* circadian rhythm (Kloss et al., 1998). Dco is a ser/thr protein kinase with highly conserved structure and sequence encoding a homologue of human casein kinase I δ/ϵ (CKI δ/ϵ). A wide range of phenotypes was identified in different *dco* mutant combinations. The loss-of-function experiments revealed the role of Dco in cell proliferation. Dco is required for inhibition of apoptosis as well as for imaginal disc growth arrest, since cells lacking this protein are unable to proliferate and die after only two or three divisions, and imaginal disc growth is strongly reduced in the *dco null* mutants, while *dco*³ mutant imaginal discs fail to stop growing even when reached the normal size (Zilian et al., 1999).

Particularly high rate of point mutations in human CKI ϵ , a homologue of *Drosophila* Dco, was found in breast cancer tissues (Fuja et al., 2004). These point mutations were introduced into the *dco* gene controlled by adjacent genomic regulatory sequences and the cancerous potential of abnormal Dco protein was tested *in vivo* (Dolezal et al., 2010). The position of point mutations is illustrated in figure 1.1. Leucine at the position 39 was mutated to glutamin, and serine at the position 101 was mutated to arginine. Dolezal et al. (2010) created flies carrying mutated *dco*^{L39Q} and *dco*^{L39Q S101R} alleles in their genomes. These mutants exhibit striking imaginal disc phenotypes. They revealed that *dco*^{L39Q} affects the Fat/Warts pathway controlling organ size (Dolezal et al., 2010). Besides these cancer-like disc phenotypes, these novel *dco* mutants have also greatly affected haematopoiesis in *drosophila* larvae which led me to this work.

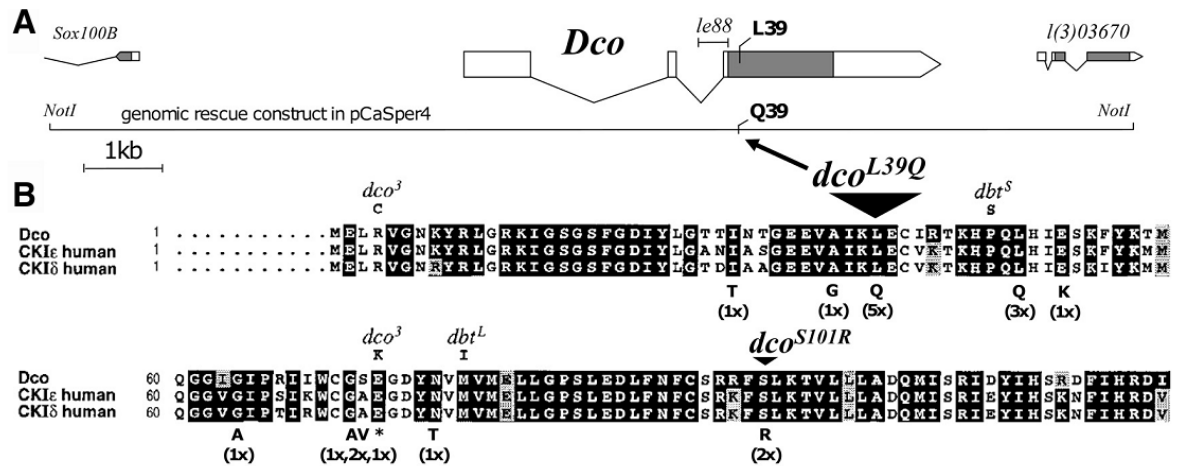


Fig. 1.1: Position of point mutations in *dco* gene (adopted from Dolezal et al., 2010).

1.2. HAEMATOPOIESIS IN *DROSOPHILA*

Haematopoiesis is a process of blood cells (haemocytes) forming in two waves in accordance with the vertebrate haematopoiesis, where the primitive and definitive waves occur (Crozatier and Meister, 2007). Since haematopoietic development and function of signalling pathways are conserved in vertebrates and *Drosophila melanogaster*, the *Drosophila* is a suitable tool for description of molecular mechanisms in this process. Haemocytes are multifunctional cells important for defensive capacity of organisms, such as seeking out and removing the dead cells during the development, encapsulation of foreign invaders, secretion of extracellular matrix components, mediating humoral immune response through the fat body and mainly mediating the cellular immune response (reviewed by Evans et al., 2003). The central role of haemocytes consists in their phagocytic features and defence against the infection (Matova and Anderson, 2006; Defaye et al., 2009). The types of haemocytes present in *Drosophila* open circulatory system are shown in figure 1.2.

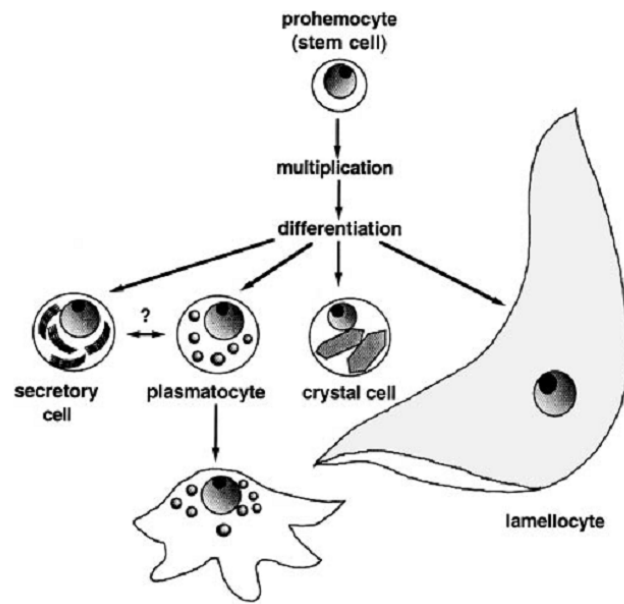


Fig. 1.2: Illustration of *Drosophila* blood cell types (adopted from Lanot et al., 2001).

Prohaemocytes contain little cytoplasmic volume, lipid droplets and many free ribosomes indicating their undifferentiated nature (Tepass et al., 1994; Lanot et al., 2001). Haemocytes are distinguishable into three basic groups – plasmatocytes, crystal cells and lamellocytes (Lanot et al., 2001). Plasmatocytes contain a bit more mass of cytoplasm than prohaemocytes. Plasmatocytes also contain abundant cytoplasmic lysosomes and endoplasmic reticulum, which is consistent with their phagocytic function in the organism. Besides their ability to recognize apoptotic cells by the Croquemort (Crq) surface receptor and subsequently remove these dead cells (Franc et al., 1996; Irving et al., 2005), they also secrete some of the extracellular matrix components, signalling molecules and antimicrobial peptides (Dimarcq et al., 1997; reviewed by Evans et al., 2003; Defaye et al., 2009). Crystal cells are nonphagocytic cells included in immune response through the melanisation process, since crystal cells produce one of the crucial enzymes involved in this process (Lanot et al., 2001; Evans et al., 2003). Melanisation results in deposition of a black pigment melanin during a wound healing. This process is controlled by serine proteases that activate enzyme prophenoloxidase catalysing the melanin synthesis (De Gregorio et al., 2002; Crozatier and Meister, 2007). Irving et al. (2005) published that also other cell types, such as lamellocytes, might produce prophenoloxidase enzyme, and therefore they are also involved in the melanisation process. Lamellocytes are large, flat, adherent, nonphagocytic cells. Their role consists in encapsulating of invaders and tissues that are too large to be engulfed by plasmatocytes. These features make them crucial for the defence against large invaders (Lanot et al., 2001; Crozatier et al., 2004). Lamellocytes form a multi-layered capsule around

the wasp egg to separate it from the inner environment of larva. This capsule becomes melanised and the parasite egg development is blocked (Carton and Nappi, 2001; Sorrentino et al., 2002). Very few or no lamellocytes are present in normal conditions in larvae (Luo et al., 1995; Lanot et al., 2001; Sorrentino et al., 2002). Mitosis was not identified in lamellocytes by the histone H3 staining (Lanot et al., 2001) and the origin of lamellocytes has not been decided yet. One theory says that lamellocytes originate from prohaemocytes (Lanot et al., 2001; Krzemień et al., 2007; Mandal et al., 2007), another theory says they originate from plasmatocytes (Rizki and Rizki, 1984), and Krzemien et al. (2010) indicated the possibility that lamellocytes might differentiate at the expense of crystal cells and that they might differentiate in circulation.

The first haematopoietic wave takes place in head mesoderm of early embryos. The lineage of haematopoietic cells expresses Serpent (Srp), a GATA family transcription factor, which is required for haematopoietic development. A fixed numbers of haemocytes emerge in the embryo, i.e. 700 plasmatocytes and 30 crystal cells (Tepass et al., 1994; Lebestky et al., 2000). Primordial haematopoietic cells are present in embryos and actively divide to give rise a pool of prohaemocytes (Krzemien et al., 2010).

The second wave of haematopoiesis occurs at the larval stage in the specialized haematopoietic organ called lymph gland (LG) (Lanot et al., 2001; Jung et al., 2005; Crozatier and Meister, 2007). From the end of embryogenesis to the second larval instar, the LG consists of only a single pair of lobes (primary lobes). The second instar LG is not immunoresponsive, i.e. the young LG is not able to activate the differentiation of lamellocytes upon the wasp parasitization (Sorrentino et al., 2002). In the 3rd larval instar, the LG is composed of the primary pair of lobes and one to six pairs of additional secondary lobes posteriorly to the first pair. Lobes are located along the dorsal vessel (Lanot et al., 2001; Evans et al., 2003). Specialized regions were determined in the primary lobes according to the expression of different specific markers and function of cells in the LG.

The posterior signalling centre (PSC) is localised posteriorly in the primary lobes. These cells are determined early in the development by expression of Serrate, a Notch ligand (Lebestky et al., 2003), and also by expression of Collier (Col) transcription factor (Crozatier et al., 1996). The *collier* gene, also known as *knot*, is the *Drosophila* orthologue of the vertebrate gene encoding early B-cell factor (EBF). Collier expression in PSC is required for activation of lamellocyte differentiation in larvae upon the wasp parasitization, since *col*

mutants fail to produce lamellocytes (Crozatier et al., 2004; Jung et al., 2005). PSC cells are specified by Antennapedia (Antp) and Hedgehog (Hh) (Mandal et al., 2007). PSC also acts in non-cell autonomous manner to maintain the haematopoietic homeostasis by preserving the JAK/STAT signalling in prohaemocytes located in the medullary zone to prevent their premature differentiation (Krzemień et al., 2007; Mandal et al., 2007). Prohaemocytes express Domeless (Dome), a transmembrane receptor molecule activating the JAK/STAT signalling pathway (Brown et al., 2001; Bourbon et al., 2002; Chen et al., 2002), and also Unpaired 3 (Upd 3), a cytokine ligand binding to Dome receptor (Agaisse and Perrimon, 2004). The expression of these proteins in LG defines the medullary zone (MZ), where the immature cells are present. When maturing occurs, the Dome expression is downregulated as well as the JAK/STAT, while expression of maturation markers, such as surface L1-antigen (Asha et al., 2003) and hemolectin (Goto et al., 2003), is initiated. These mature cells are located in the outer part of primary lobes called the cortical zone (CZ). The lineage tracing experiment revealed that the cells in the CZ came from the MZ (Jung et al., 2005). The morphology of the LG is illustrated in figure 1.3.

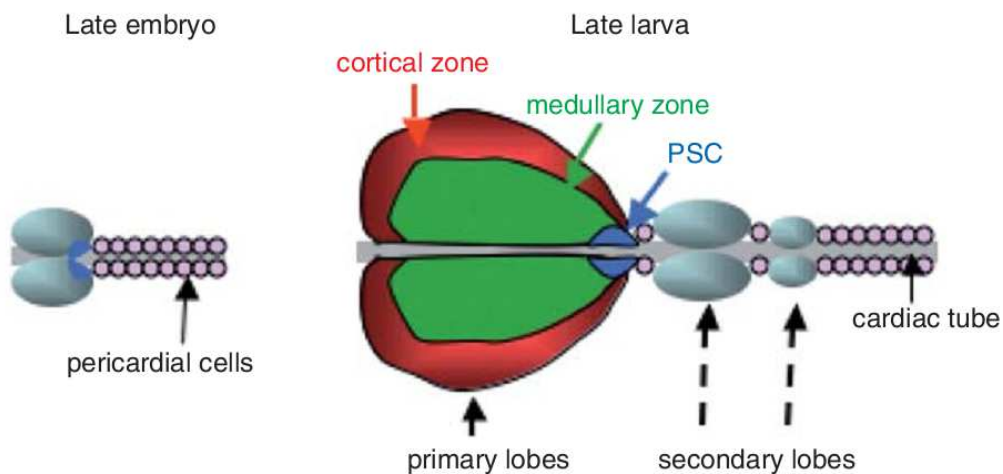


Fig. 1.3: Schematic demonstration of LG at the end of embryogenesis (left) and in the 3rd larval instar (right). Illustrative distribution of different zones in primary lobes (adopted from Crozatier and Meister, 2007).

Only few haemocytes differentiate in the secondary lobes under the normal, unchallenging situation. Circulating haemocytes present in larvae are essentially derived from the embryonic haematopoietic lineage. These posterior lobes serve as a reservoir of prohaemocytes (Lanot et al., 2001; Crozatier and Meister, 2007).

No haematopoietic organ has been found in *Drosophila* adults up to now. The adults also do not have any lamellocytes, crystal cells and mitosis was not detected in any of the present blood cells, although haemocytes are present in adult flies. At the onset of metamorphosis, most of the prohaemocytes differentiate into plasmatocytes and the LG disintegrates (Fig. 1.4) (Lanot et al., 2001; reviewed by Evans et al., 2003).

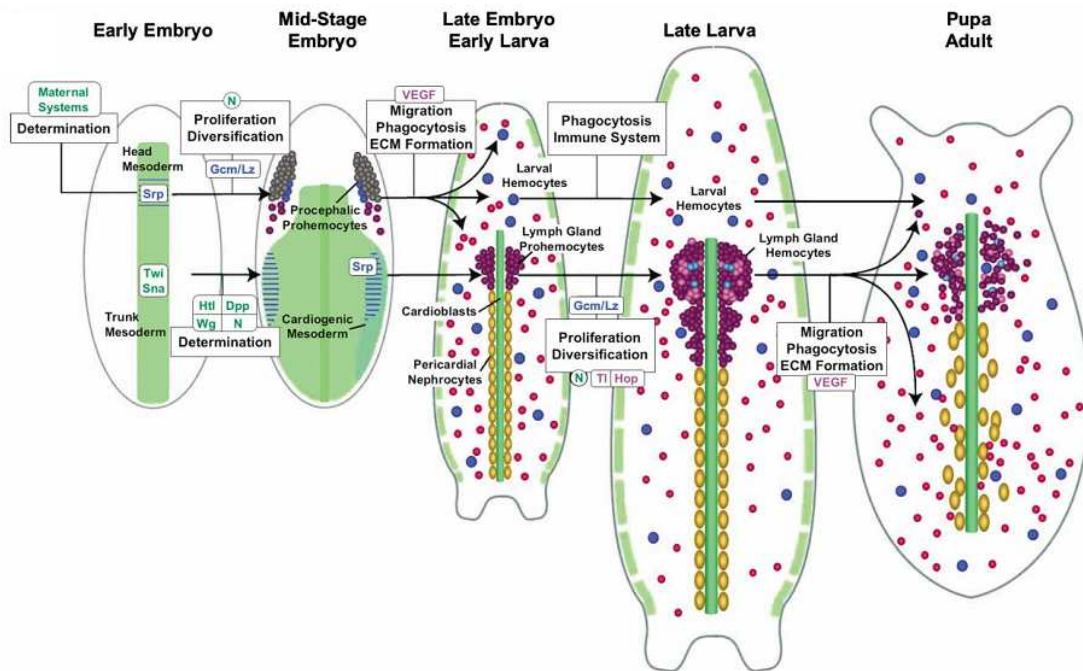


Fig. 1.4: Haematopoietic events during *Drosophila* development (adopted from Evans et al, 2003).

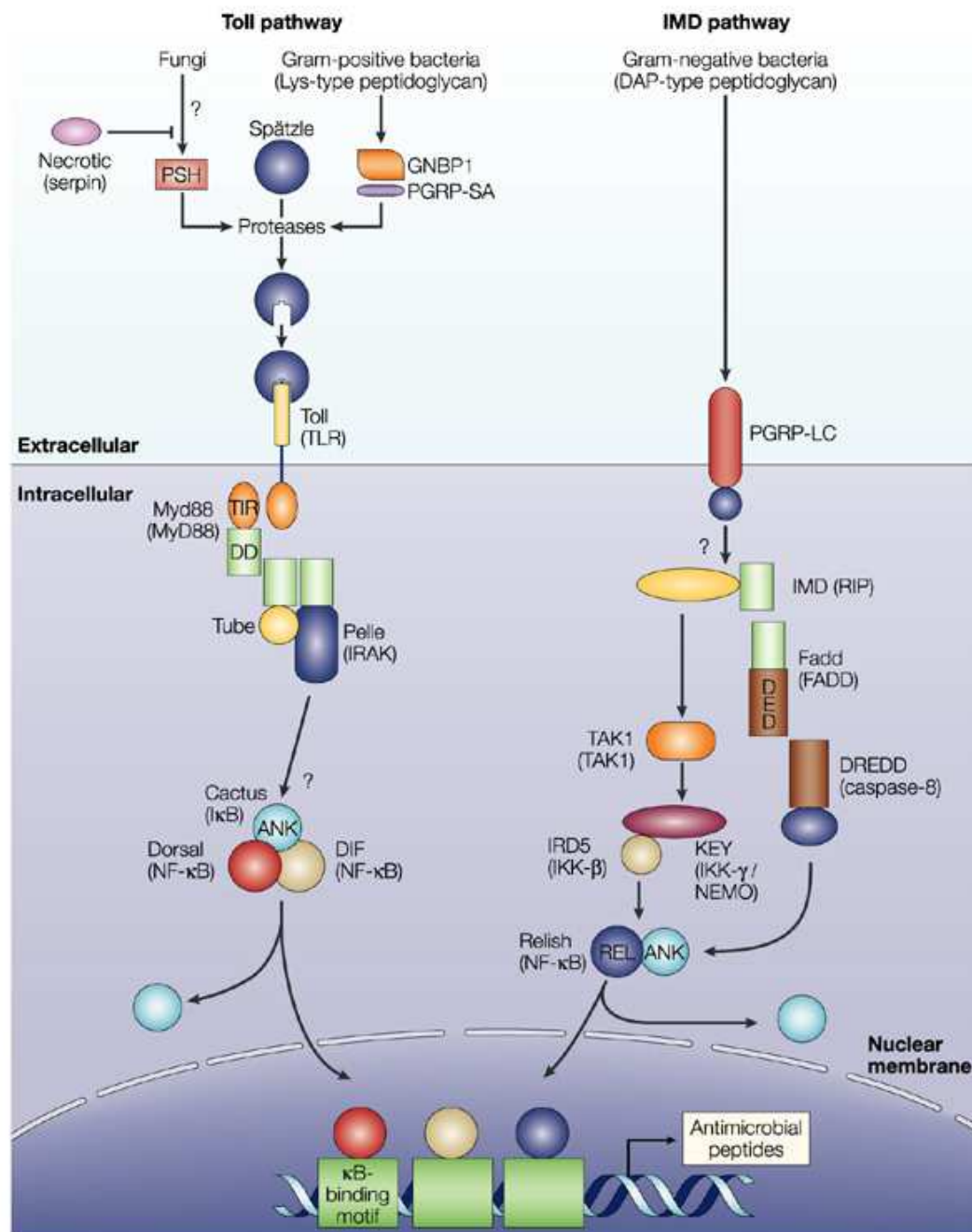
1.3. TOLL SIGNALLING PATHWAY IN HAEMATOPOIESIS

Toll signalling pathway is important for embryonic development and for specification of the dorsal-ventral axis in embryogenesis, where the Rel family transcription factors control asymmetric expression of zygotic genes along the dorso-ventral axis. However, Toll pathway was also shown to play a role in both humoral and cellular immunity, (Roth et al., 1991; Govind et al., 1993; Govind, 1999).

The Toll pathway is activated when the proteolytically cleaved ligand Spätzle (Spz) binds to the Toll receptor. The activated Toll receptor binds to the adaptor protein MyD88 followed by forming of heterotrimeric complex of MyD88, Tube and the kinase Pelle. Further, the signal results in the phosphorylation and therefore degradation of Cactus, the *Drosophila* IκB factor. In non-signalling conditions, Cactus binds to the NF-κB transcription factors Dorsal and/or Dif (Dorsal-related immunity factor), and inhibits their nuclear localisation. Once Cactus is degraded, these transcription factors can enter the nucleus and trigger the transcription of the target genes (Fig. 1.5). The Toll activation triggers both humoral immune response through the production of antimicrobial peptides (AMPs) and cellular immune response consisting in phagocytosis and encapsulation of invader (Hultmark, 2003; reviewed by Valanne et al., 2011). The linkage of Toll pathway, melanotic capsule formation, and enhanced *dorsal* mRNA level in the fat body upon injury was shown by Lemaitre et al. (1995).

The connection of Toll signalling with haematopoiesis was shown in different mutants. The loss-of-function *cactus* mutants (*cact*) and the gain-of-function TI^{10B} mutants cause an overabundance of haemocytes, melanotic capsule formation, death before pupation, and the mutant LG is considerably enlarged. Staining of mitotic process showed that the number of dividing haemocytes in the *cact* mutant LG is considerably higher than in the WT larvae. However, the loss-of-function mutations in Toll reduce the number of circulating haemocytes, and also suppress the gain-of-function-mediated phenotypes. These results suggest that the Toll/Cactus signal plays a significant role in regulation of haemocyte proliferation (Qiu et al., 1998). Dorsal and Dif were shown to be important for haemocyte survival promotion, since their transcription target is *Drosophila* IAP1 (DIAP1), an inhibitor of apoptosis. The single *dl* and *Dif* mutations do not show the haematopoietic defects in either humoral or cellular immune response. However, the *Dl Dif* double mutants have very few haemocytes, and they are constitutively infected by opportunistic infection. These

results indicate that either Dorsal or Dif is sufficient for protection so their functions are redundant. Although the *dl Dif* double mutants are able to activate the humoral immune response, it is not sufficient for their survival. Therefore, the Rel proteins are crucial regulators of the cellular immune response (Matova and Anderson, 2006, 2010).



Nature Reviews | Immunology

Fig. 1.5: Schematic illustration of Toll signalling pathway (left). Imd (immune deficiency) pathway leads to activation of AMPs genes (adopted from Lemaitre, 2004)

1.4. JAK/STAT SIGNALLING PATHWAY IN HAEMATOPOIESIS

Another signalling pathway involved in haematopoiesis regulation is JAK/STAT (Janus kinase/signal transducer and activator of transcription) pathway. When ligand binds to the transmembrane receptor, the receptor-associated JAKs are activated. These JAKs, tyrosine kinases, phosphorylate themselves and their associated receptors to generate docking sites for the STATs. STAT molecules dimerise once they phosphorylate themselves, and enter the nucleus. Thus they can bind to the target gene promoters and activate their transcription (Fig. 1.6) (Hou et al., 2002; Arbouzova and Zeidler, 2006). Three ligands, Unpaired1 (Upd1), Upd2 and Upd3 (Agaisse et al., 2003); one transmembrane receptor Domeless (Brown et al., 2001; Chen et al., 2002); one JAK kinase Hopscotch (Binari and Perrimon, 1994) and one transcription factor STAT92E (Hou et al., 1996) are known in *Drosophila* to be involved in the canonical JAK/STAT pathway.

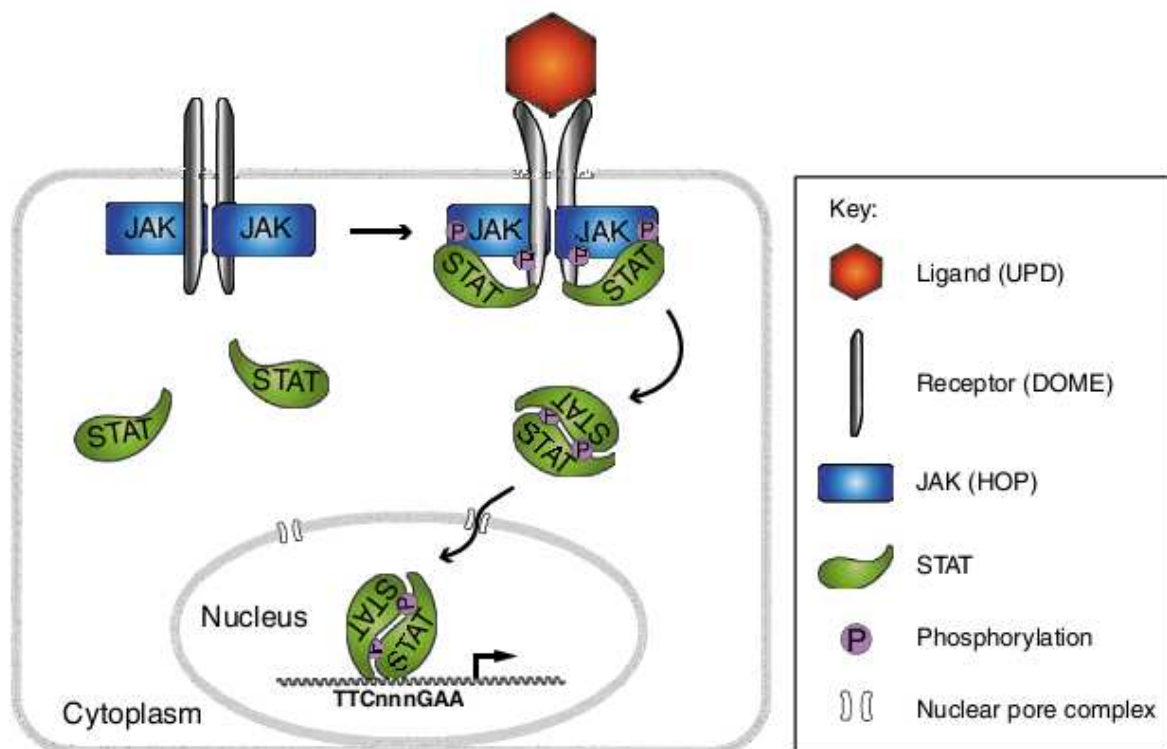


Fig. 1.6: Schematic illustration of the JAK/STAT signalling pathway (adopted from Arbouzova and Zeidler, 2006).

JAK/STAT regulates development and differentiation of multiple cell types, which makes this pathway important for embryonic segmentation. But the multiple roles played by this signalling pathway require also diverse regulatory mechanisms. Unpaired is known to be the only positive regulator, but the *upd null* mutants show less severe phenotypes than those exhibited by loss of Hop or STAT92E. This indicates that other Upd-like ligands may partially compensate for the loss of Upd (Hombría and Brown, 2002; Arbouzova and Zeidler, 2006). There are also negative regulators of the JAK/STAT pathway, such as the SOCS (suppressors of cytokine signalling) genes, and PIAS (protein inhibitors of activated STAT) proteins binding STATs and target them for degradation via SUMOylation (Luo and Dearolf, 2001; Arbouzova and Zeidler, 2006).

The JAK/STAT signalling pathway plays a role in humoral immune response through the Upd3 expression in haemocytes after septic injury. This results in activation of JAK/STAT pathway followed by activation of *totA* in the fat body. This sequence of events leads to the activation of humoral immune response (Agaisse et al., 2003; Agaisse and Perrimon, 2004). The role of JAK/STAT in the cellular immune response is shown by phenotypes in the *hop^{Tum-l}* mutants (*Tumorous-lethal* mutation in *hopscotch*). *hop^{Tum-l}* is a dominant gain-of-function mutation causing defects in haematopoiesis resulting in melanotic capsule forming and leukemia-like phenotypes (Hanratty and Dearolf, 1993; Harrison et al., 1995; Luo et al., 1995).

In haematopoietic process, the PSC controls haematopoietic homeostasis through the maintaining of JAK/STAT in prohaemocytes. The JAK/STAT signalling is necessary to be switched off in the MZ of the LG upon the wasp parasitization for massive differentiation of lamellocytes. Latran, a short type I cytokine-related receptor lacking the intracellular domain required for signal transduction, acts as a negative regulator of JAK/STAT. Just like Domeless, Latran is expressed in the MZ and forms a heterodimer with Dome. Latran antagonises the function of Domeless in dose dependent manner. So after the wasp parasitization, the expression of Latran is activated followed by the increase of Latran/Dome ratio, which eventually results in the JAK/STAT switch off. As figure 1.7 shows, *lat* mutants are unable to mount the cellular immune response upon the wasp parasitization (Makki et al., 2010).

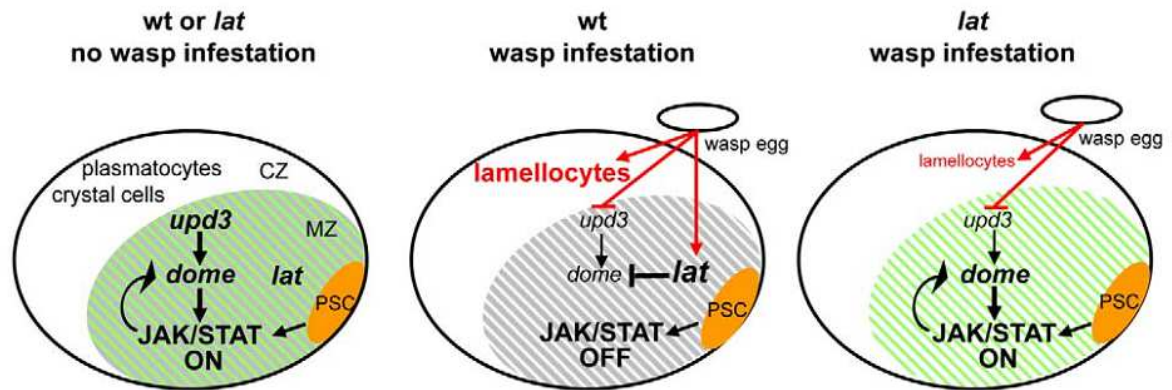


Fig. 1.7: Model for Latran function in *Drosophila* larval haematopoiesis. Schematic illustration of the processes in LG lobes under different conditions. Left-WT, no immune challenge; Middle-WT upon the wasp parasitization; *lat* mutant upon the wasp parasitization (adopted from Makki et al., 2010).

1.5. CKI ϵ IN HAEMATOPOIESIS

Although the Dco mammalian orthologue CKI ϵ have already been shown to be expressed in immune system cells, and that its expression levels dynamically change as the cell development proceeds, the CKI ϵ specific biological function is not clarified yet (Utz et al., 2010). The evidence that CKI ϵ is involved in haematopoietic cell differentiation in mammals was shown by Okamura et al. (2004). They discovered the connection of human granulocyte differentiation with the downregulation of CKI ϵ (in vitro) and CKI ϵ involvement in cytokine-induced activation of STAT3, a signal transducer and activator of transcription involved in JAK/STAT signalling. Furthermore, CKI ϵ was shown to bind the SOCS3 (suppressors of cytokine signalling) protein, a regulator of JAK/STAT, possibly to stabilise this protein (Okamura et al., 2004). Recently, the role of CKI ϵ in haematopoietic survival through the modification of PI3K/Akt signalling was discovered. The CKI ϵ activates PTEN, a negative regulator of PI3K/Akt signalling, resulting in the downregulation of Akt phosphorylation, and therefore in downregulation of PI3K/Akt signalling. The consequence of these events causes an increased sensitivity to apoptosis, which might be related to the cell immortalisation in many human leukemia cell lines where the CKI ϵ is suppressed (Okamura et al., 2006).

1.6. AIMS OF THIS THESIS

The aim of my work is to test the role of Dco (homologue of mammalian CKIε) in *Drosophila* haematopoiesis and describe different phenotypes in *dco*^{L39Q S101R} and *dco*^{L39Q} mutants. The next goal is to determine the mechanism how the Dco affects haematopoietic proces that is so important for cellular immunity.

2. MATERIAL AND METHODS

2.1. *DROSOPHILA* STOCKS:

Larvae for all the experiments were raised on a cornmeal diet (120g cornmeal; 75g glucose; 60g instants yeast; 15g agar; 1.5 l water and 25ml of 10% methylparaben in ethanol) at 25°C. Diet where the larvae for the Toll experiments were made (chapter 3.2), was supplied with 40µl of penicillin streptomycin (Sigma-Aldrich, Missouri, USA). Stocks that I used for crosses are listed in table 2.1.

Genotype	Function	FlyBase ID
yw dco[L39Q+S101R]P3D34	here <i>dco</i> ^{L39Q S101R}	
yw dco[L39Q]P6-70	here <i>dco</i> ^{L39Q}	
dl[1] cn[1] sca[1]/CyO, 1(2)DTS100[1]	<i>dl</i> ¹ is Dorsal loss-of-function allele	FBst0003236
Df(2L)TW119, cn[1] bw[1]/CyO	Df(2L)TW119 is a large chromosomal deletion covering <i>dorsal</i> and <i>Dif</i> region	FBst0006073
Df(2L)J4/CyO	Df(2L)J4 is a chromosomal deletion removing <i>dorsal</i> and <i>Dif</i> region	FBab0001479
Df(3R)A177der22, ry[+] / TM6B, Tb	Df(3R)A177der22 (here <i>dco</i> ^{der}) is a chromosomal deletion of <i>dco</i>	FBab0027660
yw ; FRT82 dco[le88] / TM6B, Tb	<i>dco</i> [le88] (here <i>dco</i> ^{le}) is Dco loss-of-function allele	FBal0032019
w; HmlΔ-Gal4 UAS-GFP	Hml-Gal4 is hemolymph GAL4 driver	FBtp0040877
y w ; FRT82 dco[3] / TM6B, Tb	<i>dco</i> [3] (here <i>dco</i> ³) is an unusual hypomorphic <i>dco</i> allele	FBal0032016
UAS-Grim	proapoptotic effects	FBal0092965
Pcol85-Gal4 UAS-mcd8GFP/CyO Tubby	Collier GAL4 driver and GFP construct	FBti0077825 and FBtp0002652
PG125/FM7; UAS-mcd8GFP	PG125 is Domeless GAL4 driver	FBal0130418
yw; pFlyFos{020844}-dco:GFP-attP2	FF:dco is a transgenic Dco coupled with GFP	

Tab. 2.1: List of stocks I used for crosses. (FlyBase ID is the identification number registered in online database www.flybase.org)

2.2. TERMINOLOGY

Genotypic combinations of mutants and the terminology how I use it in the text are listed in figure 2.1.

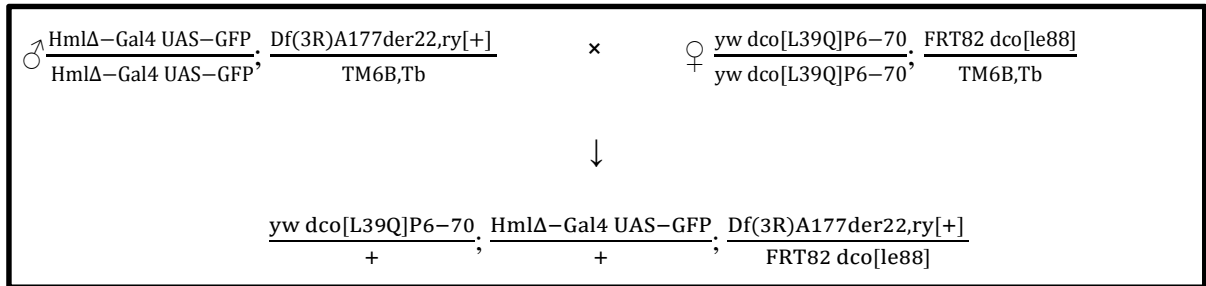
$\frac{yw\ dco[L39Q]P6-70}{+/Y}; \frac{Df(3R)A177der22,ry[+]}{FRT82\ dco[le88]}$	dco^{L39Q} homozygous mutant
$\frac{yw\ dco[L39Q+S101R]P3D34}{+/Y}; \frac{Df(3R)A177der22,ry[+]}{FRT82\ dco[le88]}$	$dco^{L39Q\ S101R}$ homozygous mutant
$\frac{yw\ dco[L39Q]P6-70}{+/Y}; \frac{Df(3R)A177der22,ry[+]}{+}$	dco^{L39Q} heterozygous mutant
$\frac{yw\ dco[L39Q+S101R]P3D34}{+/Y}; \frac{Df(3R)A177der22,ry[+]}{+}$	$dco^{L39Q\ S101R}$ heterozygous mutant
$\frac{Df(3R)A177der22,ry[+]}{FRT82\ dco[3]}$	dco^3 mutant
$\frac{Df(3R)A177der22,ry[+]}{FRT82\ dco[le88]}$	dco null mutant
$\frac{Df(3R)A177der22,ry[+]}{+}$	$dco^{der/+}$ heterozygous control
$\frac{Df(2L)J4}{dl[1]\ cn[1]\ sca[1]}$	$dorsal$ (DI-)
$\frac{Df(2L)J4}{Df(2L)TW119,cn[1]\ bw[1]}$	$dorsal\ Dif$ double mutant

Fig. 2.1: List of mutant genotypes as used in this text.

2.3. CROSSES:

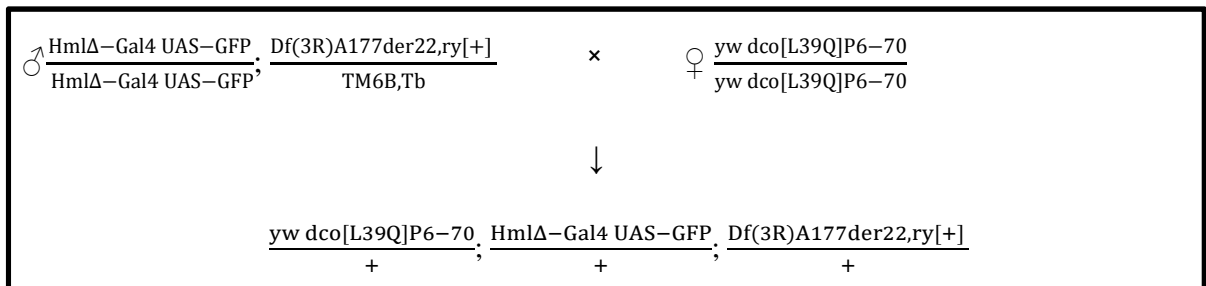
The final crossing schemes are listed in this chapter according to the type of experiment. Larvae with resulting genotypes were analysed.

2.3.1. HEMOLECTIN EXPRESSION



The same crossing procedure was applied also for $\text{♀} \frac{\text{yw dco[L39Q+S101R]P3D34}}{\text{yw dco[L39Q+S101R]P3D34}}; \frac{\text{FRT82 dco[le88]}}{\text{TM6B,Tb}}$.

Fig. 2.2: Crossing scheme for hemolectin expression experiment in dco^{L39Q} and $dco^{L39Q S101R}$ homozygous mutants.



The same crossing procedure was applied also for $\text{♀} \frac{\text{yw dco[L39Q+S101R]P3D34}}{\text{yw dco[L39Q+S101R]P3D34}}$.

Fig. 2.3: Crossing scheme for hemolectin expression experiment in dco^{L39Q} and $dco^{L39Q S101R}$ heterozygous mutants.

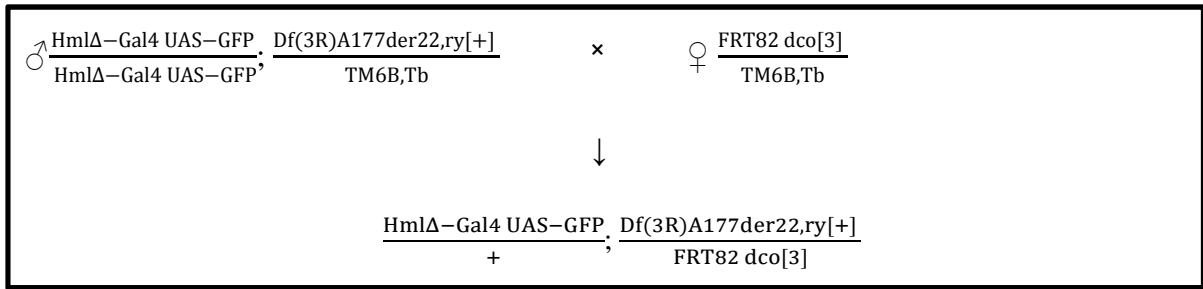


Fig. 2.4: Crossing scheme for hemolectin expression experiment in *dco*³ mutants.

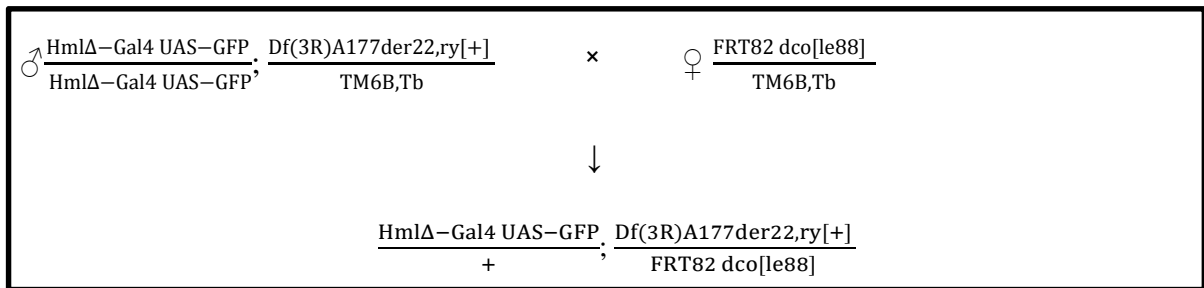
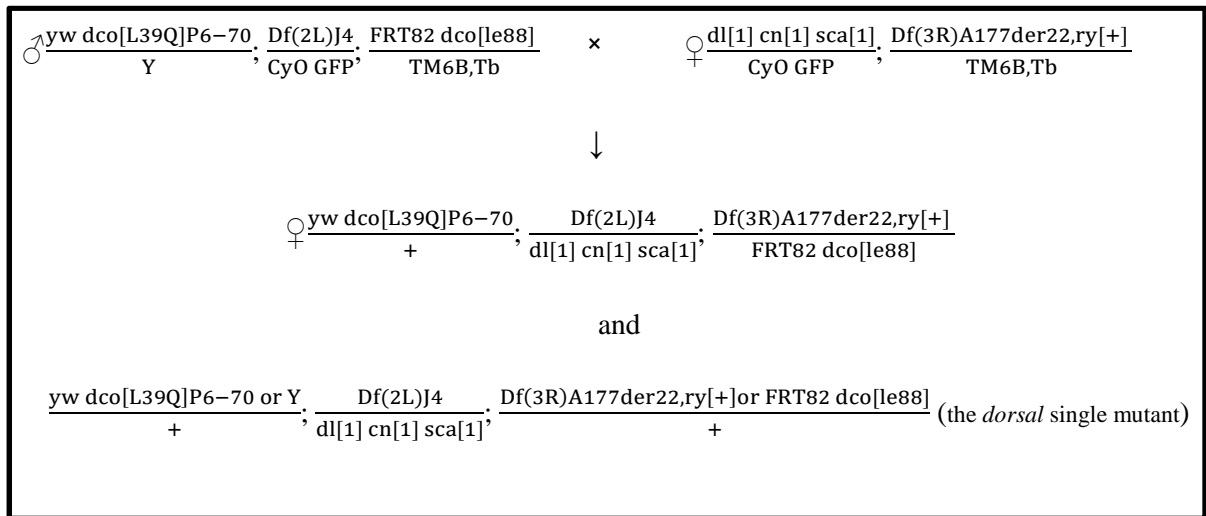


Fig. 2.5: Crossing scheme for hemolectin expression experiment in *dco null* mutants.

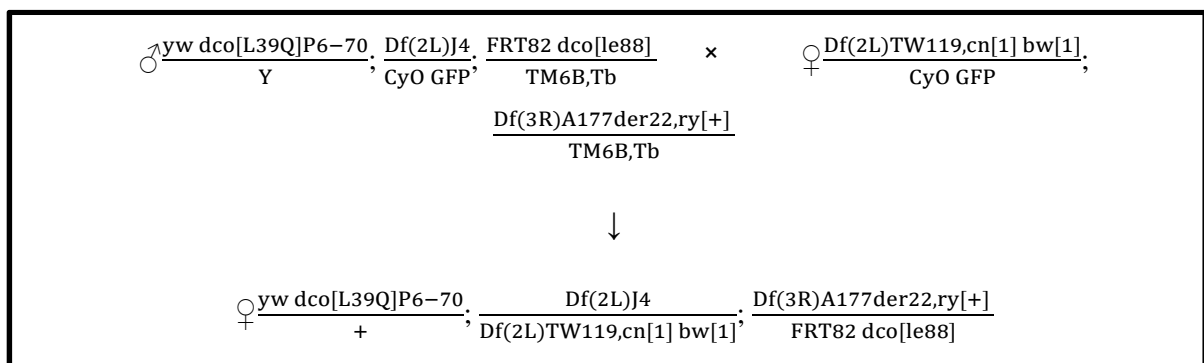
2.3.2. TOLL MUTANTS



The same crossing procedure was applied also for

$$\text{♂ } \frac{yw \text{ dco}[L39Q+S101R]P3D34}{Y}; \frac{Df(2L)J4}{CyO \text{ GFP}}; \frac{FRT82 \text{ dco}[le88]}{TM6B,Tb}$$

Fig. 2.6: Crossing scheme for *dco dorsal* double mutants.



The same crossing procedure was applied also for

$$\text{♂ } \frac{yw \text{ dco}[L39Q+S101R]P3D34}{Y}; \frac{Df(2L)J4}{CyO \text{ GFP}}; \frac{FRT82 \text{ dco}[le88]}{TM6B,Tb}$$

Fig. 2.7: Crossing scheme for *dco dorsal Dif* triple mutants.

2.3.3. COLLIER EXPRESSION

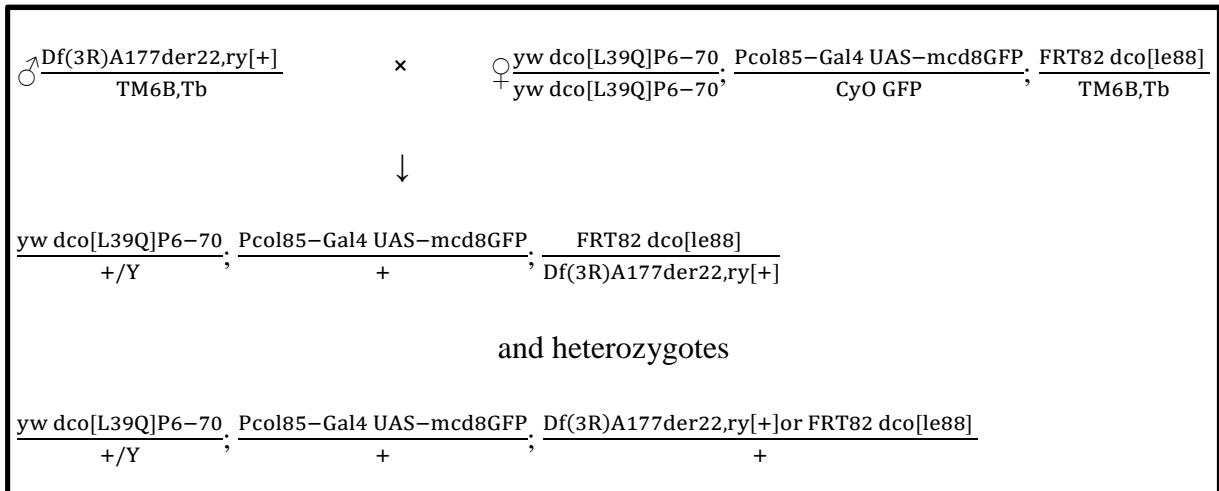


Fig. 2.8: Crossing scheme for Collier expression experiment in *dco^{L39Q}* and *dco^{L39Q S101R}* homozygous and heterozygous mutants.

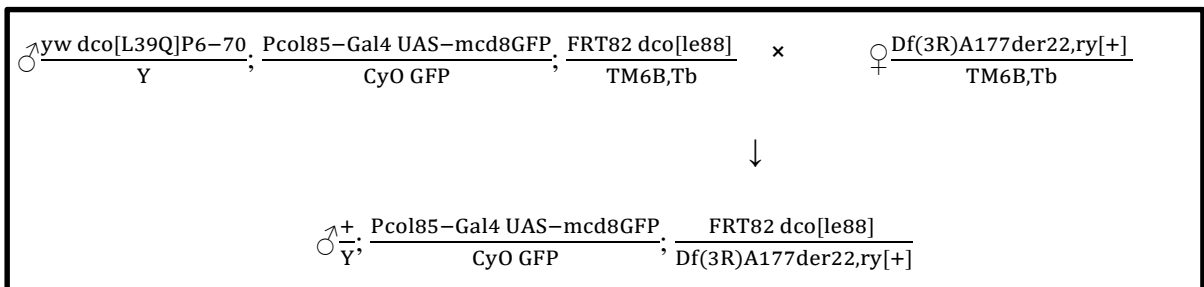
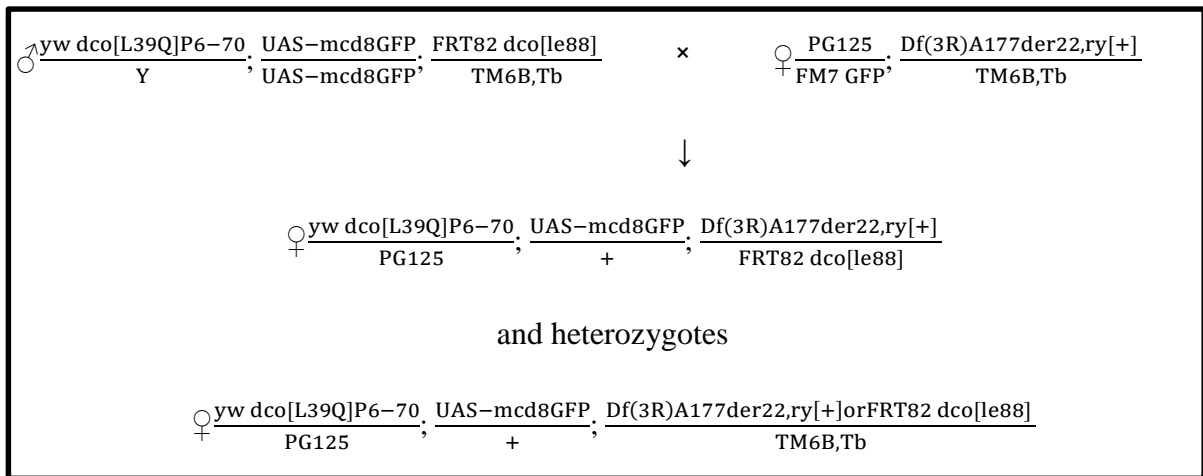


Fig. 2.9: Crossing scheme for Collier expression experiment in *dco null* mutants.

2.3.4. DOMELESS EXPRESSION



The same crossing procedure was applied also for

$$\text{♂} \frac{yw \ dco[L39Q+S101R]P3D34}{Y}; \frac{UAS-mcd8GFP}{UAS-mcd8GFP}; \frac{FRT82 \ dco[le88]}{TM6B,Tb}$$

Fig. 2.10: Crossing scheme for Domeless expression experiment in *dco*^{L39Q} and *dco*^{L39Q S101R} homozygous and heterozygous mutants.

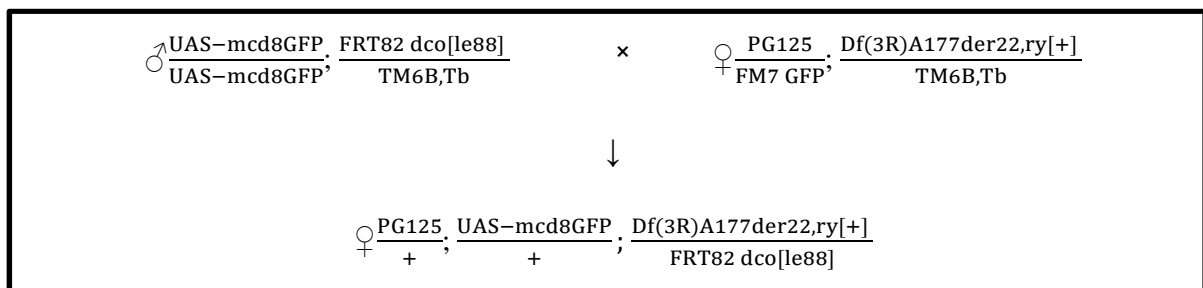


Fig. 2.11: Crossing scheme for Domeless expression experiment in *dco null* mutants.

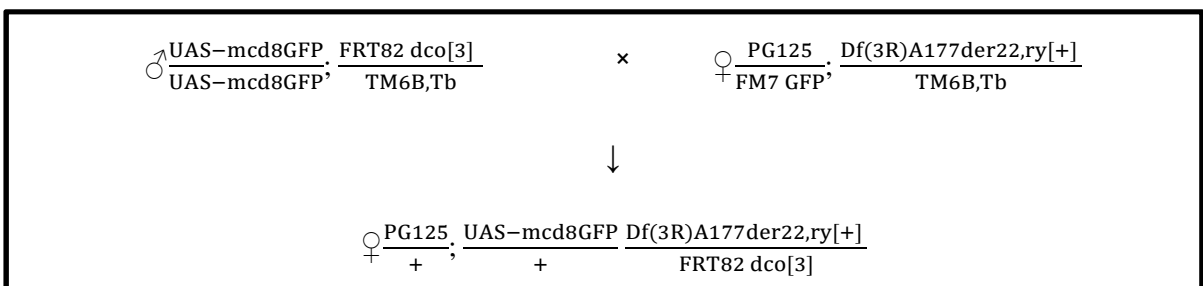


Fig. 2.12: Crossing scheme for Domeless expression experiment in *dco*³ mutants.

2.4. TISSUE IMAGING:

Larvae were dissected with the use of two forceps (size 5) in PBS buffer. Tissues were analysed as living samples without any fixating step. Dissection steps were performed with the use of inverted binoculars (OLYMPUS SZX12). All the figures, except the figures in chapter “Confocal microscopy”, were made with inverted microscope (OLYMPUS IX71) by differential interference contrast microscopy (DIC) and fluorescence lamp (Hg) if needed. OLYMPUS FluoView FV1000 Laser scanning microscope was used for confocal microscopy (<http://www.olympus-global.com>).

2.5. HAEMOCYTES COUNTING:

Two larvae of appropriate age were opened in abdominal region and turned inside out in 30µl of PBS buffer. Circulating haemocytes were bled and mixed into the PBS with gentle pipetting. 10µl of this cell suspension were recovered on the Neubauer improved haemocytometer. I counted haemocytes in the central square, where the total volume is 0.1µl. Because two larvae were bled into 30µl of PBS, these counts were multiplied by 150 to obtain an expression of haemocytes quantity per animal. The age of larvae as used throughout this work for all the experiments is specified in the table 2.1.

days	hours*
3	49-72
4	73-96
5	97-120
6	121-144
7	145-168
8	169-192
9	193-216
10	217-240
11	241-264

Tab. 2.2: Specification of the age of larvae. This scaling was used in full extent of this work. (*AEL – after egg laying)

2.6. EVALUATING THE HAEMOCYTE COUNTS:

The data were processed with the use of Microsoft Excel 2010 and Statistica 10 (Stat. Soft., Inc., Tulsa USA) programs. For comparing of haemocyte counts in different mutants I used the nonparametric test Kruskal-Wallis ANOVA (comparison of multiple independent samples).

2.7. WASP TREATMENT:

Larvae at the age of 72 hours (i.e. late 2nd instar) were challenged by parasitization with *Lepropolina boulandi* parasitic wasps for two hours.

2.8. APOPTOSIS:

In situ cell death detection kit, fluorescein (Roche Applied Science, Penzberg, Germany) was used for apoptosis detection. I used the procedure recommended for adherent cells, cell smears, and cytospin preparations as described in the instruction manual. When the protocol did not work, I adjusted concentration of paraformaldehyde (to 2%), fixation time and also permeabilising step (combination of Triton X-100 and Tween 20, prolonged incubation with the permeabilisation solution). As positive control, larvae with apoptosis triggered by UAS-Grim/Hml-GAL4 system were used. In these larvae, apoptosis is triggered in all haemocytes expressing hemolectin. Another positive control were haemocytes treated with DNase I (Ambion, Austin, TX) as recommended and described in the Instruction manual for the kit.

2.9. CRYSTAL CELLS:

Crystal cells in larvae were visualized by heating larvae in tube with PBS at 75°C, 10min.

2.10. FLYFOS CONSTRUCT:

Flies carrying the FlyFos-dco:GFP construct were created by Michaela Fencková. The procedure is described in her PhD. thesis (Fenckova, 2011). The combination of recombineering and transgenesis allows introduction of large constructs into the genome by homologous recombination. This system is based on a fosmid vector (pFlyFos) containing *attB* site recognised by Φ C31 integrase and also the dominant selectable marker dsRed and approximately 36kb of genomic DNA fragment (Ejsmont et al., 2009). The Φ C31 integrase is a serine integrase from bacteriophage. It mediates the sequence-directed recombination between the *attB* site and the *attP* site in a genome (Bischof et al., 2007). This system enables functional analysis of a gene in the context of its intact *cis*-regulatory neighbouring regions by imaging of the gene product in living tissues and it also enables rescue the mutant phenotypes (Ejsmont et al., 2009). In the case of FF:dco, the GFP tag is attached to the C-terminal of the *dco* gene without stop codon in between (Fenckova, 2011). Therefore the Dco protein originating from this construct is linked with the GFP that is easily visualised by fluorescent microscopy.

RECOMBINATION OF FLYFOS:DCO CONSTRUCT TO THE LOSS-OF-FUNCTION *DCO* ALLELE:

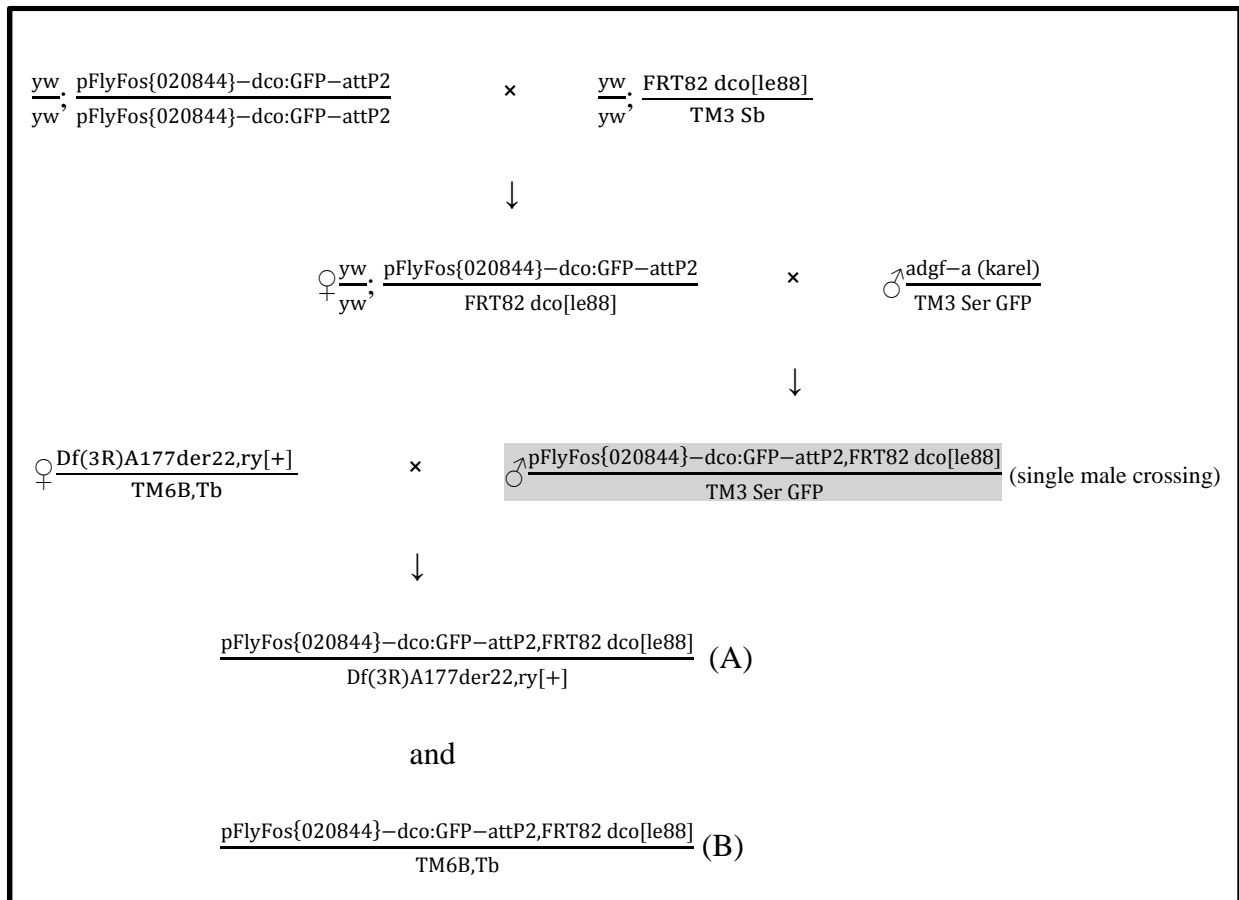


Fig. 2.13: Crossing scheme for FlyFos:dco recombination to the *dco^{le}*. (A) This combination was used for first testing if FlyFos:dco present in larvae is functional, i.e. normal imaginal discs are present. (B) Larvae of this genotype were used for establishing of stock.

DNA from males of the genotype marked by the grey rectangle was isolated by squishing these single males in squishing buffer (10mM Tris-HCl, pH 8.2; 1mM EDTA; 25mM NaCl; water). This suspension was treated by Proteinase K (20mg/ml) and then heated 30min at 37°C and 2min at 95°C. This DNA was used for molecular identification of presence of the *dco^{le}* allele (Fig. 2.14).

Primers (5' - 3' direction) used for PCR amplification of genomic section enabling distinguishing different *dco* alleles:

dco-seq3: AAGTTGCGGAAGAGTTTG

bam-dcoF2: GAAGGATCCACACAGGCAGGTTTTGAGGTTAGA

PCR program with annealing temperature 57°C was used for the amplification.

94°C – 240s		
94°C – 30s	}	30 cycles
57°C – 30s		
68°C – 180s		
68°C – 300s		

Size of WT allele section: 2742bp

Size of *dco^{le}* allele section: 2373bp

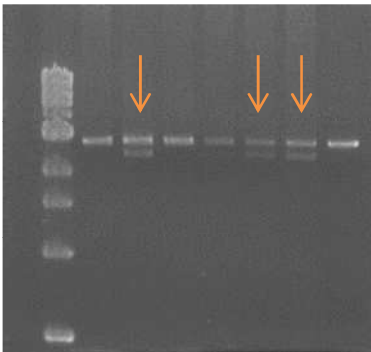


Fig. 2.14: PCR products identifying if there is only WT *dco* copy or WT and *dco^{le}* copy. The upper band is the WT *dco* and the lower band is the *dco^{le}* allele containing a short deletion.

Progeny of those three males were kept as stocks. Two of them maintain the TM6B balancer, but one of them is viable in homozygous constitution. This homozygous pFlyFos{020844}–dco:GFP–attP2,FRT82 dco[le88] / pFlyFos{020844}–dco:GFP–attP2,FRT82 dco[le88] larvae (here referred as FF:dco) were used in my work for identification of Dco localization (Figs. 3.56 and 3.60-3.62). Presence of the FlyFos construct was visually tested by presence of dsRed in brain.

2.11. IMMUNOSTAINING:

Larval tissues were dissected in PBS on ice and incubated for 40min in 4% paraformaldehyde in PBS at RT (25°C). Tissues washing 3x 20min in PBT (PBS with 0.3% Triton X-100) was followed by blocking in blocking buffer (see below) for 1 hour. Further, tissues were incubated in blocking buffer with primary antibodies overnight at 4°C:

for FF:dco tissues: mouse anti-discs large 1:500 (DSHB - Developmental Studies Hybridoma Bank, University of Iowa) and anti-GFP rabbit 1:500 (G1544, Sigma-Aldrich, Missouri, USA).

for WT tissues: mouse anti-discs large 1:100 (DSHB - Developmental Studies Hybridoma Bank, University of Iowa) and rabbit anti-Dco (kindly provided by Jeffrey L. Price, Ph.D., Associate Professor of Biology, University of Missouri-Kansas City) 1:50.

The washing step follows again (3x 20min in PBT) and incubation in blocking buffer with secondary antibodies - goat anti-mouse and goat anti-rabbit:

for FF:dco tissues: CyTM 2 conjugated affinity purified goat anti-rabbit IgG (JIR 111-225-003; Jackson Immuno Research laboratories, West Grove, PA) and Cy 3.5 conjugated affinity purified goat anti-mouse IgG 1 (Rockland 610-112-12; Rockland Immunochemicals Inc., Gilbertsville, PA), both diluted 1:500 in blocking buffer.

for WT tissues: Alexa Fluor® 555 Goat Anti-Mouse IgG and Alexa Fluor® 488 Goat Anti-Rabbit IgG (both from Life technologies, www.lifetechnologies.com), both diluted 1:200 in blocking buffer.

Tissues are then washed as follows: 1x 20min in PBT, 1x 20min in PBT with DAPI (1:10000) and 2x 20min in PBT. Tissues are then mounted in Vectashield mounting medium (Vector Laboratories Inc.; Burlingame, CA) overnight. Tissues recovered on slides were prepared to imaging.

Blocking buffer consists of: 5% NGS - Normal goat serum (JIR 005-000-121; Jackson Immuno Research laboratories, West Grove, PA) and 0.1% BSA (Serva electrophoresis, Heidelberg, Germany) in PBT.

2.12. RNA ISOLATION AND cDNA SYNTHESIS:

Tissue dissections were carried out in RNase free Ringer buffer and forceps were cleaned with RNase Zap (Ambion, Austin, TX). Tissues were collected for 30min and then frozen in liquid nitrogen.

The total RNA was isolated with the use of NucleoSpin RNA II (Macherey Nagel, Düren, Germany) following suppliers instructions. All samples were treated with the DNase (Turbo DNase free kit, Ambion, Austin, TX). Samples were diluted in DEPC treated water to concentration 200ng/μl. Reverse transcription was performed on 600ng of total RNA with the use of SuperScript III reverse transcription kit (Invitrogen, Carls-bad, CA) and the oligo dT primer was used for selective reverse transcription of only mRNA. The quality and amount of cDNA was measured with NanoDrop (Thermo Scientific, Wilmington, USA).

RT-PCR:

I compared relative rates of *dco* mRNA in different tissues (gut, fat body, brain, salivary glands, ring gland, lymph gland, discs and haemocytes). All data were normalized to the relative levels of *β-actin* mRNA in these tissues. The quantification of gene expression was analysed with C1000 Thermal Cycler with the use of iQ-SYBR Green Supermix kit (both from BioRad laboratories, Hercules, CA).

Program:

94°C – 180s

94°C – 30s

56°C – 30s

72°C – 35s

} 40 cycles

72°C – 300s

Program was followed by melting analysis from 50°C to 98°C.

The data were evaluated in CFX manager software (BioRad laboratories, Hercules, CA).

Primer sequences (5' - 3' direction):

dco-seq2: CCTCGATTGTGGTGCTGTGC

dco-seq3: AAGTTGCGGAAGAGTTTG

act5CF: TACCCCATGAGCACGGTAT

act5CR: GGTCATCTTCTCACGGTTGG

3. RESULTS

3.1. CHARACTERISATION OF PHENOTYPES

3.1.1. LYMPH GLAND (LG)

The lymph gland (LG) is a haematopoietic organ in *Drosophila* larvae; therefore I first compared the impact of mutant *dco* alleles on the LG morphology. As a control in this work, I usually used the *dco^{der/+}* heterozygous larvae if not stated or *w*. The *dco^{der/+}* heterozygotes do not differ from the WT (or *w*) flies (larvae) in this case.

Figure 3.1 shows the wild type (WT – *w*) lymph gland and a detail of its lobes. This is the normal size of the LG, where the form is rather solid. Initially, there is only the first pair of lobes at the 4th day. At the 5th day, just before pupation, the secondary pair of lobes emerges. A different situation is in the case of the *dco null* mutant in figure 3.2. The primary lobes are noticeably smaller than those of the WT larvae at the 4th day. The size of lobes does not significantly change with time and does not reach the size of the WT lobes in spite of the fact that the *dco null* larvae live for 10 days. After these ten days, they either die without any signs of pupation or manage to pupate and then die without starting the metamorphosis. The homozygous *dco^{L39Q S101R}* mutant lymph glands at day 4 and 6 are depicted in figure 3.3. The morphology of this mutant LG does not noticeably differ from the WT LG. But at the 6th day, the morphology already changes - the first lobes are overgrown and start disintegrating as seen in figure of LG in detail at the 6th day. Lobe margins are broken and lobes are slowly falling apart. The secondary lobes of homozygous *dco^{L39Q S101R}* mutants are enlarged too, and this trend continues with time. These mutants also do not reach the adult stage. Larval development of *dco^{L39Q S101R}* homozygotes is prolonged up to 11 days (rarely even longer) when they usually die. In sporadic cases, the prepupae can be seen but the metamorphosis does not occur. A similar phenotype is seen for homozygous *dco^{L39Q}* mutants. The *dco^{L39Q}* homozygous mutant LGs at the 4th and 7th day are depicted in figure 3.4. The mutant LG at day 4 is similar to the WT lymph gland. At the 7th day, the LG is greatly enlarged. The primary lobes as well as the secondary lobes are overgrown. Unlike the homozygous *dco^{L39Q S101R}* mutants, the *dco^{L39Q}* homozygote lobes do not disintegrate at this point. The lobe margins are rather solid and smooth.

WILD TYPE (WT)

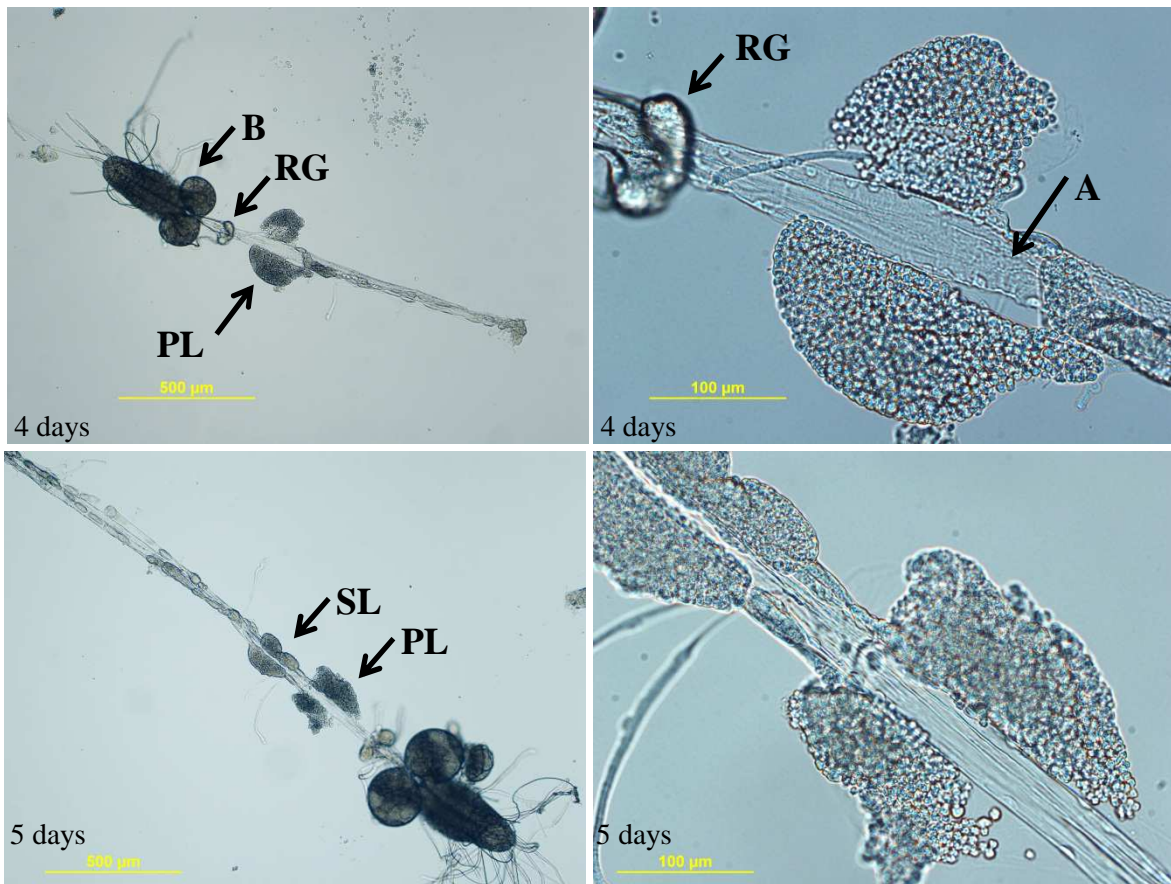


Fig. 3.1: The third instar wild type (WT) lymph gland (LG). (left – the whole LG; right – detail) B – Brain, RG – ring gland, PL – primary lobes of the lymph gland (LG), SL – secondary lobes of the LG, A – dorsal vessel (aorta).

DCO NULL MUTANT

Fig. 3.2: The lymph gland of the *dco null* (*dco^{der/le}*) mutant. (left – the whole LG; right – detail)

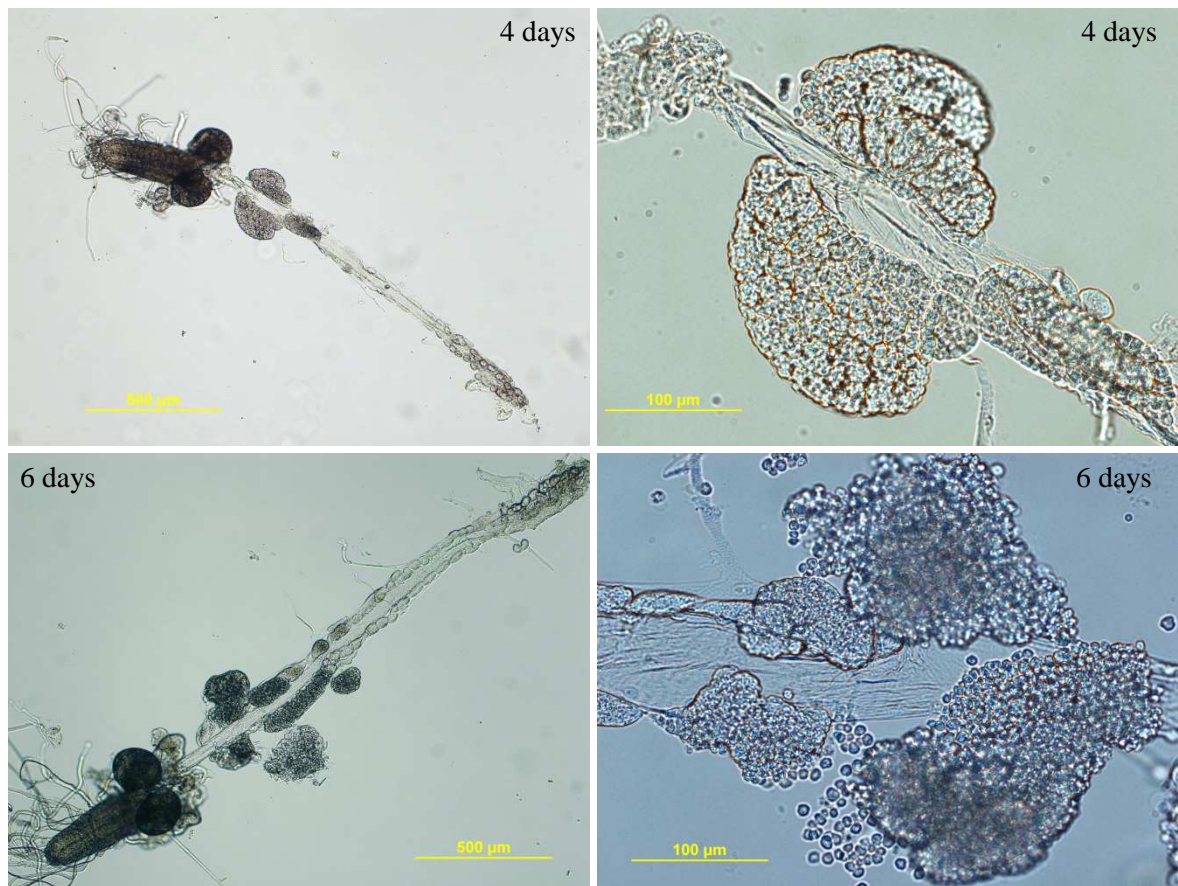
DCO L39Q S101R MUTANT

Fig. 3.3: The LG of homozygous *dco L39Q S101R* mutants. (left – the whole LG; right – detail)

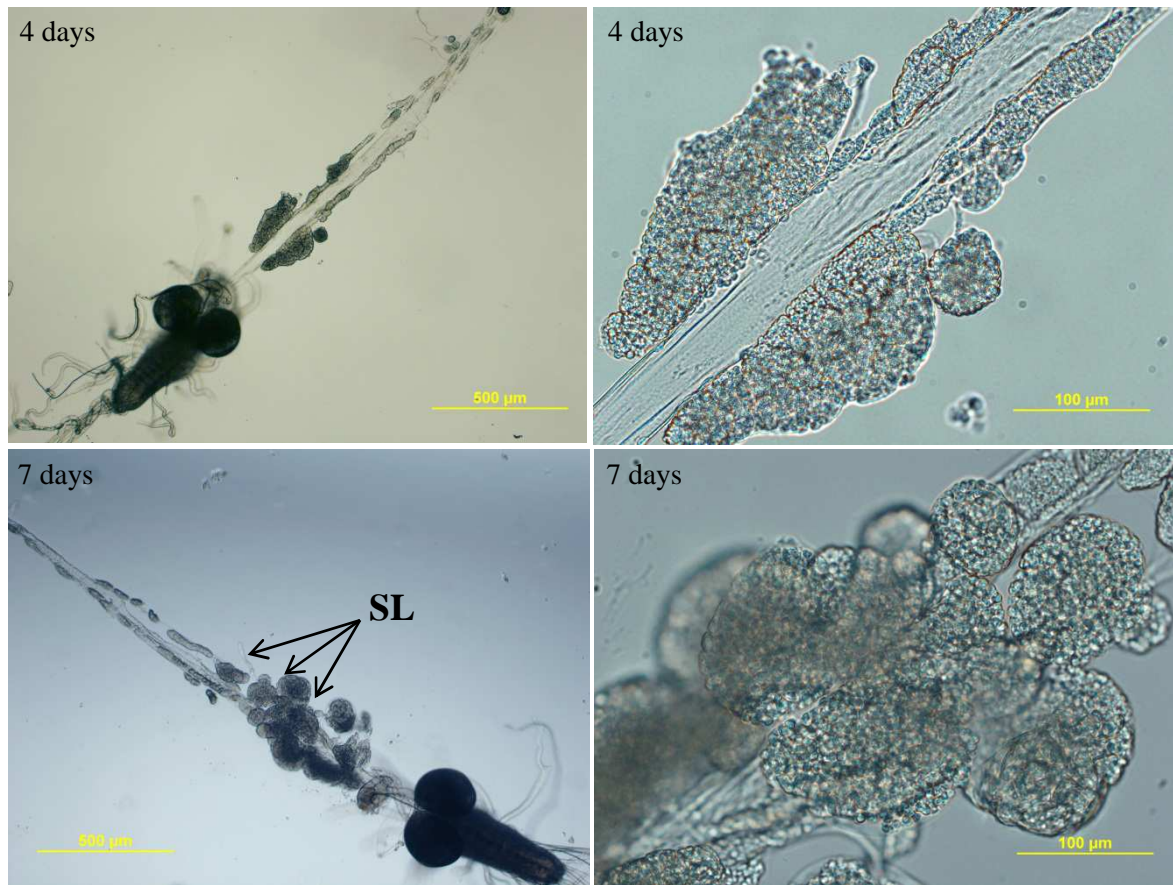
DCO^{L39Q} MUTANT

Fig. 3.4: The Lymph gland of homozygous *dco*^{L39Q} mutants. (left – the whole LG; right – detail; SL secondary lobes).

3.1.2. CHANGES IN HAEMOCYTE PROLIFERATION AND DIFFERENTIATION

Since there are noticeable changes in the larval haematopoietic organ, the lymph gland, I assumed that there could also be changes in the counts of circulating haemocytes. Therefore I compared the counts of haemocytes (*Drosophila* blood cells) per larva in each of the mutant constitution. Although all the hemolymph cannot be yielded from the larva body, i.e. there is an underestimating effect on haemocyte counts to a certain extent; the estimation of hemolymph volume is not required. Since the size of mutant larvae greatly differs from

the size of the WT larvae, the hemolymph volume estimation can be labourious. Therefore, I counted the haemocytes per larva.

For the first characterisation of mutant phenotypes based on haemocyte counts, I used the UAS-GAL4 system. I counted haemocytes in the flies where hemolectin ($Hml > GFP$) marker was used to distinguish between the mature and immature haemocytes. Hemolectin is expressed in a subpopulation of plasmatocytes and crystal cells, but not in lamellocytes (Goto et al., 2003). The haemocyte morphology and $Hml > GFP$ marker, which are features used to distinguish between different haemocyte types in this work, are demonstrated in figure 3.5.

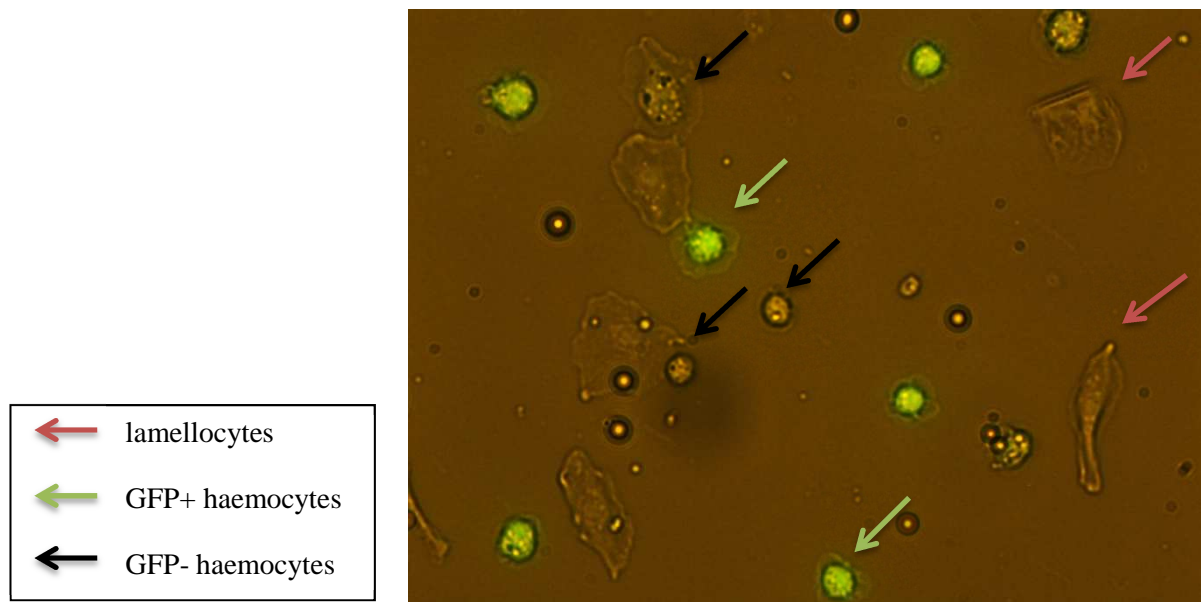


Fig. 3.5: Specification of the different types of haemocytes.

The dependency of the haemocyte counts (y-axis) on the length of larval life (x-axis) for individual genotypic combinations is illustrated in figures 3.6 and 3.7. For figure 3.6, the average numbers of the particular types of haemocytes for different genotypes are used. For more accurate illustration of the state in different genotypes, I used box-and-whisker plots in figure 3.7. I counted haemocytes for all the genotypes starting the 4th day AEL except the heterozygous control, for which I started counting at the 3rd day AEL, because the control larva size at this age is similar to the *dco* mutant larva body size (late 2nd stage/early 3rd stage). From charts (Fig. 3.6 and 3.7), it is obvious that the main difference between mutants

is in the counts of Hml-, i.e. undifferentiated haemocytes. Counts of haemocytes in both *dco*^{L39Q S101R} and *dco*^{L39Q} heterozygotes do not exceed the heterozygous control haemocyte counts. The *dco*^{L39Q} homozygous mutants have significantly increased counts of haemocytes in comparison to the heterozygous control. Furthermore, the *dco*^{L39Q S101R} homozygotes have even more increased counts of haemocytes than the mutants mentioned before. The *dco*³ mutants have a similar amount of haemocytes as the heterozygous control. The larvae with this mutant constitution pupate at the 6th day and then die. The *dco null* mutants have less haemocytes per larva in comparison to the heterozygous control and the haemocyte counts are kept at steady level during the larval life without any noticeable increase.

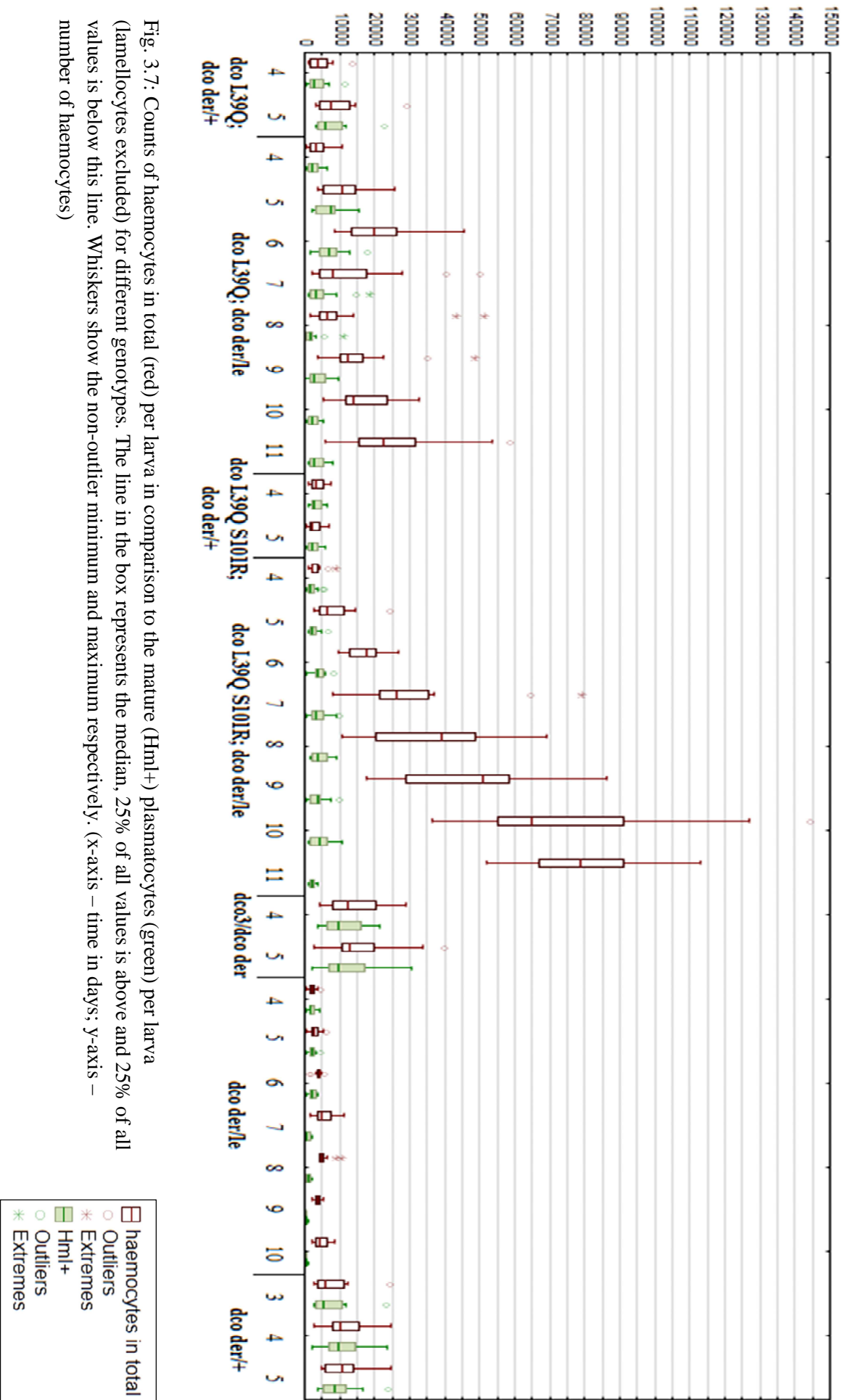


Fig. 3.7: Counts of haemocytes in total (red) per larva in comparison to the mature (Hml+) plasmatocytes (green) per larva (lamellocytes excluded) for different genotypes. The line in the box represents the median, 25% of all values is above and 25% of all values is below this line. Whiskers show the non-outlier minimum and maximum respectively. (x-axis – time in days; y-axis – number of haemocytes)



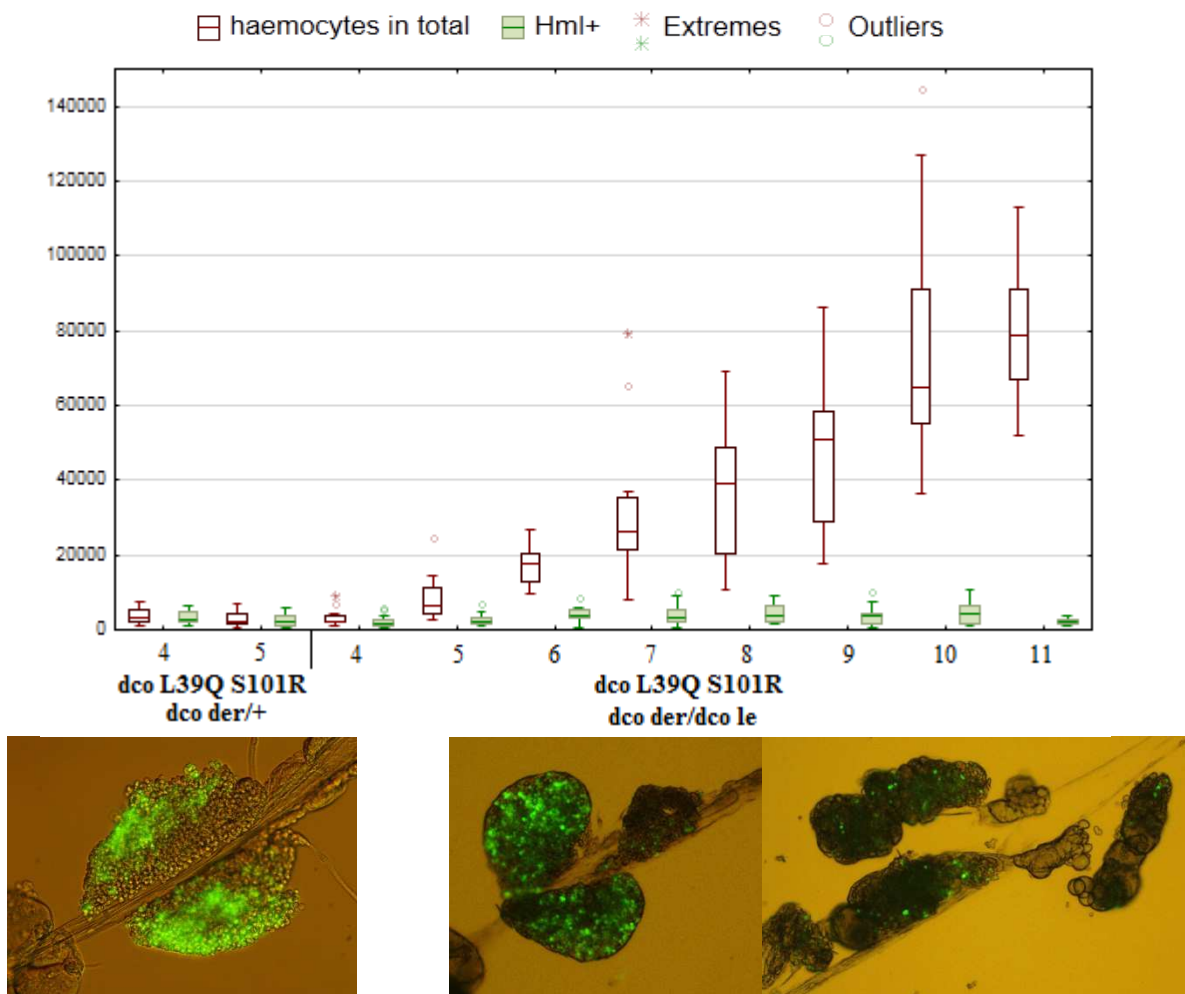
DCO ^{L39Q S101R} MUTANT

Fig. 3.8: Counts of haemocytes per larva in the *dco* ^{L39Q S101R} mutants (lamellocytes excluded) and representative figures of lymph glands with illustrative distribution of different haemocyte types (Hml+ and Hml-) corresponding to the changes happening in the mutant LG (left – heterozygote, right – homozygote; x-axis – time in days; y-axis – number of haemocytes).

I compared the individual mutants with its mutant heterozygous control. The illustrative pictures of the *dco* ^{L39Q S101R} mutant lymph glands are in figure 3.8. The green signal is the Hml marker (GFP) to present how the proportion of Hml+ and Hml- haemocytes changes with time. As the proportion of Hml+ haemocytes decreases with time

in comparison to the Hml- haemocytes in the chart above, the proportion of these Hml+ cells also decreases in the LG though the LG is bigger than at the beginning of larval life. The haemocyte counts in the dco^{L39Q} mutants in both heterozygous and homozygous constitution are shown in figure 3.9. Here we can also see the increased counts of Hml- haemocytes in comparison to the heterozygous dco^{L39Q} mutants. But in this case, the increase is much weaker than in the $dco^{L39Q S101R}$ homozygotes. Unlike the homozygous $dco^{L39Q S101R}$ mutants where the increase of Hml- haemocytes is continuous, the dco^{L39Q} homozygote Hml- haemocyte counts increase in two waves. After the first growing wave, there is a decrease and then an increase again. As it can be seen in the chart of the haemocyte counts, the ratio of the Hml+ haemocytes in the LG also changes as the Hml- counts are raising.

DCO ^{L39Q} MUTANT

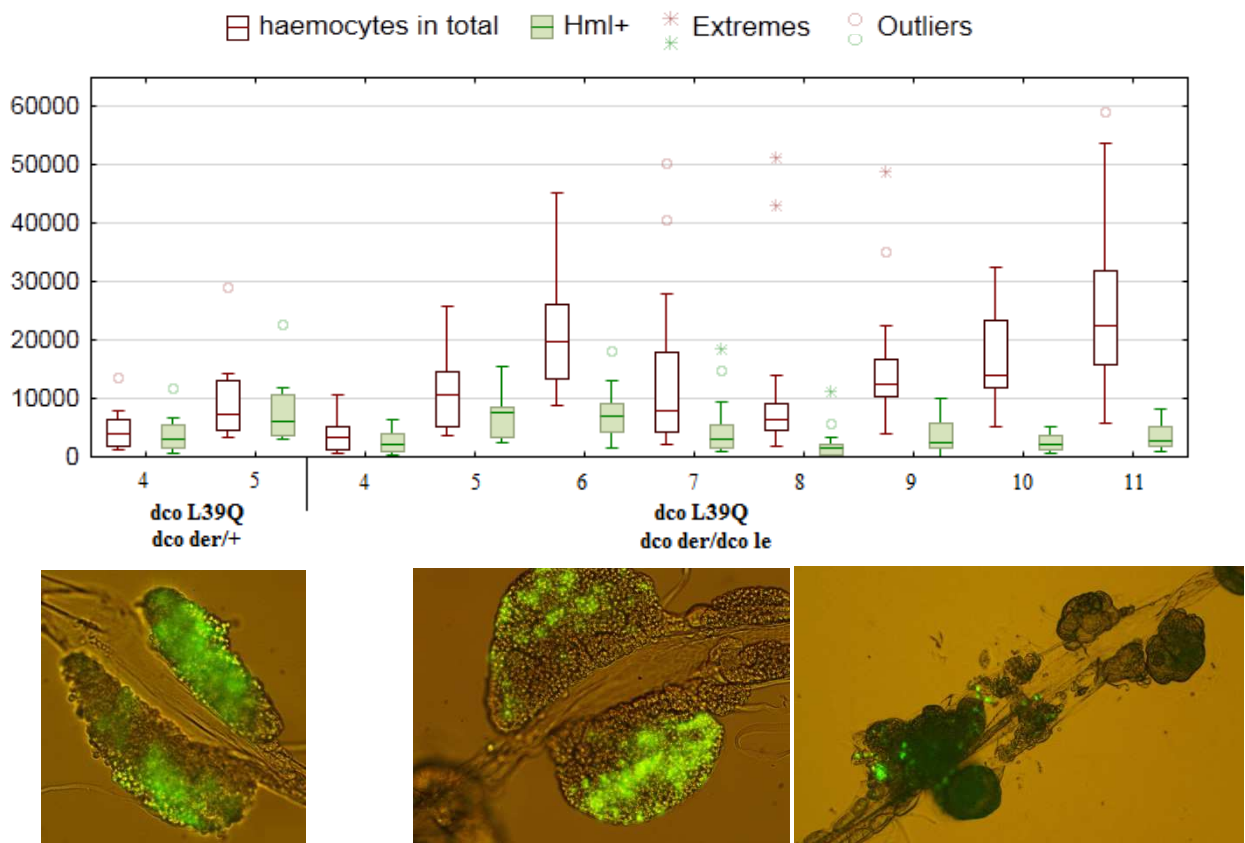


Fig. 3.9: Counts of haemocytes per larva in the dco^{L39Q} mutants (lamellocytes excluded) and representative figures with illustrative distribution of the different haemocyte types (Hml+ and Hml-) corresponding to the changes happening in the lymph gland. (left – heterozygote, right – homozygote; x-axis – time in days; y-axis – number of haemocytes).

COMPARISON OF MUTANT PHENOTYPES

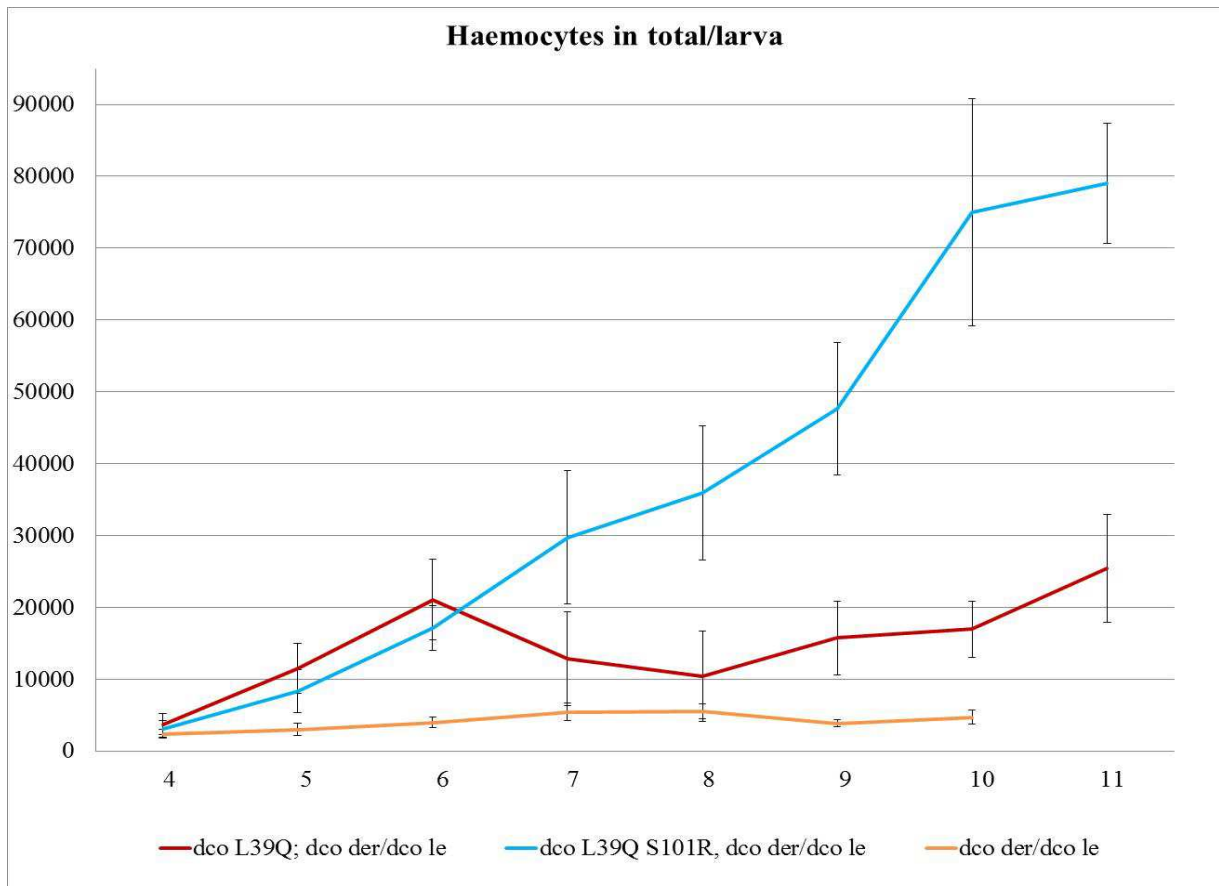


Fig. 3.10: Average numbers of plasmatocytes in total per larva (lamellocytes excluded). (x-axis – time in days; y-axis – number of haemocytes)

I compared plasmatocyte total counts (i.e. mature and immature; lamellocytes are excluded) in the mutants. The homozygous *dco*^{L39Q} and *dco*^{L39Q S101R} mutants and *dco* null mutants are compared in figure 3.10. The *dco* null mutant total plasmatocyte counts do not develop any significant progress throughout the life, despite the larvae live for 10 days. The identical increasing trend is observed in both *dco*^{L39Q S101R} and *dco*^{L39Q} homozygotes up to the 6th day. After the 6th day, the homozygous *dco*^{L39Q S101R} mutant haemocyte counts keep growing continuously in time, without any sign of decrease, up to the end of larval life. The *dco*^{L39Q} homozygote haemocyte counts decrease after the 6th day up to the 8th day, and increase again after the 8th day up to the 11th day, when these larvae die. But these mutants cannot reach the counts of the *dco*^{L39Q S101R} homozygotes. In previous figures, it looks like

the Hml+ haemocyte counts do not significantly change with time or between the $dco^{L39Q S101R}$ and dco^{L39Q} homozygous mutants. Therefore, I tested if the $dco^{L39Q S101R}$ and dco^{L39Q} homozygous mutants significantly differ in the Hml+ and/or Hml- haemocyte counts. Figure 3.11 shows that they do not significantly differ from each other in the Hml+ haemocyte counts. Moreover, the Hml+ counts do not exhibit any dynamic development of their quantity throughout the lifetime. The mutants vary in the counts of Hml- haemocytes after the 6th day. Unlike the dco^{L39Q} homozygotes, the $dco^{L39Q S101R}$ homozygous mutant Hml- haemocyte counts keep growing throughout the whole larval stage. The Hml+ haemocyte counts in dco mutants (homozygous $dco^{L39Q S101R}$ and dco^{L39Q} mutants and dco null mutants) are depicted in figure 3.12 in more detail. Hml+ haemocytes in the dco null mutants very slightly increase at the beginning (up to the 6th day) and then only decrease. The Hml+ haemocyte counts in homozygous dco^{L39Q} mutants quickly increase (2.5 fold) from the 4th to the 6th day. After the 6th day, the Hml+ counts decrease and stay more or less at the same level for the rest of the life. In the $dco^{L39Q S101R}$ homozygotes, the increase of mature plasmatocyte counts is slower than in case of the homozygous dco^{L39Q} mutants and there is no decreasing trend.

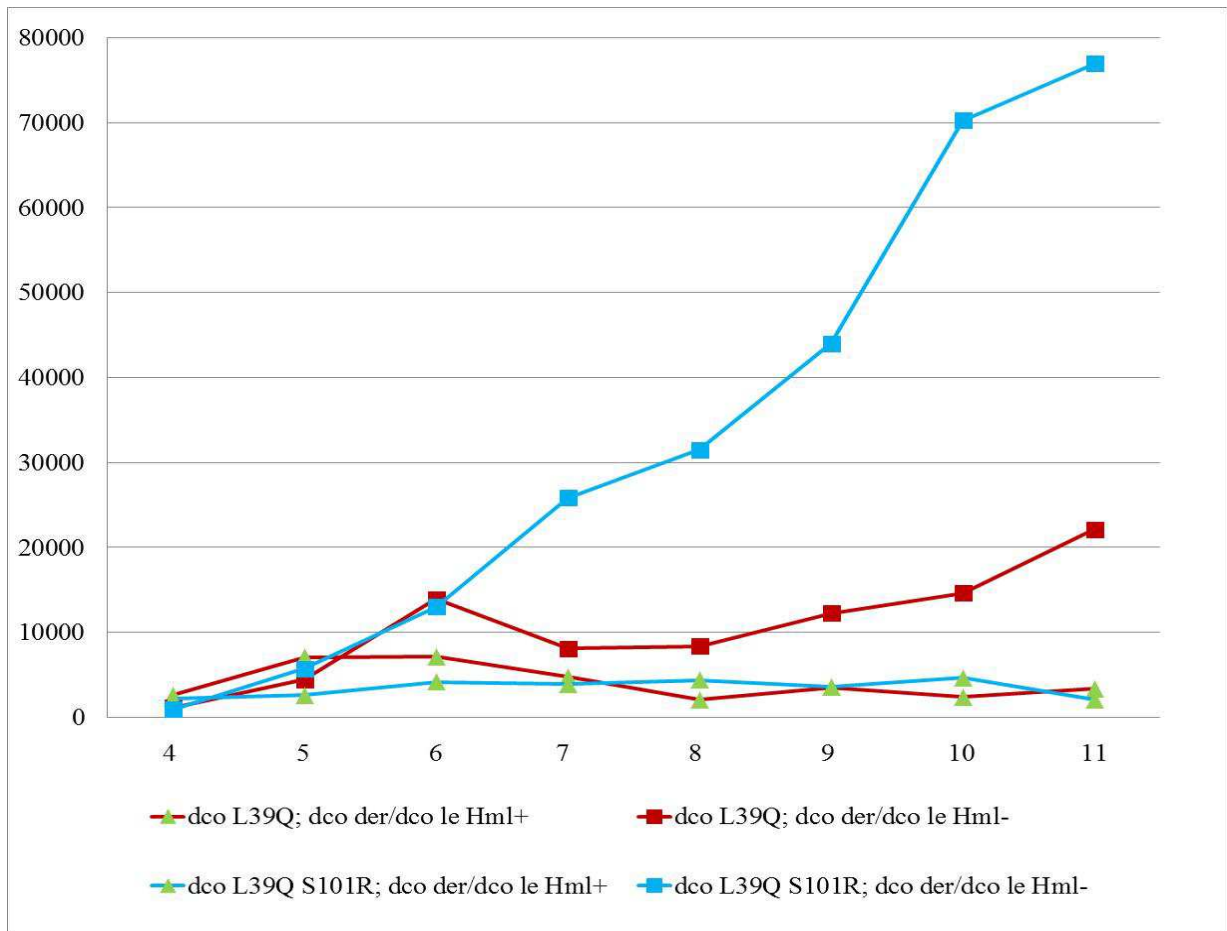


Fig. 3.11: Comparison Hml+ and Hml- plasmatocyte counts in *dco* mutants. (x-axis – time in days; y-axis – number of haemocytes).

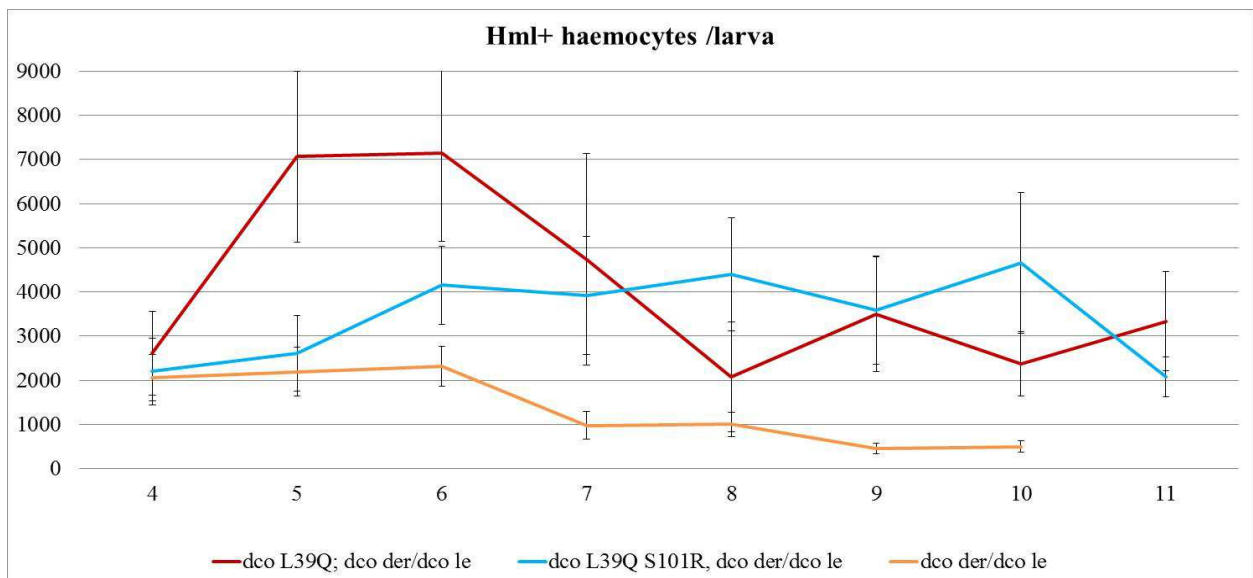


Fig. 3.12: Counts of Hml+ haemocytes in mutants per larva. (Whiskers – standard deviation; x-axis – time in days; y-axis – number of haemocytes)

I further examined the effect of the heterozygous constitution of mutant alleles on both haematopoiesis and imaginal wing discs (Fig. 3.13), and I compared these results with the heterozygous control and *dco null* mutants. The *dco null* mutants have greatly reduced imaginal discs (Zilian et al., 1999), as well as counts of haemocytes. The *dco null* mutants cannot reach the heterozygous control haemocyte counts even after 10 days AEL. The heterozygous control does not differ from the wild type larvae in this case either in the imaginal disc or haematopoiesis. Here I compare imaginal wing discs from heterozygous control larvae with heterozygous mutant wing discs at the 4th day AEL. The *dco*^{L39Q} heterozygotes have overgrown imaginal discs in comparison to the heterozygous control. A bit slighter effect on imaginal wing disc size is present in the *dco*^{L39Q S101R} heterozygotes. Although the imaginal wing disc size is changed in heterozygous mutants, their morphology and folding do not seem to be changed. Haemocyte counts in the *dco*^{L39Q S101R} heterozygotes are lower than those in the heterozygous control at both the 4th and the 5th day (p<0,001). But in the case of *dco*^{L39Q} heterozygotes, haemocyte counts differ from heterozygous control only at the 4th day and the haemocyte counts are alike at the 5th day (p<0,001). It means that even heterozygous mutant allele constitution is sufficient for a gentle phenotype changes in both haemocyte counts and imaginal wing disc size. The comparison of the heterozygous control with the *dco*³ mutants is depicted in figure 3.15. Haemocyte counts in *dco*³ mutants do not differ from the heterozygous control either in Hml+ haemocytes (p=0.9342) or in haemocytes in total (p=0.5905), although the *dco*³ mutant imaginal wing discs (at the 4th day) are significantly bigger than the control imaginal wing discs. After the 5th day, both heterozygous control and *dco*³ mutants pupate.

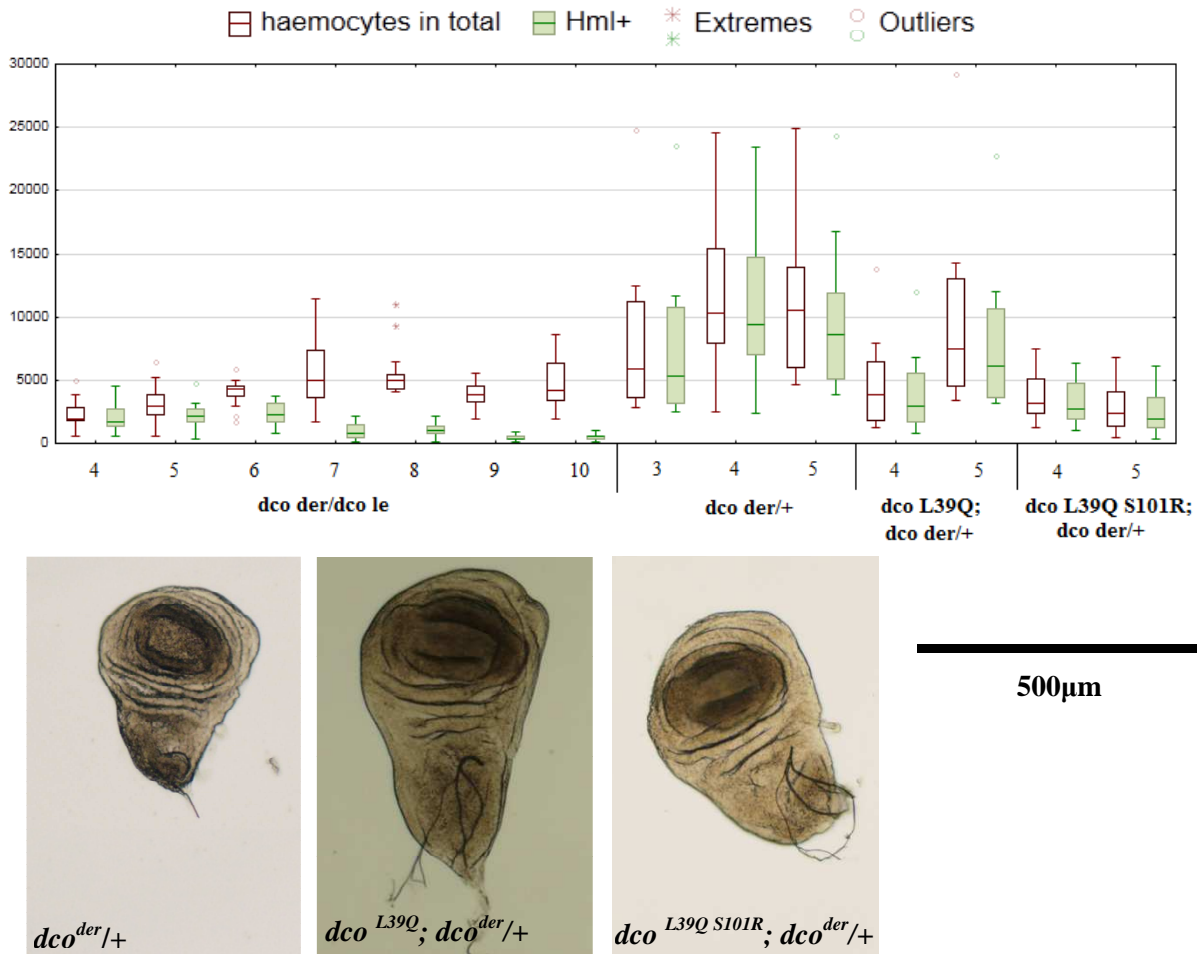


Fig. 3.13: Counts of haemocytes in heterozygous controls and *dco null* mutants (x-axis – time in days; y-axis – number of haemocytes; lamellocytes excluded) and the effect of heterozygous mutant allele constitution on imaginal wing discs at the 4th day AEL.

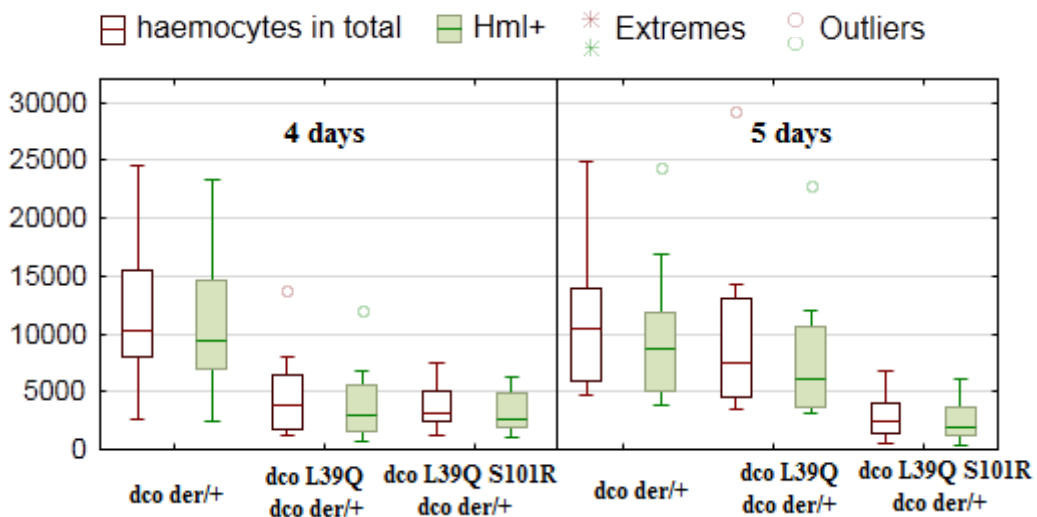


Fig. 3.14: Haemocyte counts in heterozygous mutants compared to the heterozygous control counts (x-axis – time in days; y-axis – number of haemocytes).

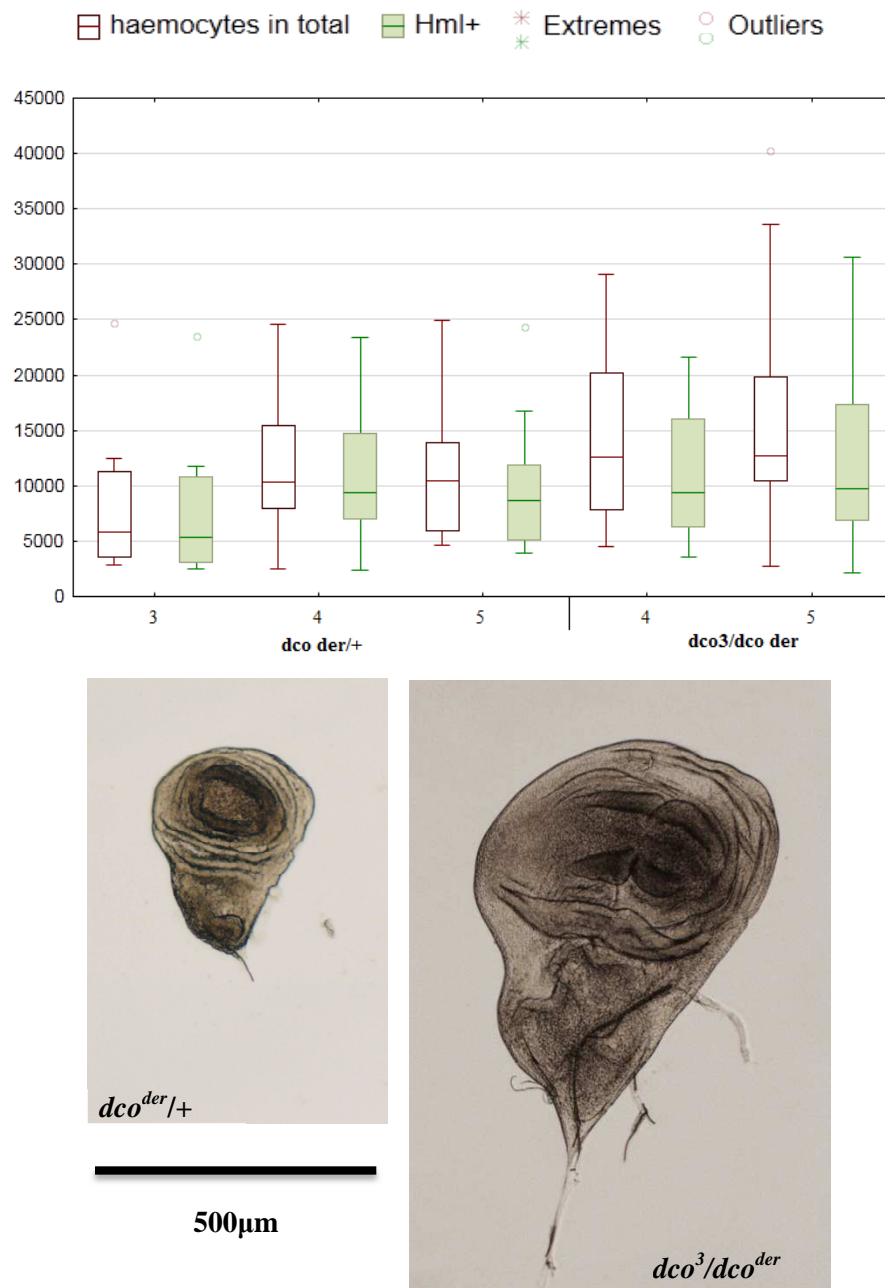


Fig. 3.15: Haemocyte counts in heterozygous control (*dco^{der/+}*) and *dco³* mutants with illustrative figures of imaginal wing discs (x-axis – time in days; y-axis – number of haemocytes).

HML-/HML+ RATIO

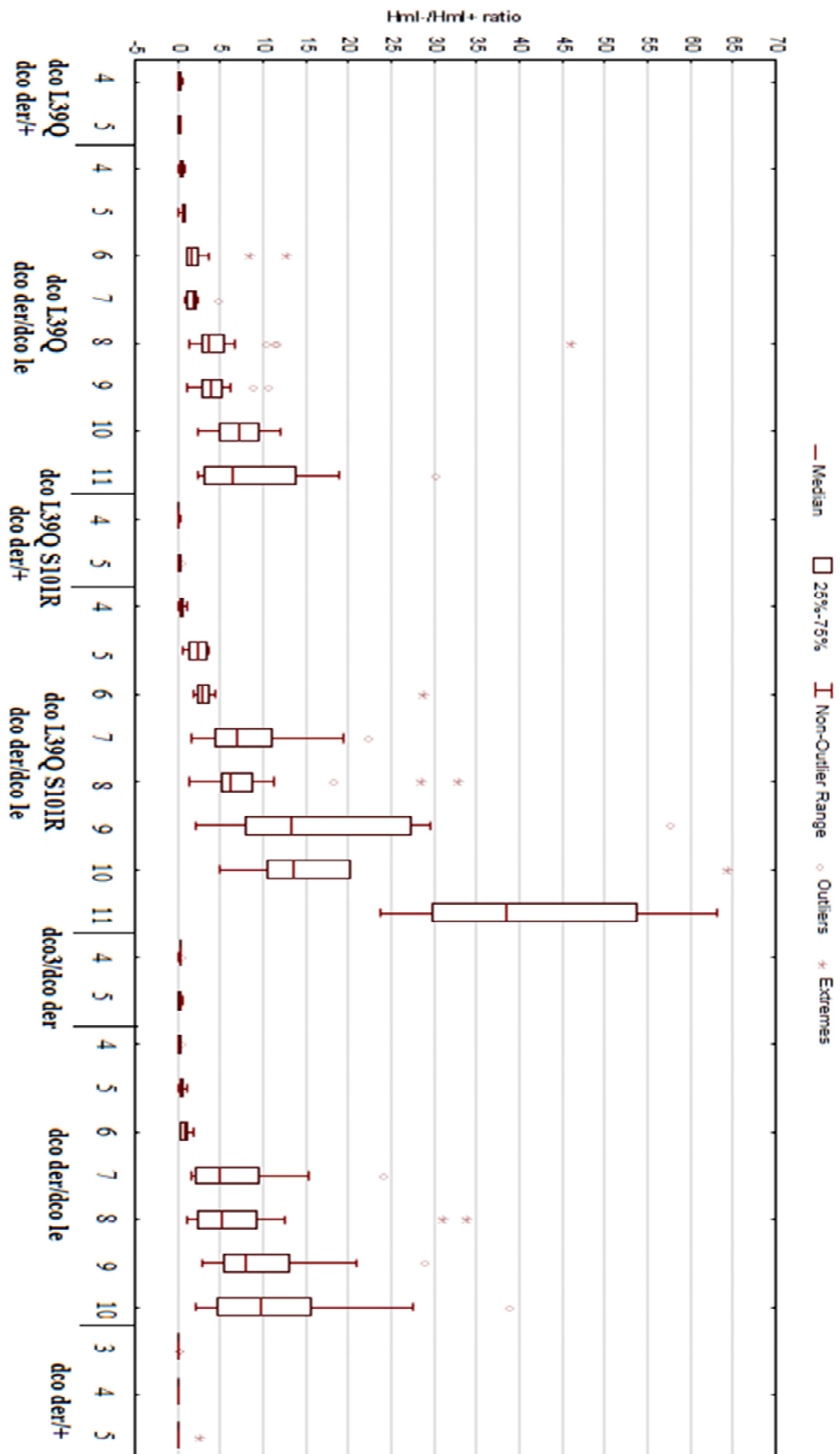


Fig. 3.16: Ratios of Hml- to Hml+ haematocytes in *dco* mutants. (x-axis – time in days; y-axis – ratio)

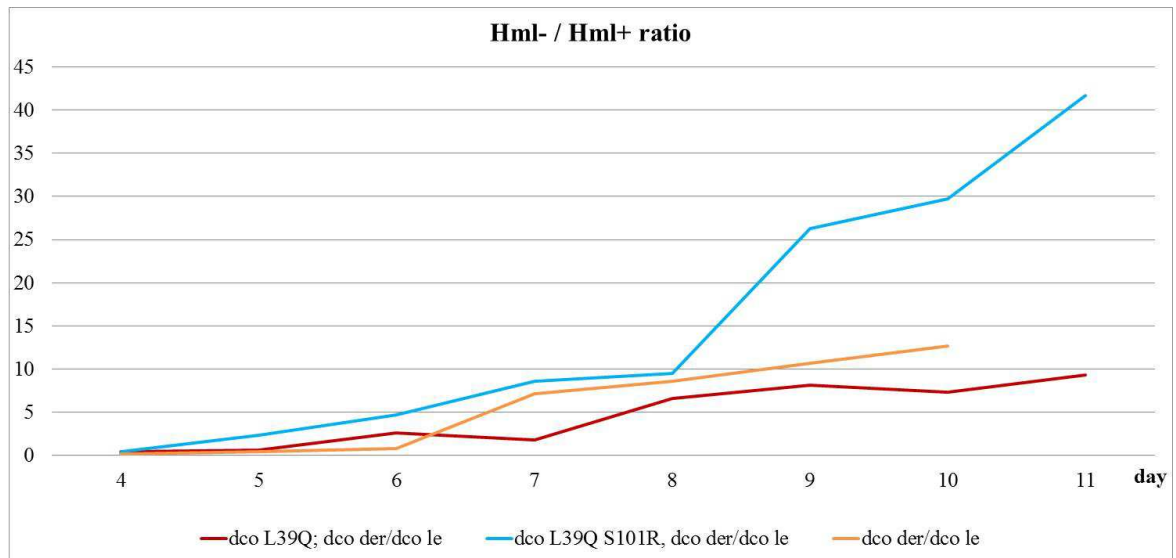


Fig. 3.17: Comparison of Hml-/Hml+ haematocyte ratios in *dco*^{L39Q S101R} and *dco*^{L39Q} homozygotes and *dco null* mutants. (x-axis – time in days; y-axis – ratio)

From the results above (Fig. 3.17), one could say that the *dco* mutants are rather affected by ratio of different haemocyte types – for instance the ratio of mature and immature plasmatocytes. On that account, I compared these ratios in larvae of genotypes I used in this work (Fig. 3.16). There are two main distinguishable categories: group 1 – genotypes with normal lifetime where the ratio is always fewer than 1 (heterozygous *dco*^{L39Q S101R}; *dco*^{L39Q} mutants and control heterozygote), and group 2 – genotypes with prolonged larval lifetime and other abnormalities (homozygous *dco*^{L39Q S101R} and *dco*^{L39Q} mutants and *dco null* mutants) where the ratios are higher than 1, presenting the prevalence of the Hml- haemocytes. I compared these ratios in homozygous mutants in figure 3.17. Based on statistical test, the homozygous *dco*^{L39Q} mutant Hml-/Hml+ haemocyte ratios do not significantly differ from the *dco null* mutants ($p < 0,001$). Furthermore, the ratios for the *dco*^{L39Q S101R} homozygotes do not significantly differ from the *dco null* mutants up to the 8th day AEL ($p < 0,001$).

LAMELLOCYTES

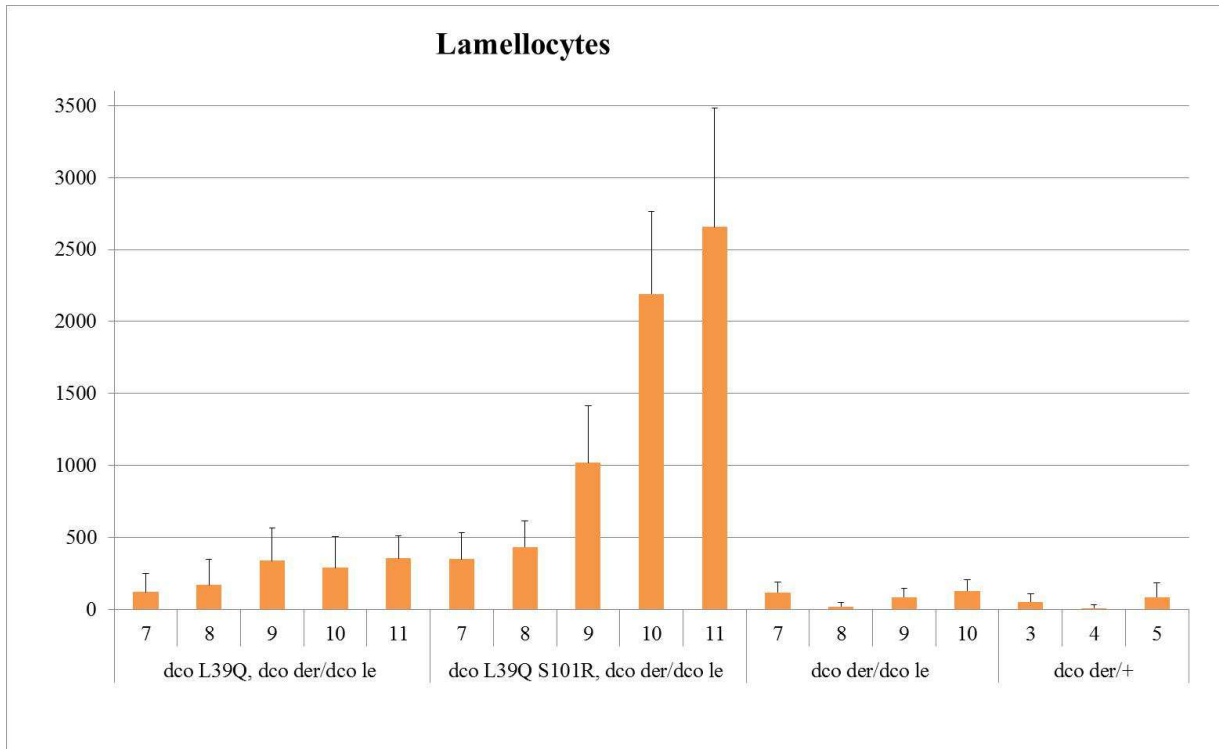


Fig. 3.18: Counts of lamellocytes per larva in different *dco* mutants. (x-axis – time in days; y-axis – number of haemocytes)

As I mentioned above, lamellocytes are type of *Drosophila* blood cells, which emerges after the immune challenge, such as wasp parasitization. If lamellocytes appeared in heterozygous control larvae, it was probably because of the conditions they met during their life. The numbers of lamellocytes per larva in the *dco* null mutants do not seem to differ from the heterozygous control. The *dco*^{L39Q} homozygotes have increased numbers of lamellocytes per larva kept at a steady level, whereas the homozygous *dco*^{L39Q S101R} mutant haemolymph contains more lamellocytes per larva in comparison to both heterozygous control and homozygous *dco*^{L39Q} mutants (Fig. 3.18). Although the haemocyte production is slightly reduced in the *dco* null mutants (Fig. 3.13), they are capable of differentiation of lamellocytes after the wasp parasitization (Fig. 3.19), indicating that the Dco protein is not required for lamellocyte differentiation. On the contrary, the Dco could be required for inhibition of apoptosis since the morphology of the *dco* null mutant haemocytes seems to be broken and bubbling (Fig. 3.20). These features strikingly remind the morphology of cells undergoing apoptosis (see Discussion).

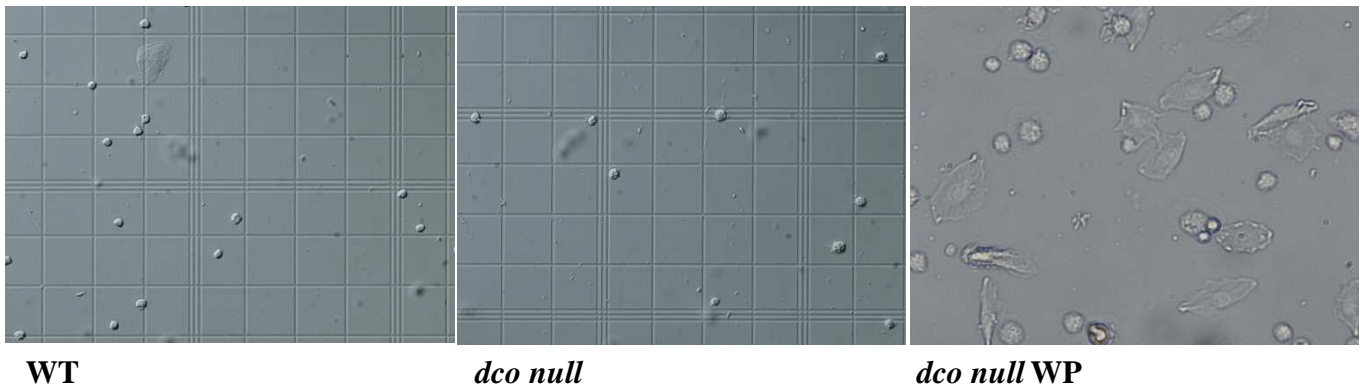


Fig. 3.19: Haemocytes in the WT (*w*), in the *dco null* mutant and in the *dco null* mutant after the wasp parasitization (WP).



Fig. 3.20: WT (*w*) and *dco null* mutant haemocytes in detail.

3.1.3. MELANOTIC CAPSULES FORMING

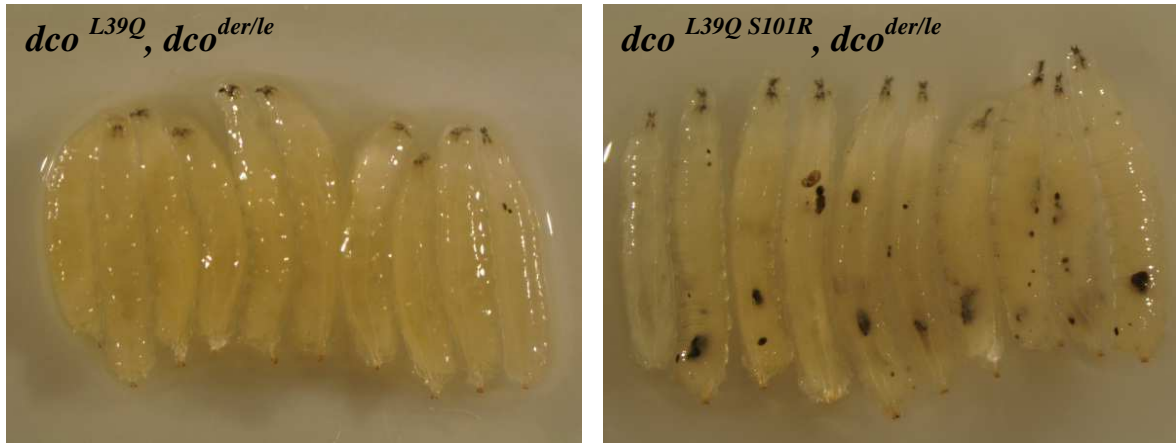


Fig. 3.21: Melanotic capsules incidence in homozygous dco^{L39Q} and $dco^{L39Q S101R}$ mutants.

One of the striking features of tested *dco* mutants is also the occurrence of melanotic capsules in larvae. Melanotic capsules incidence in both dco^{L39Q} and $dco^{L39Q S101R}$ homozygotes is depicted in figure 3.21. Melanotic capsules are present in 1 out of 10 homozygous dco^{L39Q} mutant larvae. The inverse situation is in the $dco^{L39Q S101R}$ homozygotes, where 1 out of 10 larvae does not have any melanotic capsules. Melanisation is an immune reaction that results in the deposit of a black pigment melanin during the wound healing. This process occurs thanks to the prophenoloxidase, which is an enzyme present in crystal cells (Crozatier and Meister, 2007). Lamellocytes are involved in this process as wrapping cells to form a multi-layered capsule around the wasp egg or other invader. The capsule is then melanised (Lanot et al., 2001; Crozatier et al., 2004; Crozatier and Meister, 2007). It is known that both lamellocytes and crystal cells are able to produce prophenoloxidase, an enzyme necessary for this process. Lamellocytes are thus capable of lamellocyte-mediated spontaneous melanisation process (Sorrentino et al., 2002; Irving et al., 2005). Therefore, I tested the presence of crystal cells in larvae (Fig. 3.22). Both dco^{L39Q} and $dco^{L39Q S101R}$ homozygotes have a decreased amount of crystal cells similarly to the *dco null* mutants. Also the localization is changed when compared to the WT control (*w*). Crystal cells are mostly localized in the posterior part of larva in the WT control, while the crystal cells in the dco^{L39Q} and $dco^{L39Q S101R}$ homozygotes are mostly localized anteriorly in the larva. Crystal cells do not seem to be present at all in posterior part larva body in the *dco*

mutants. Crystal cells in the *dco null* mutants are distributed both anteriorly and posteriorly, but in a less extent than in the control larvae. My results support the idea that melanotic capsules in *dco*^{L39Q S101R} homozygous mutants could be so-called “pseudotumors” caused by the extensive presence of lamellocytes, which is probably an overreaction of the cellular immune response. Mutations that activate the Toll and JAK/STAT pathways show similar phenotypes (Gateff, 1994; Lanot et al., 2001; Zettervall et al., 2004) to that seen in homozygous *dco*^{L39Q S101R} and *dco*^{L39Q} mutants. Regarding JAK/STAT signalling, mutations causing the constitutive activation of JAK kinase Hopscotch lead to both hyperproliferation of haemocytes and formation of melanotic capsules (Harrison et al., 1995; Luo et al., 1995). The same phenotype was observed in gain-of-function mutants in the transmembrane receptor Toll and in loss-of-function *cactus* mutants (Qiu et al., 1998). In the next chapters, I tested a connection of phenotypes seen in *dco* mutants with both Toll and JAK/STAT signalling pathways.

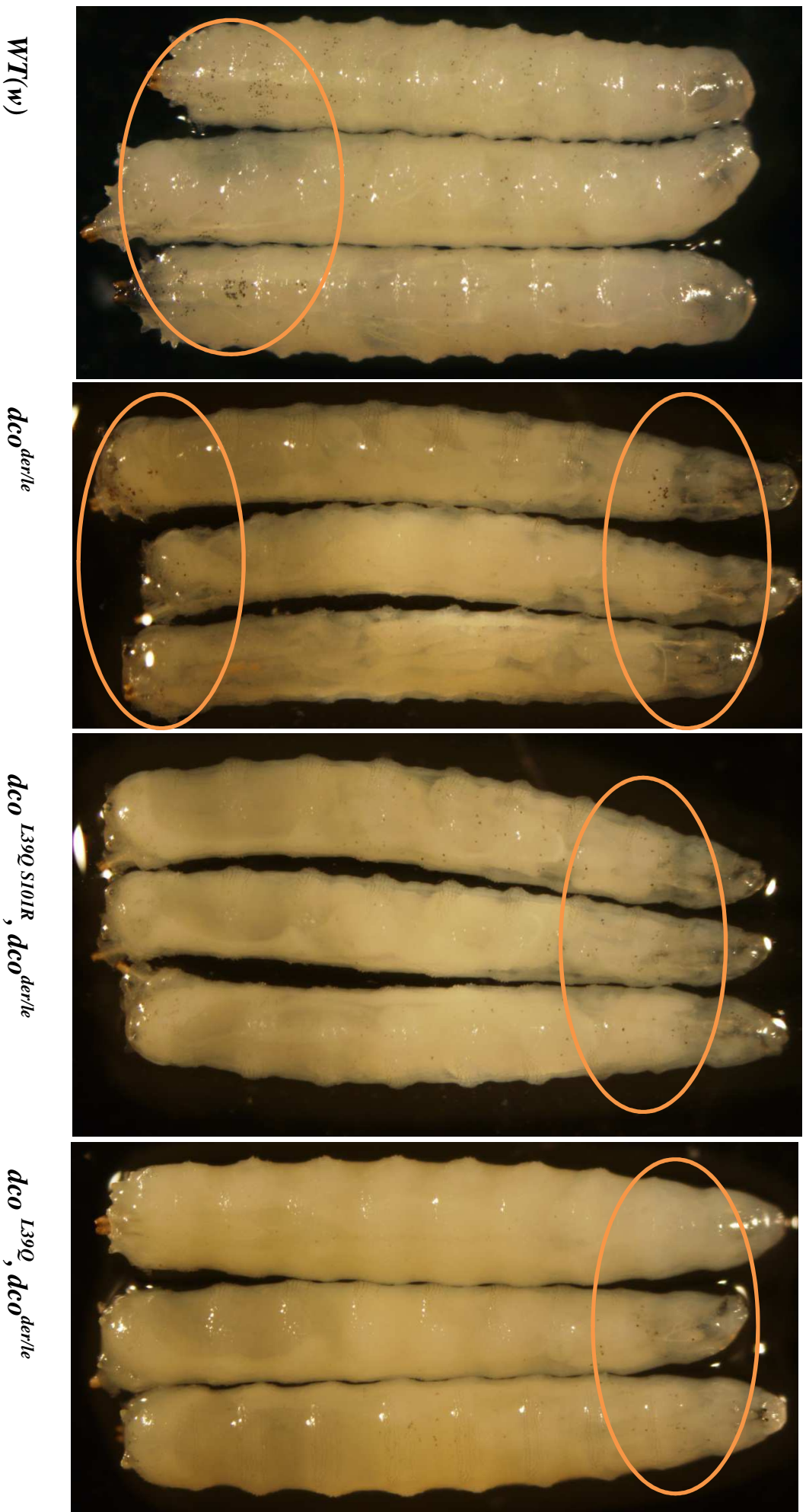


Fig. 3.22: Presence of crystal cells in larvae and their main localisation in the larva body (circle).

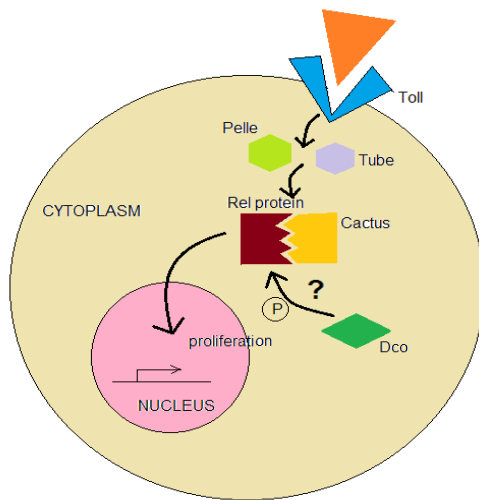
3.2. *DCO* / *TOLL* DOUBLE MUTANTS

Fig. 3.23: Hypothetical role of Dco through the Toll signalling pathway (adjusted by Qiu et al., 1998). Orange triangle presents a ligand triggering the Toll signalling pathway, Spätzle.

Toll signalling pathway is activated after the Spätzle ligand is bound to the Toll transmembrane receptor. The Toll/Tube/Pelle signal mediates phosphorylation and degradation of Cactus. Once Cactus is degraded in response to the signal, Dorsal is free to move into the nucleus where it regulates transcription of specific target genes (Belvin and Anderson, 1996). Analysis of *cactus* mutants revealed that the LGs of *cactus* larvae are considerably enlarged and that a lack of the Cactus protein causes an overabundance of haemocytes, formation of melanotic capsules and *cactus* mutant larvae die before reaching pupae stages (Qiu et al., 1998). I tested the possibility that the phenotype of *dco* mutants is triggered through the Toll signalling pathway. If the phenotype of the *dco*^{L39Q S101R} and/or *dco*^{L39Q} mutants would be caused by the activation of Toll signalling pathway, a removal of the transcription factors *dorsal* and *Dif* involved in Toll pathway should lead to suppression of the phenotypes. Therefore, I crossed both *dorsal* and *dorsal*, *Dif* deficiencies into the *dco* mutant background. For this purpose I used mutant combination of *dl*¹ with *Df(2L)J4* and *Df(2L)TW119* with *Df(2L)J4*, where *dl*¹ is a loss-of-function allele of *dorsal*, *Df(2L)J4* is a deletion of both *dorsal* and *Dif* and *Df(2L)TW119* is larger deletion where besides other genes are also deleted *dorsal* and *Dif*. These combinations cause the loss-of-function

mutations of *dorsal* and *dorsal Dif* respectively. However, in this work I present only results with *dorsal* (hereinafter referred to as DI-) mutation because larvae with constitution *dco*^{L39Q S101R} or *dco*^{L39Q}; *dorsal Dif*; *dco*^{der/le} emerge very rarely so I did not have sufficient amount of larvae for testing.

3.2.1. HAEMATOPOIESIS IN *DCO DORSAL* DOUBLE MUTANTS

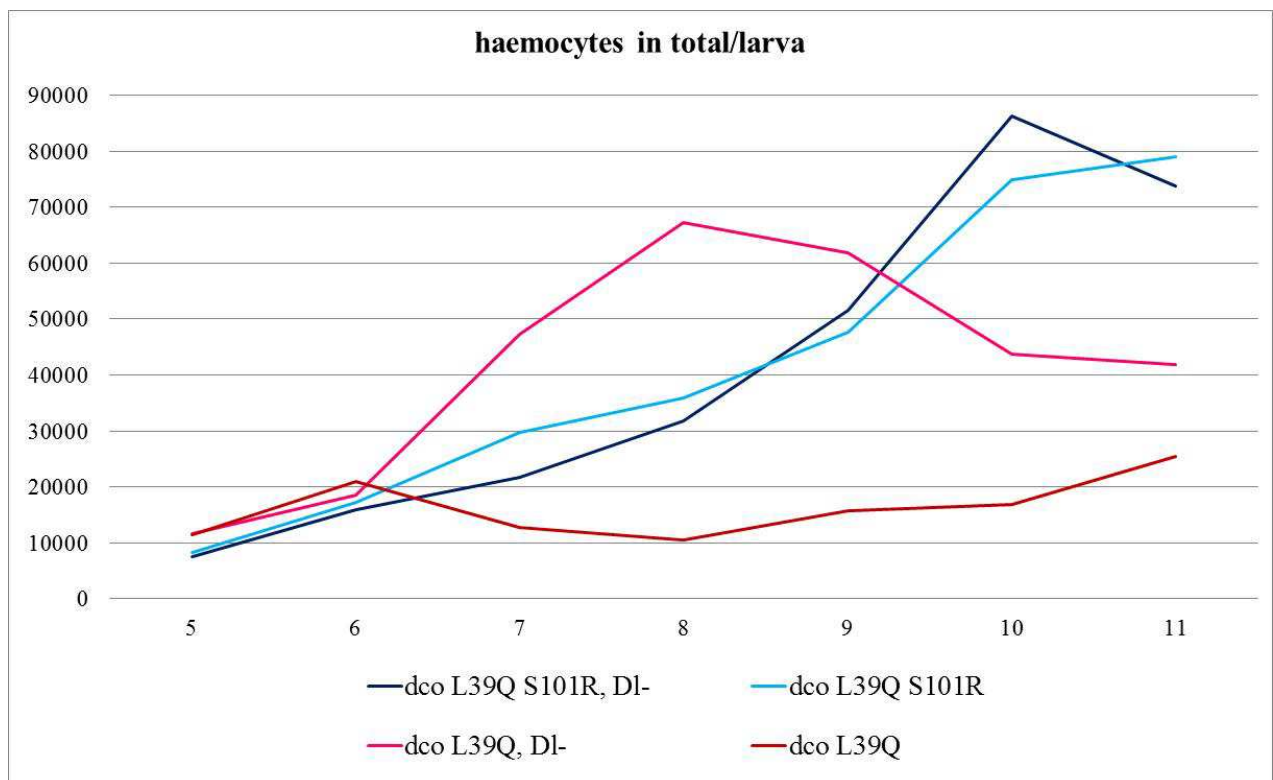


Fig. 3.24: Counts of haemocytes in total per larva in *dco* mutants along with the *dorsal* (DI-) deficiency. (x-axis – time in days; y-axis – number of haemocytes)

I counted the haemocytes in the *dco* and *dorsal* double mutants (Fig. 3.24). There is no significant change of haemocyte counts in total per larva in the *dco*^{L39Q S101R} homozygotes after the addition of *dorsal* gene deletion (DI-). There is an opposite trend in the *dco*^{L39Q} homozygotes where haemocyte counts noticeably changed after the addition of DI-. Haemocyte counts in homozygous *dco*^{L39Q} mutants by its own decrease after the 6th

day, and then gently increase again after the 8th day. The addition of *dorsal* deletion to the *dco*^{L39Q} homozygous mutation rather increases the counts – haemocyte counts greatly increase after the 6th day, and decrease after the 8th day. Further, I counted lamellocytes per larva in the same mutants (Fig. 3.25). In both cases, there is a significant increase in lamellocyte counts. The increase is a bit slighter in case of the *dco*^{L39Q S101R} homozygotes than in the other mutant combination.

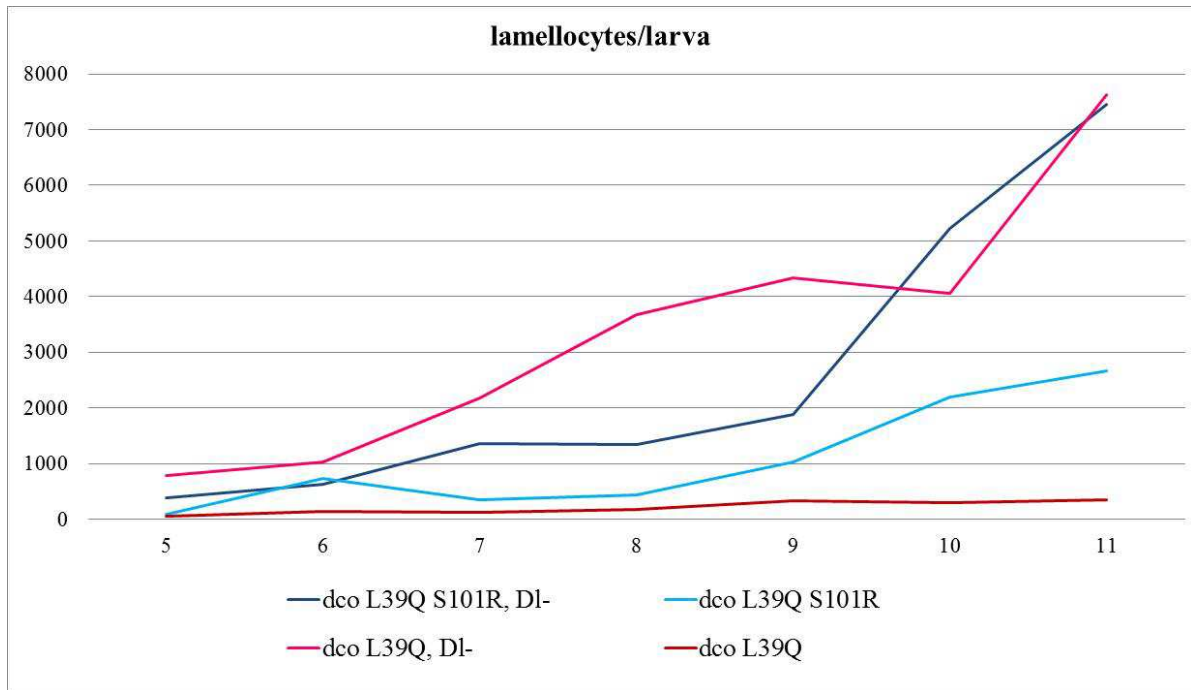


Fig.3.25: Counts of lamellocytes per larva in *dco* mutants along with the *dorsal* (DI-) deficiency. (x-axis – time in days; y-axis – number of haemocytes)

Haemocyte and lamellocyte counts in *dorsal* mutant (i.e. *dco*^{L39Q(S101R)}; DI-; *dco*^{der(or le)/+} *dco* heterozygous siblings – see methods) are indicated in figure 3.26. I did not count the same amount of larvae for this analysis as for the other analysis. I usually counted at least 30 larvae per each day for each genotypic combination. But the data in fig. 3.26 represent only 4 to 8 larvae per single day so it is just an indication of how haemocyte counts change in the *dorsal* mutant. Here we can see a similar growing trend of haemocyte counts in *dorsal* mutant when compared to homozygous *dco*^{L39Q}; DI- mutants. These results indicate that *dorsal* deficiency does not rescue *dco* mutant phenotypes. The *dorsal* deficiency has rather an additional effect on counts of both haemocytes in total and lamellocytes in *dco*^{L39Q} homozygotes. In the case of homozygous *dco*^{L39Q S101R} mutants, haemocyte counts in total do not change but there is still the additional effect on lamellocyte counts.

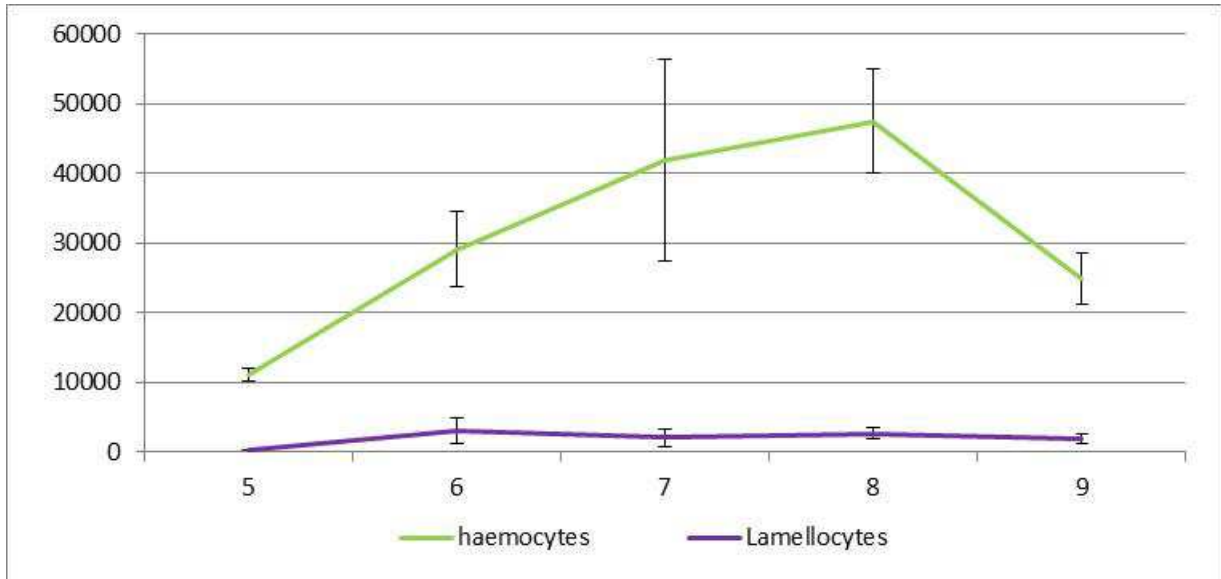


Fig. 3.26: Preliminary counts of both haemocytes in total per larva and lamellocytes per larva in *dorsal* mutants ($dco^{L39Q/S101R}; DL-$; $dco^{der(or\ le)/+}$). (Whiskers – standard deviation, x-axis – time in days; y-axis – number of haemocytes)

Morphology of haemocytes in homozygous $dco^{L39Q/S101R}; DL-$ and $dco^{L39Q}; DL-$ mutants is depicted in figure 3.27. Haemocyte morphology became noticeably changed in both cases. Haemocyte surface is not smooth and the inner space seems to be disrupted. Haemocytes and mainly lamellocytes changed their size and they also have unfolded structure. Similar effect can be seen in the lymph glands of these mutants. LGs became fragmented and they are greatly fragile. This can be the reason why these mutants have increased counts of circulating blood cells.

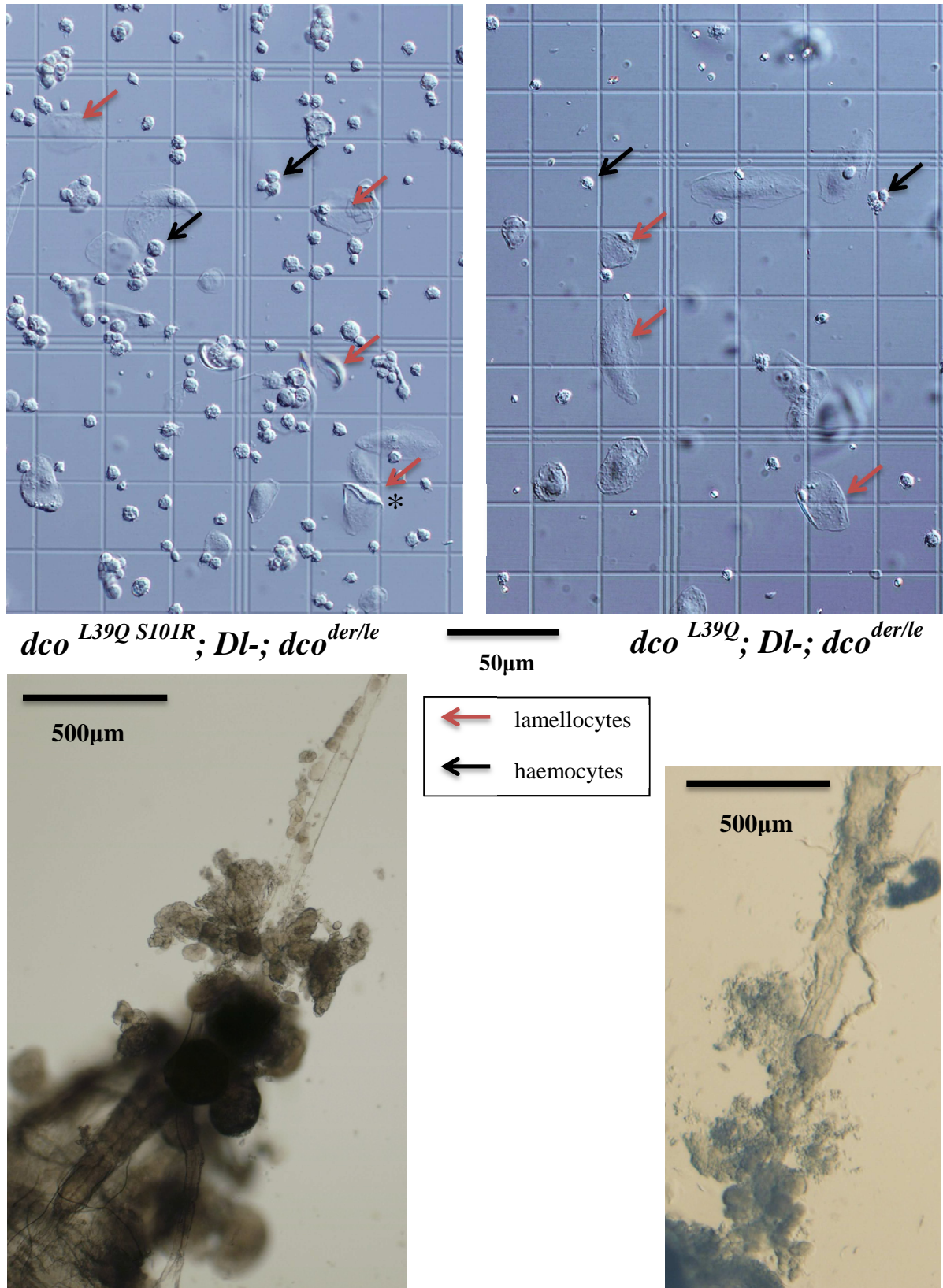


Fig. 3.27: Haemocyte appearance of *dco* mutants in combination with the *D1-*. A star * marks the typical lamellocyte how it also looks like in wild type.

3.2.2. IMAGINAL WING DISCS

Dolezal et al. (2010) showed the role of mutated Dco in Fwt/Warts signalling pathway that affects imaginal discs and also plays a role in cancer development. Thus I tested if removal of Dorsal protein, i.e. downregulation of the Toll signalling pathway, could rescue the phenotype observed in imaginal discs. All the imaginal wing disc phenotypes are summarized in figure 3.28. It was already mentioned above that the *dco*^{L39Q S101R} and *dco*^{L39Q} mutant alleles have a slight effect on imaginal wing disc size even in the heterozygous *dco*^{der/+} background (Fig. 3.13), but the morphology remains unchanged. Imaginal wing discs in the *dco*^{L39Q S101R} homozygotes cannot reach the size of heterozygous control even after 11 days (Fig. 3.28 upper right corner). The morphology is greatly changed and discs are often strongly fragile, so they easily disintegrate or even completely fall apart (arrow). Imaginal wing discs in the *dco*^{L39Q} homozygous larvae are greatly overgrown and their morphology is noticeably changed too. Also the *dco*³ mutant imaginal wing discs are markedly overgrown, but their morphology rather resembles the WT wing discs.

Switching off the Toll signalling pathway with the removal of Dorsal protein does not rescue imaginal discs in the *dco* mutants. The change in solidity of homozygous *dco*^{L39Q}; *Dl*- mutant wing discs is presented in figure 3.29. They became fragile, which was never seen in the *dco*^{L39Q} homozygotes. Wing disc conditions do not change for homozygous *dco*^{L39Q S101R}; *Dl*- mutants, because the fragility can be found also in *dco*^{L39Q S101R} homozygotes alone. Therefore, Dorsal is not a key player driving these phenotypes in *dco* mutants.

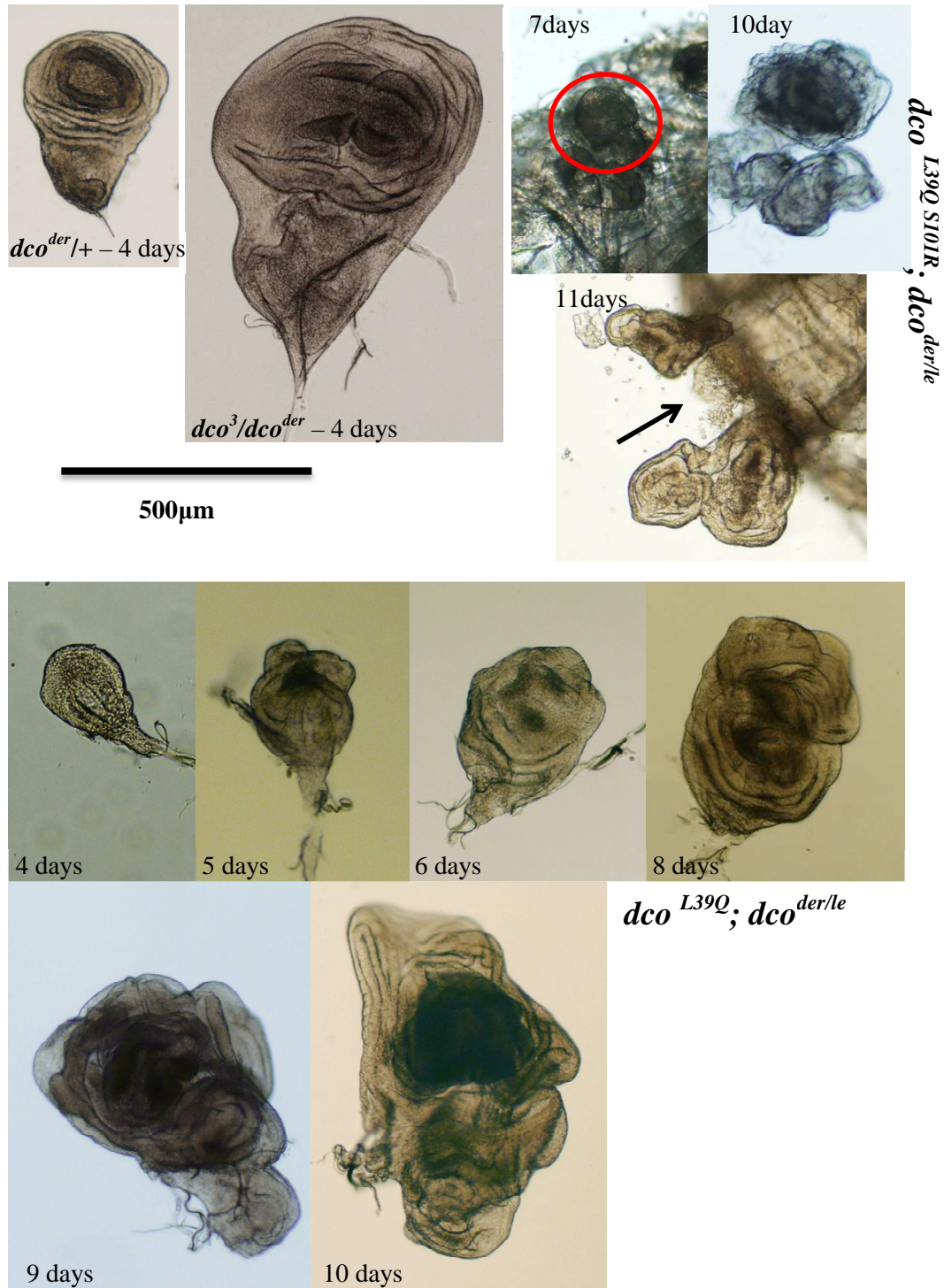


Fig. 3.28: Morphology and size of imaginal wing discs in the *dco* mutants.

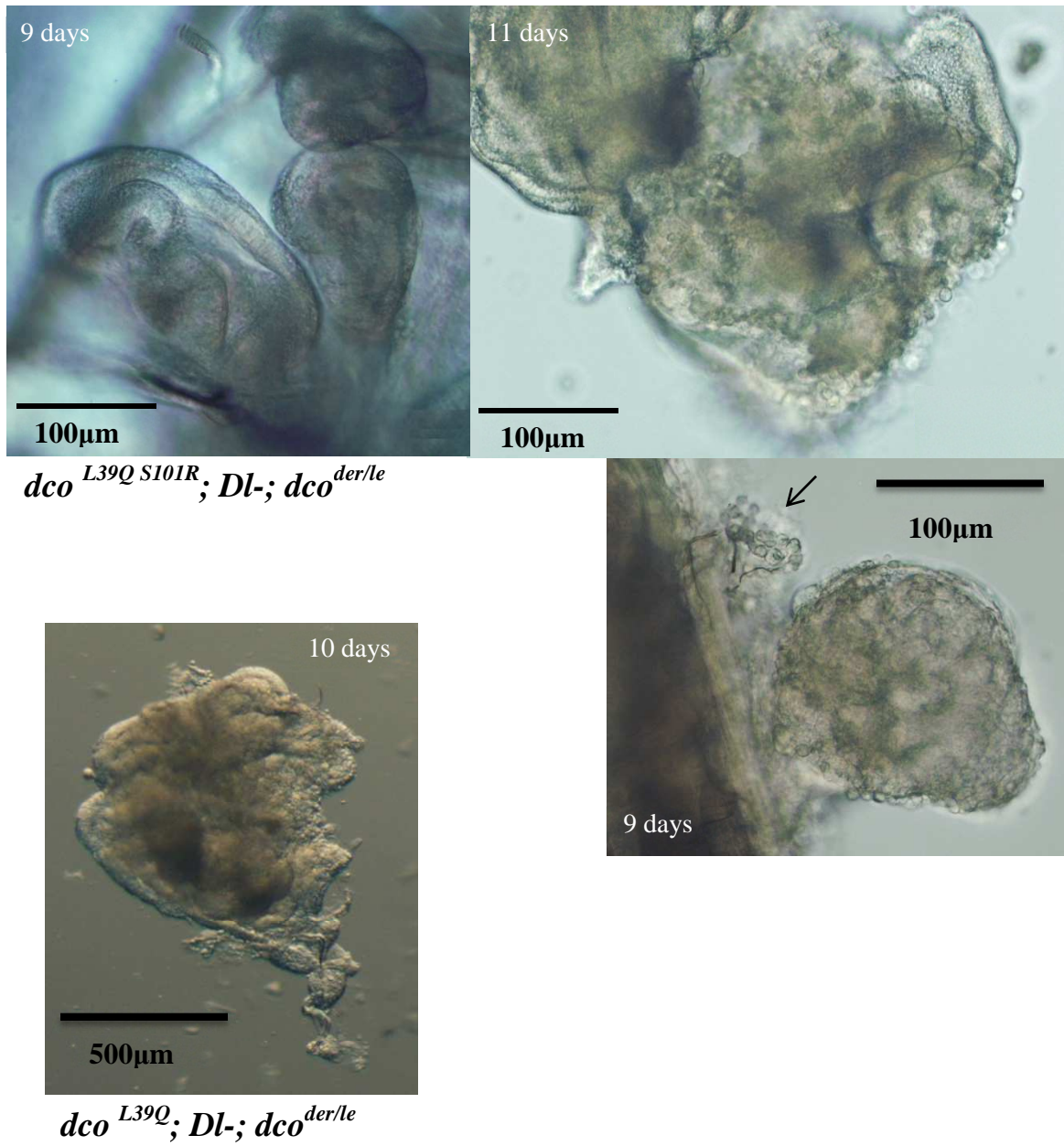


Fig. 3.29: Effect of genetic combination of *dco* mutation and absence of Dorsal on imaginal wing discs.

3.2.3. MELANOTIC CAPSULES FORMING

CRYSTAL CELLS

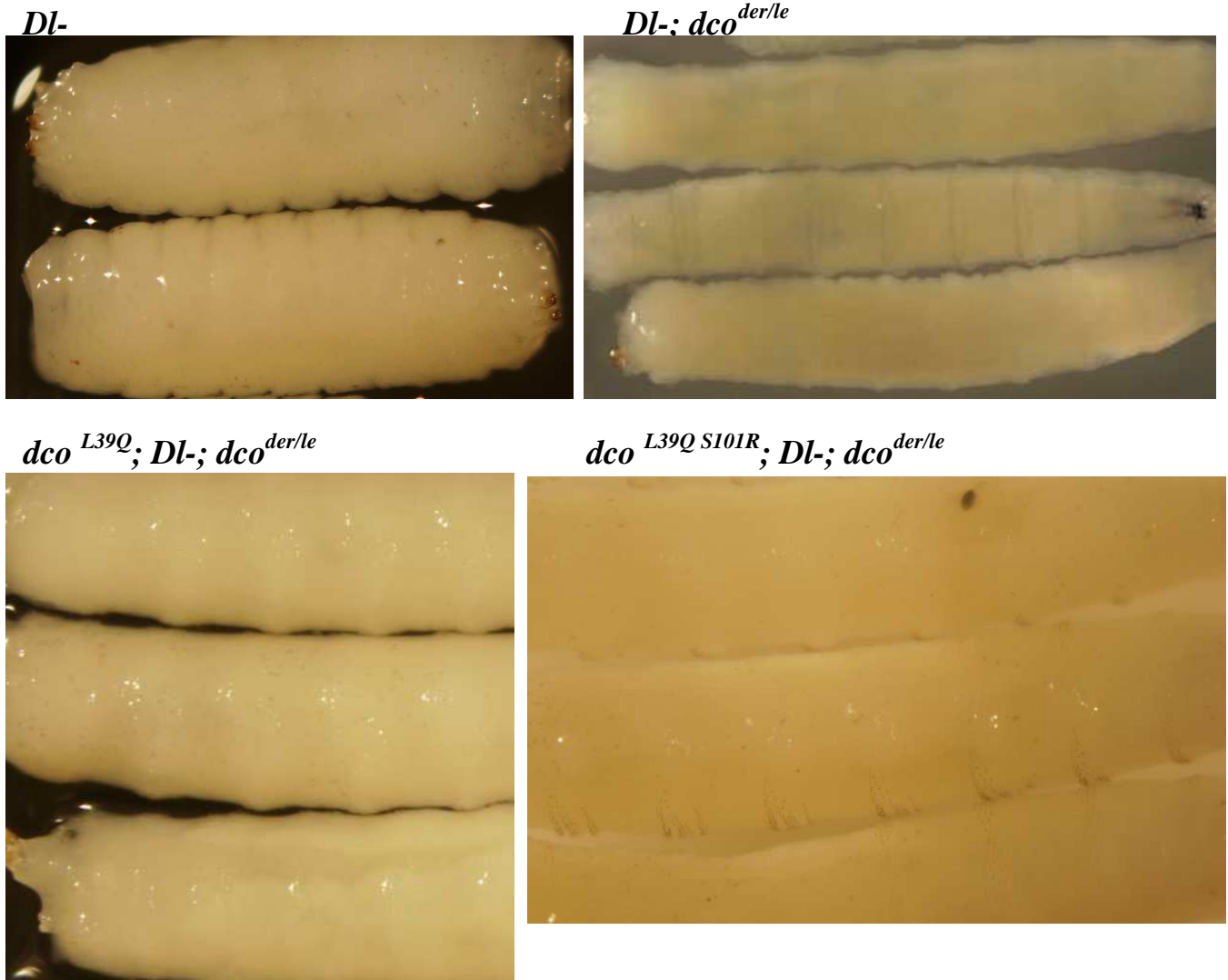


Fig. 3.30: Presence of crystal cells in *dco* and *dorsal* double mutants.

Further, I tested the effect of *dorsal* deficiency on crystal cell counts and melanotic capsule formation in *dco* mutants (Fig. 3.30). Noticeably, the *DL-; dco null* mutants do not have any crystal cells at all, and they also do not form any melanotic capsules, whereas the single *dorsal* mutants contain both crystal cells and melanotic capsules in their larva bodies. After comparison of crystal cell amount in *dco* mutants (Fig. 3.22) and *dorsal dco* double mutants (Fig. 3.30), we can conclude that the quantity of crystal cells increased after the

addition of *dorsal* mutation in both $dco^{L39Q S101R}; Dl-$ and $dco^{L39Q}; Dl-$ homozygous mutants. In these mutants, the ratio of larvae with or without melanotic capsules also slightly changed. Seven out of ten homozygous $dco^{L39Q S101R}; Dl-$ mutant larvae do form melanotic capsules. The ratio (1 out of 10 larvae forms melanotic capsules) in homozygous $dco^{L39Q}; Dl-$ mutants does not differ from the ratio of dco^{L39Q} homozygous mutant alone. In *dorsal* mutants, the ratio of larvae forming melanotic capsules to larvae without them is 8 to 2. All the ratios were counted at the 10th day, except for the *dorsal* mutants that were counted at the 9th day.

As I already mentioned above, I had some difficulties to get the *dorsal Dif* and *dco* triple mutants. But I noticed that heterozygous constitution of *dorsal Dif* mutation is sufficient to decrease the incidence of melanotic capsules in the $dco^{L39Q S101R}$ homozygous mutants (Fig. 3.21 right compared to fig. 3.31).



Fig. 3.31: Melanotic capsules incidence in $dco^{L39Q S101R}; Dl- Dif/+; dco^{der/le}$ mutants at the 10th day AEL.

3.3. MARKERS FOR HAEMATOPOIESIS

For further characterisation of *dco* mutants, I used the UAS-GFP/GAL4 system to see the expression of different markers in LGs. First, I used hemolymph GAL4 driver for mapping fully differentiated mature larval plasmatocytes, normally present in the cortical zone of the LG. Hemolymph is not expressed in lamellocytes (Goto et al., 2003). I used the same GAL4 driver for haemocyte counting (chapter 3.1.2). For testing JAK/STAT signalling pathway, I used the *domeless* GAL4 driver. Domeless is expressed in immature haemocytes, called prohaemocytes, but not in the PSC or in lamellocytes. This means that Domeless is expressed in the medullary zone of the LG. *Domeless* encodes a transmembrane receptor molecule known to mediate the activation of the JAK/STAT pathway upon binding of the ligand Unpaired (Jung et al., 2005; Brown et al., 2001). For detection of PSC in the LGs, I used *collier* GAL4 driver. The PSC plays a crucial role in differentiation of lamellocytes upon the immune challenge (Crozatier et al., 1996, 2004). JAK/STAT activity is required to prevent premature differentiation of multipotent prohaemocytes into plasmatocytes or crystal cells (Crozatier and Meister, 2007). PSC cells act in a non-autonomous manner to maintain the JAK/STAT signalling activity in prohaemocytes, resulting in maintenance of the multipotent cell character (Krzemień et al., 2007; Mandal et al., 2007).

3.3.1. HEMOLECTIN MARKER

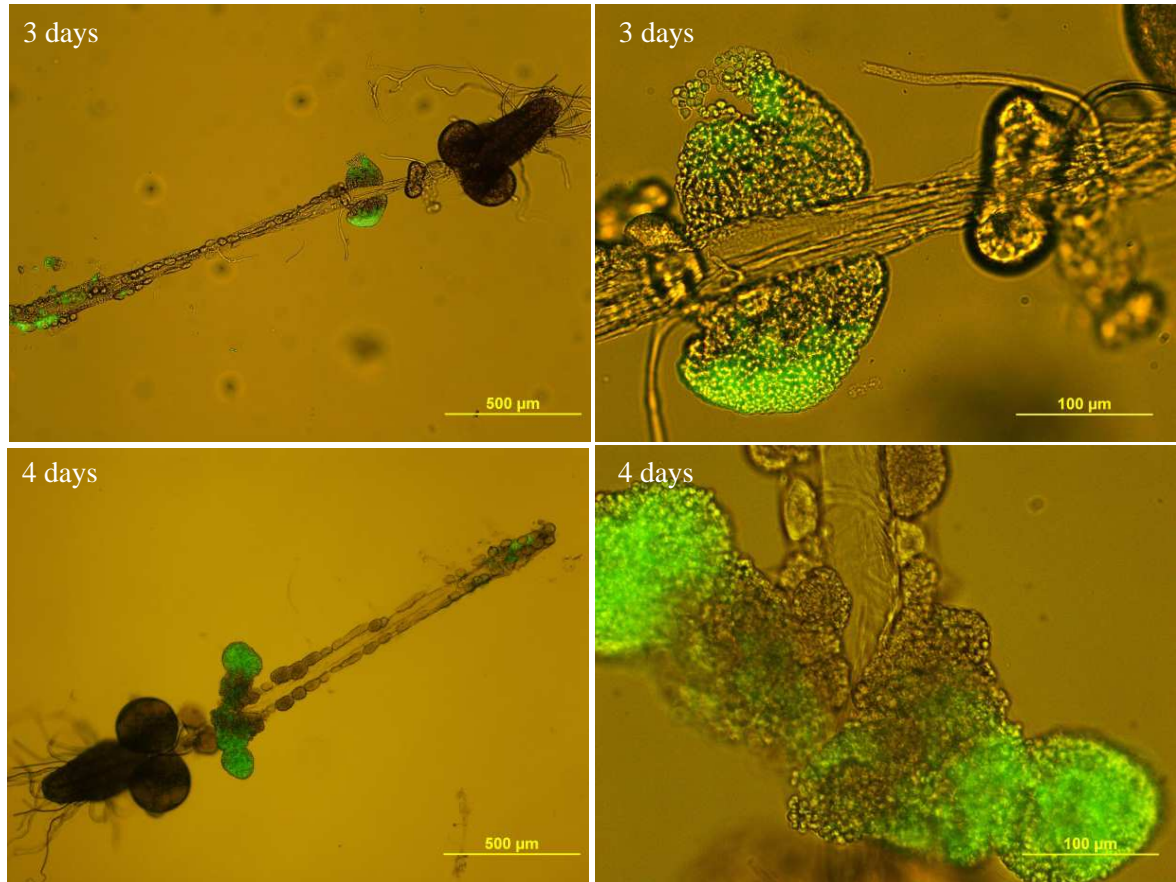
DCO^{DER/+} (HETEROZYGOUS CONTROL)

Fig. 3.32: A distribution of the Hml+ blood cells in the LG of the heterozygous control.

The normal distribution of mature plasmatocytes (haemocytes expressing hemolectin) in the LGs is depicted in figure 3.32. These mature haemocytes are present in the outer part of the primary lobes, which corresponds to the cortical zone (CZ). Similarly to heterozygous control, the localisation of the mature plasmatocytes in *dco^{L39Q S101R}* heterozygous mutants (Fig. 3.34) and *dco^{L39Q}* heterozygous mutants (Fig. 3.36) corresponds to the CZ, though there is a slower development of the primary lobes in *dco^{L39Q S101R}* heterozygotes if compared to the heterozygous control LG. Only sporadic presence of the mature blood cells can be seen in the *dco null* mutant LGs (Fig. 3.33) and they are not found exclusively in the CZ. When primary lobes fall apart (right bottom in fig. 3.33) no other Hml+ plasmatocytes appear, and just a few of them are still present in the rest of the LG.

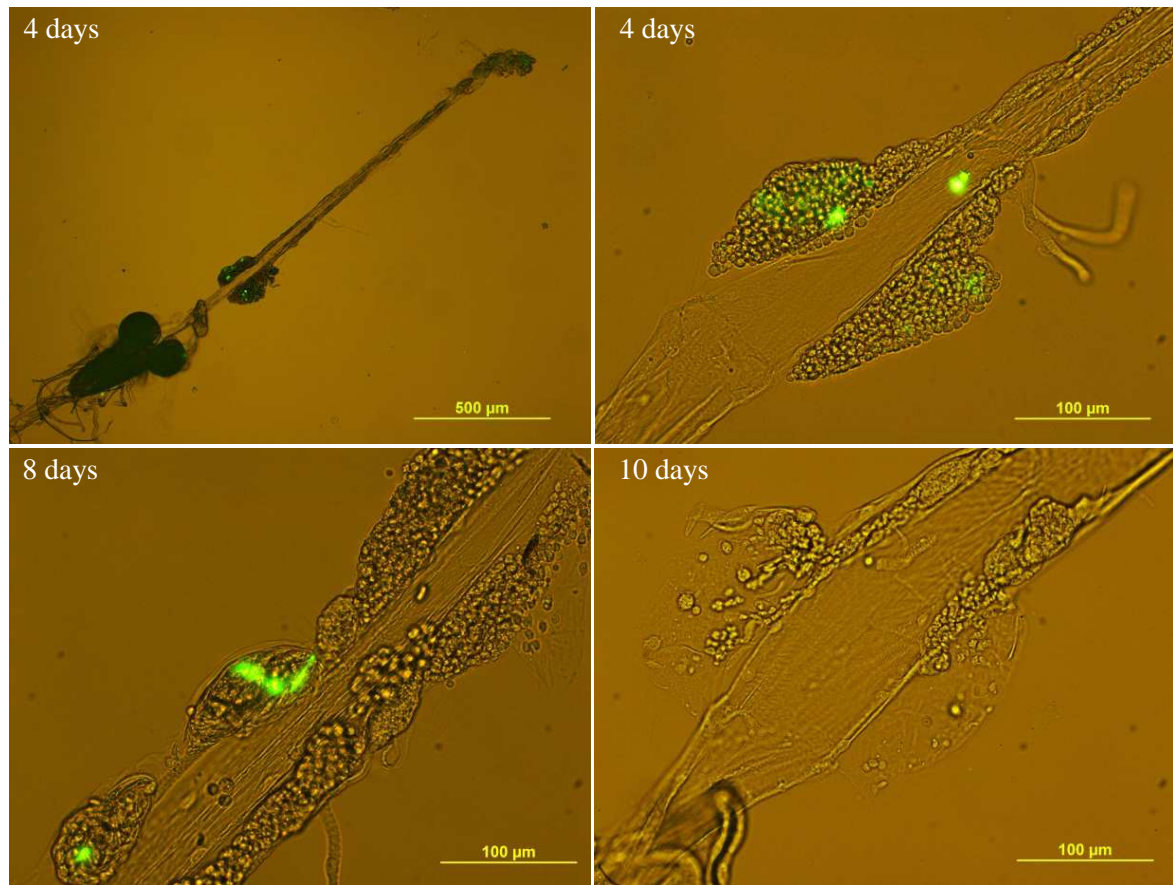
DCO NULL

Fig. 3.33: Distribution of the mature plasmatocytes in the *dco null* mutant LGs.

DCO^{L39Q S101R}

HETEROZYGOTES

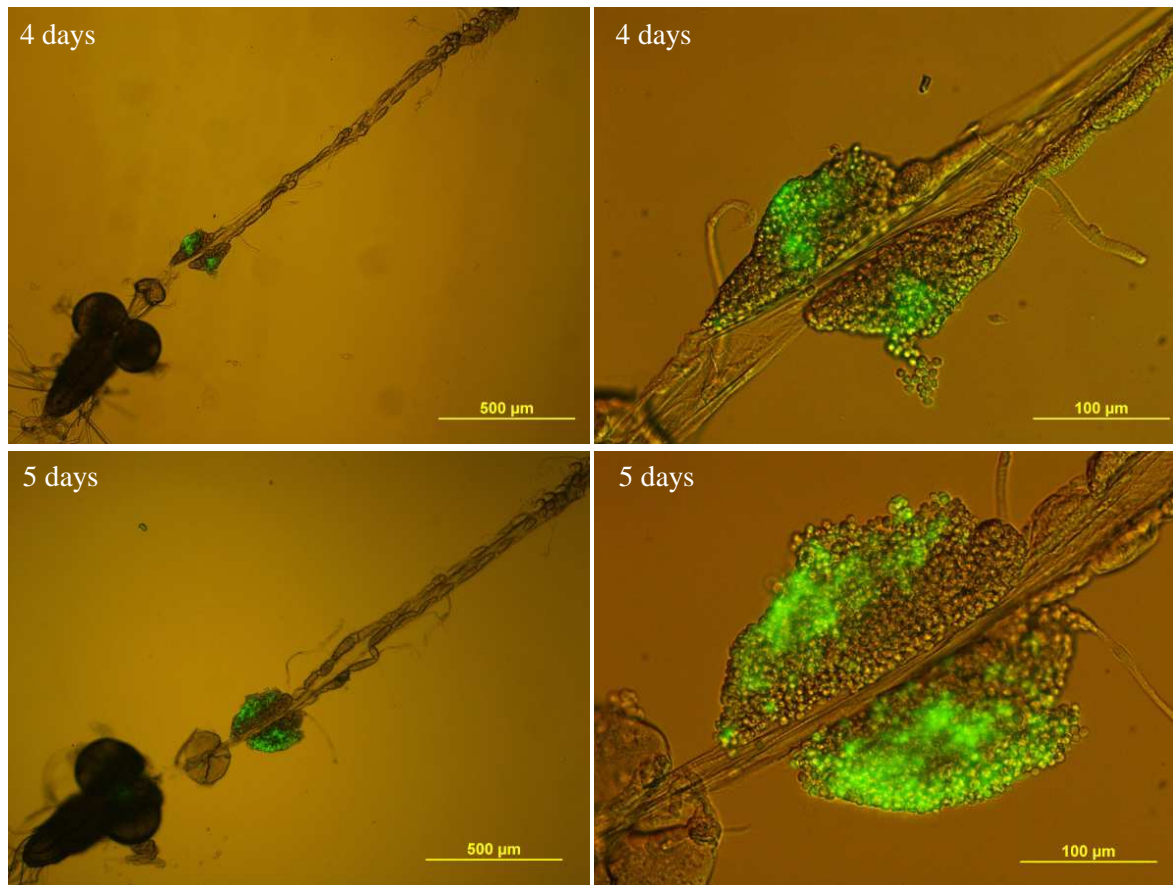
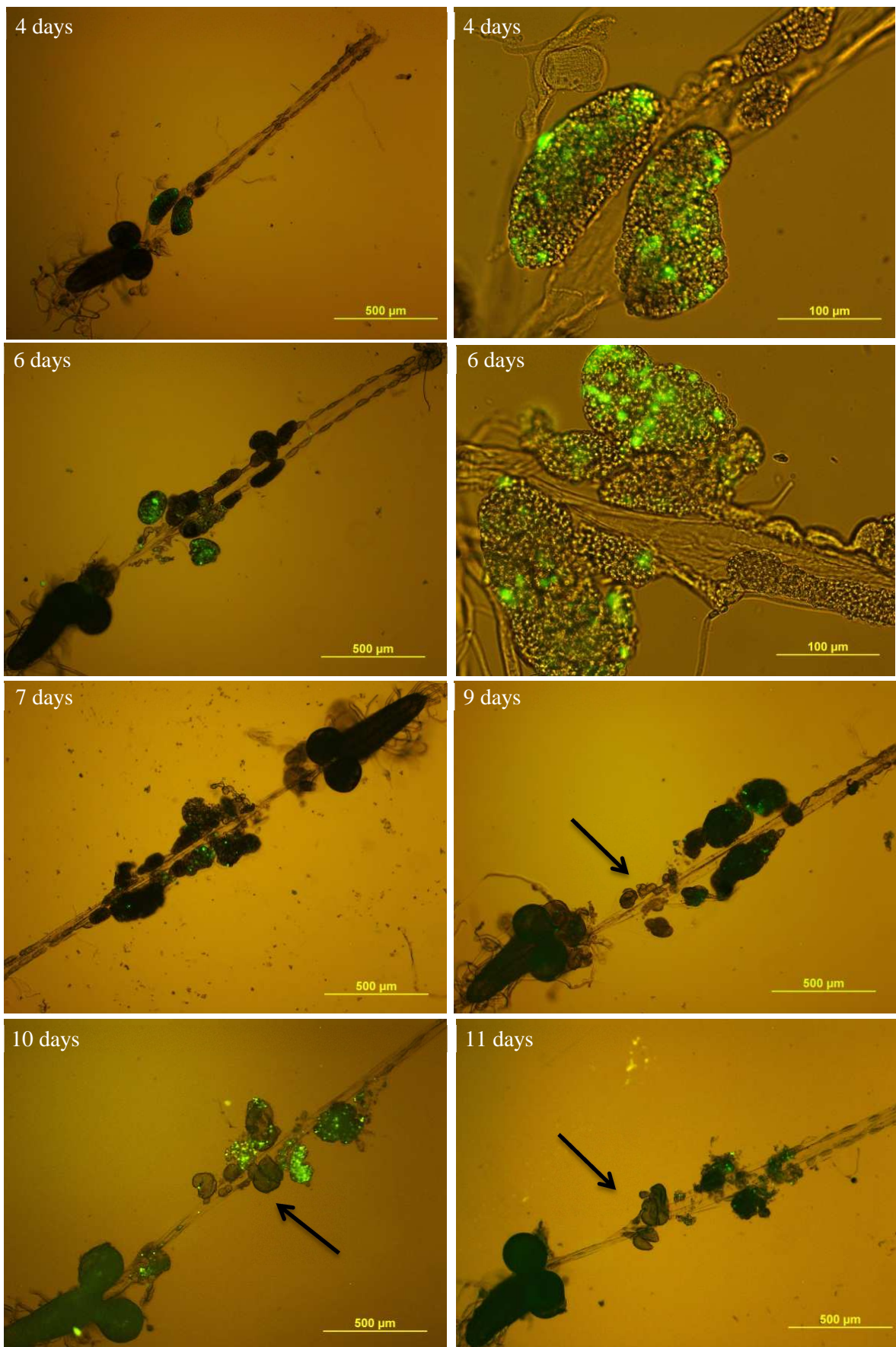


Fig. 3.34: Distribution of mature plasmatocytes in the LG of *dco*^{L39Q S101R} heterozygotes.

Fig.3.35 (next page): Distribution of the mature plasmatocytes in the LG of homozygous *dco*^{L39Q S101R} mutants. In later stages, 9-11 days, the first lobes leave just the rest of the envelope of the primary lobes (←).

HOMOZYGOTES



DCO^{L39Q}

HETEROZYGOTES

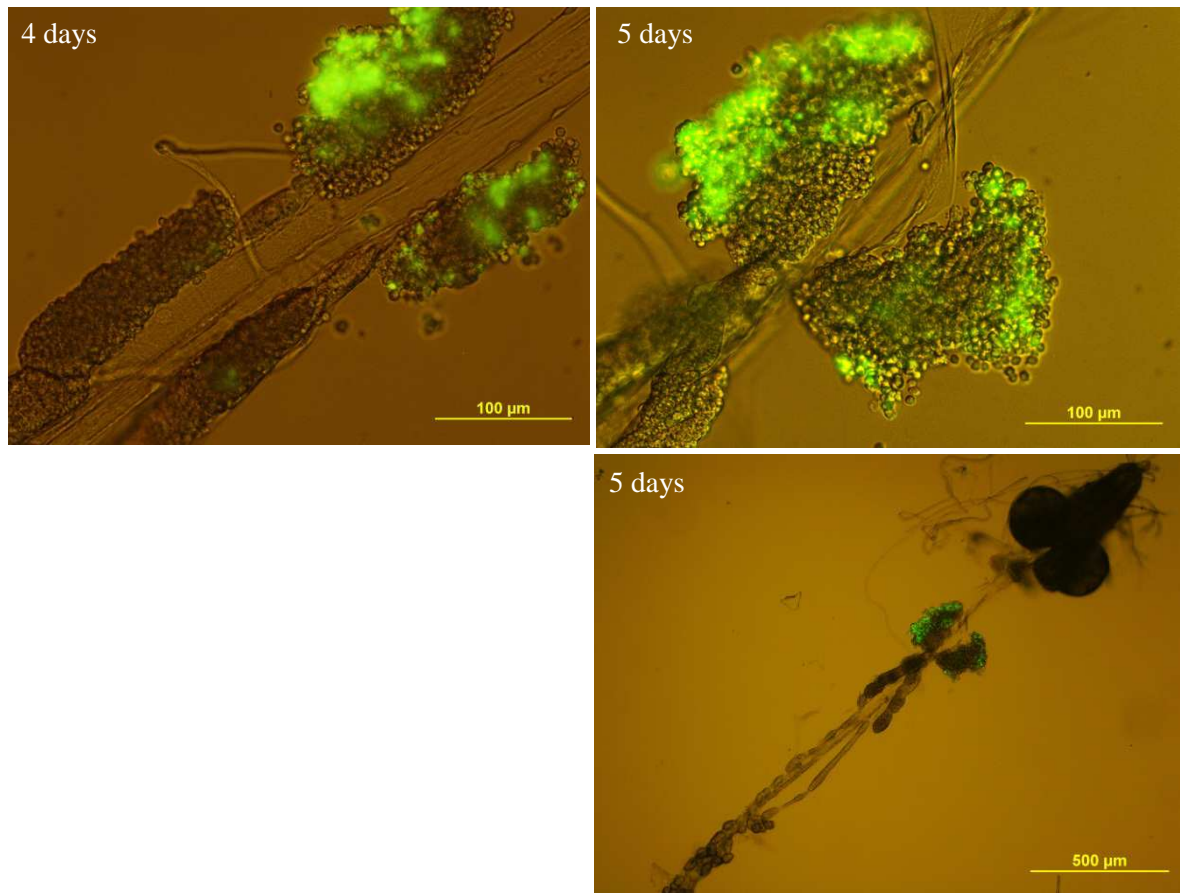


Fig. 3.36: Distribution of mature plasmatocytes in the LG of heterozygous *dco^{L39Q}* mutants.

In *dco^{L39Q S101R}* homozygotes (Fig. 3.35), the mature plasmatocytes expressing hemolectin are more or less evenly distributed throughout the primary lobes without any specific pattern corresponding to the CZ. The mature plasmatocytes are also in the secondary lobes later on the development. The first lobes disintegrate as the haemocytes proceed from the lymph gland into hemolymph. In the *dco^{L39Q}* homozygotes (Fig. 3.37), the mature plasmatocytes are at first localized in the outer part of the primary lobes, which closely corresponds to the CZ. The mature plasmatocytes spread out through when other lobes grow. Similarly to the *dco^{L39Q S101R}* homozygotes, the first lobes disintegrate as the haemocytes proceed from the lymph gland into hemolymph to circulate through the body. The *dco³* mutant LG is depicted in figure 3.38. Here, mature haemocytes are spread out all over the lymph gland in all lobes without any specific localisation. Moreover, they are present also in all secondary lobes even at the 4th day, which we cannot see in heterozygous control (Fig. 3.32, bottom).

HOMOZYGOTE

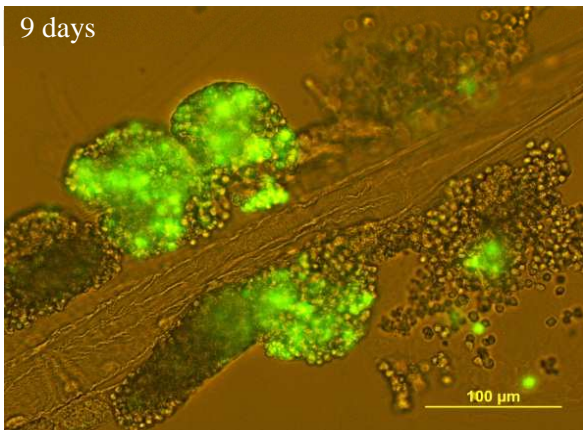
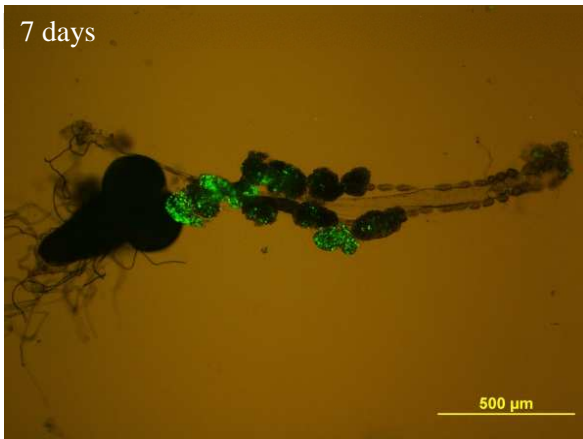
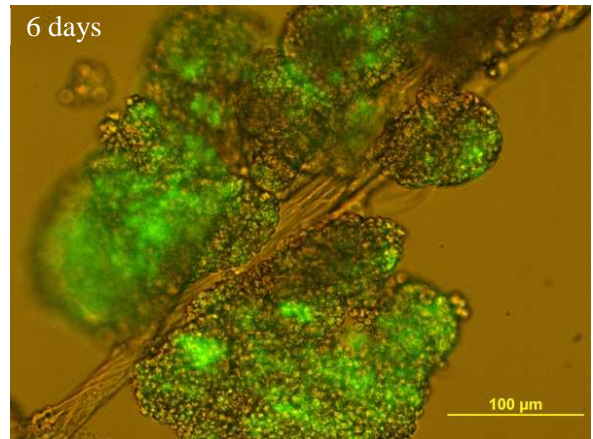


Fig.3.37 (previous page): Distribution of the mature plasmatocytes in the homozygous *dco*^{L39Q} mutant LG. (the envelope of the primary lobes ←→)

*DCO*³

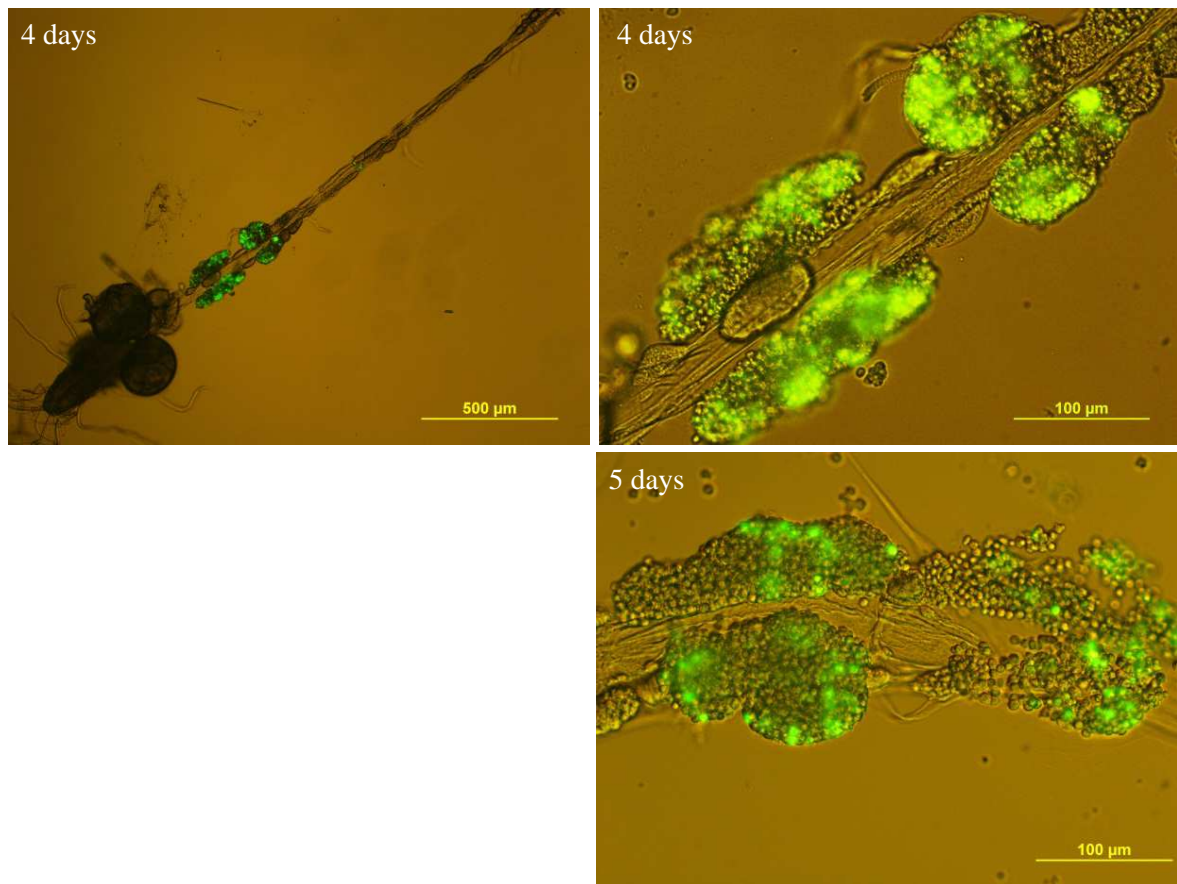


Fig. 3.38: Distribution of the mature haemocytes in the *dco*³ mutant LG.

3.3.2. COLLIER EXPRESSION

WT

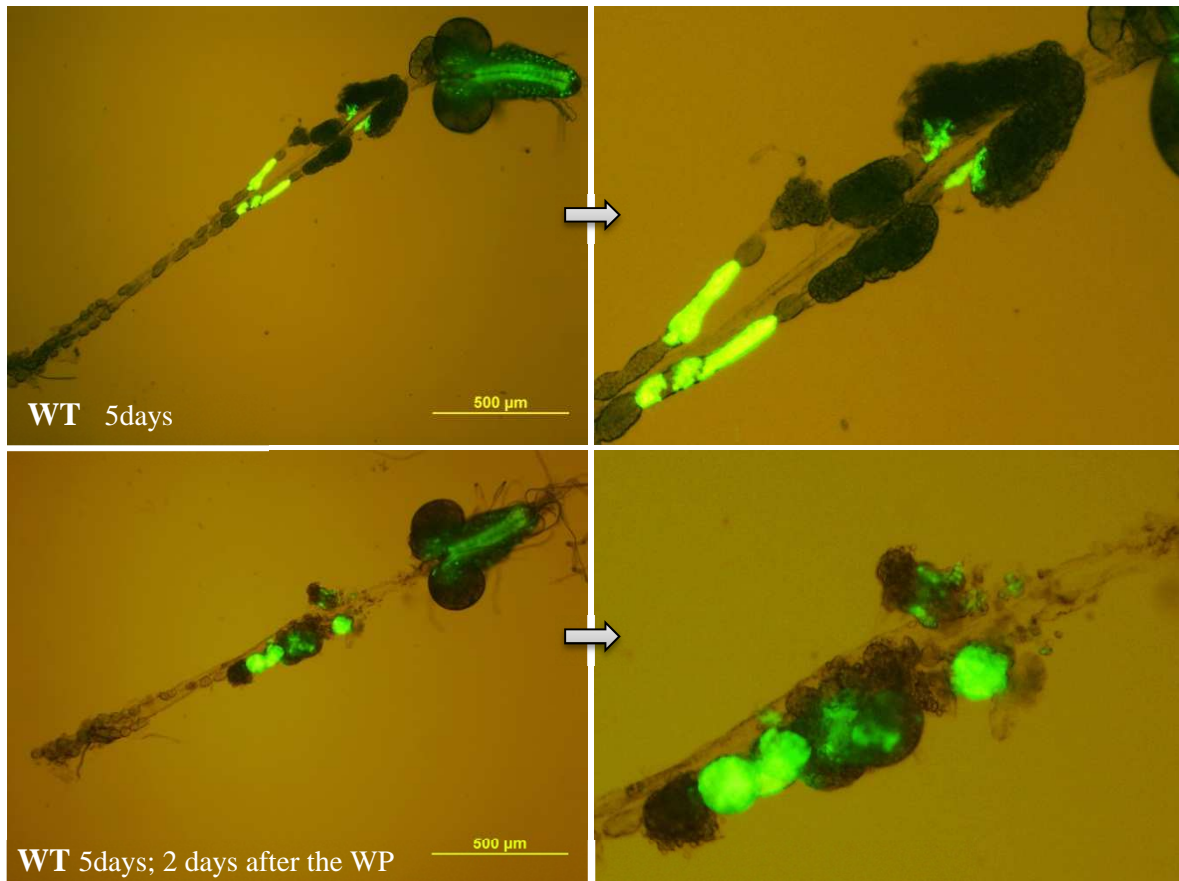


Fig. 3.40: Localisation of the Collier expression in the WT control LG and in the WT after the wasp parasitization (WP) at the 5th day.

The expression of Collier in wild type background is in figure 3.40. Collier is expressed in the PSC. In the infected larvae, the LG lobes start growing and Collier expression spreads out through the lymph gland. Primary lobes disintegrate as haemocytes proceed into hemolymph. Collier expression in the *dco null* mutants is alike the wild type expression, i.e. posteriorly in the primary lobes (Fig. 3.41). Heterozygous *dco*^{L39Q S101R} (Fig. 3.42) and *dco*^{L39Q} (Fig. 3.44) mutants have also quite similar Collier expression pattern to the WT control. Collier expression in the homozygous *dco*^{L39Q S101R} (Fig. 3.43) and *dco*^{L39Q} (Fig. 3.45) mutants spreads out across the lobes and is rather similar to the WT LGs after the wasp parasitization.

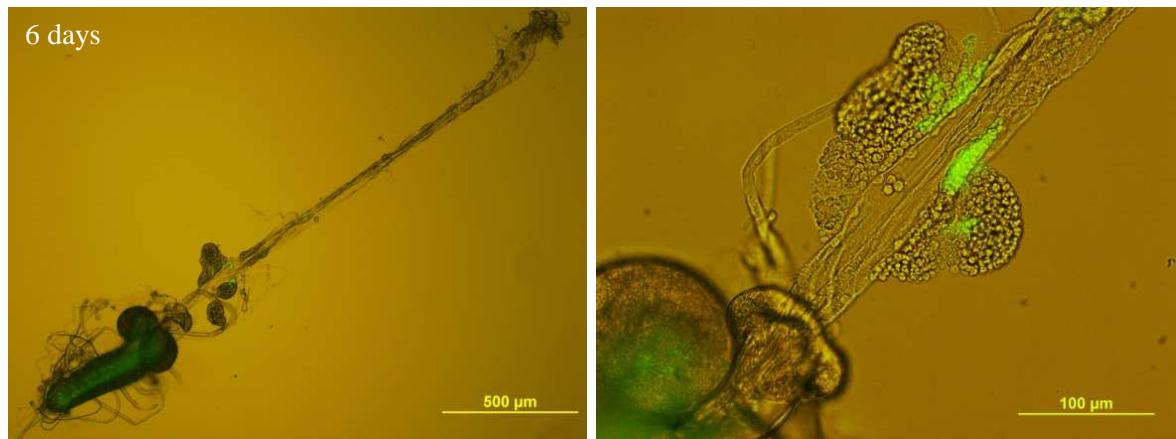
DCO NULL

Fig. 3.41: Collier expression in the *dco null* mutants.

DCO ^{*L39Q_S101R*}

HETEROZYGOTES

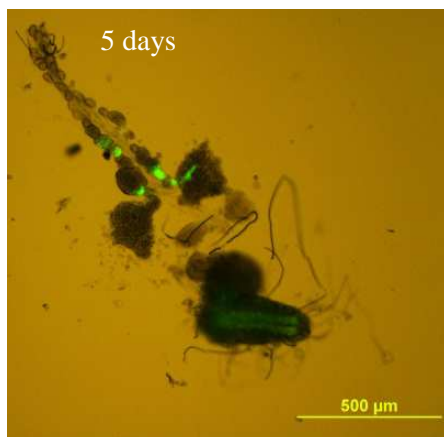


Fig. 3.42: Localisation of Collier expression in the *dco*^{*L39Q_S101R*} heterozygotes.

HOMOZYGOTES



Fig. 3.43: Collier expression in the *dco*^{L39Q S101R} homozygous mutant lymph glands.

DCO^{L39Q}

HETEZYGOTES

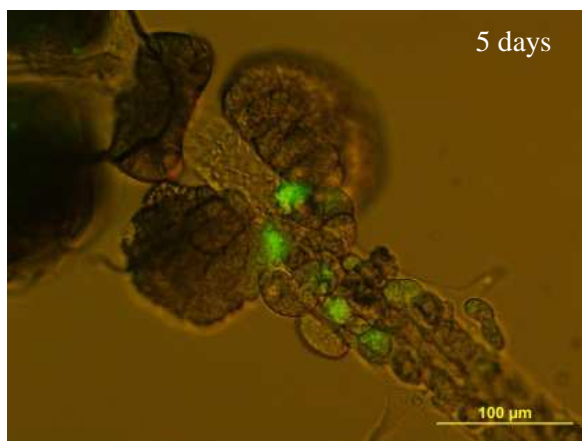


Fig. 3.44: Localisation of Collier expression in the *dco*^{L39Q} heterozygotes.

HOMOZYGOTES

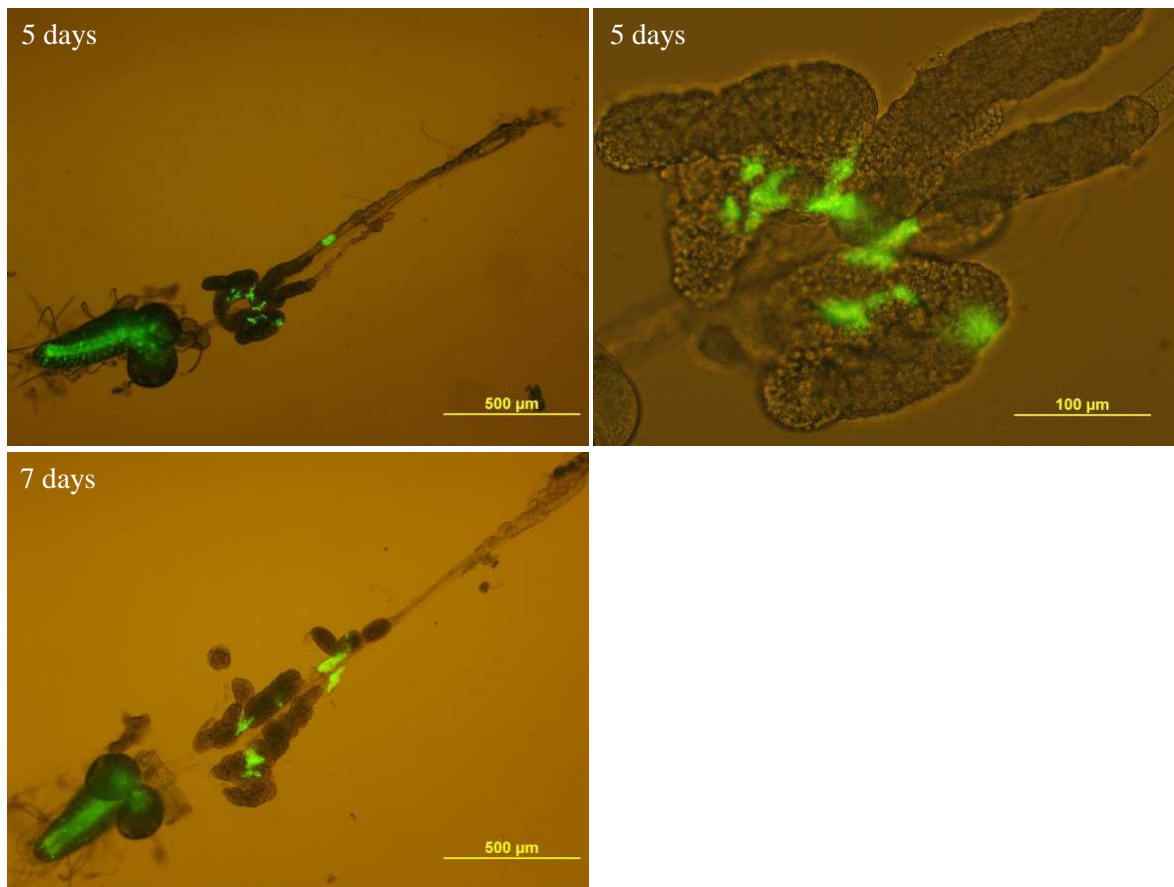


Fig. 3.45: Collier expression in the *dco*^{L390} homozygous mutant lymph glands.

3.3.3. DOMELESS EXPRESSION

WT (CONTROL)

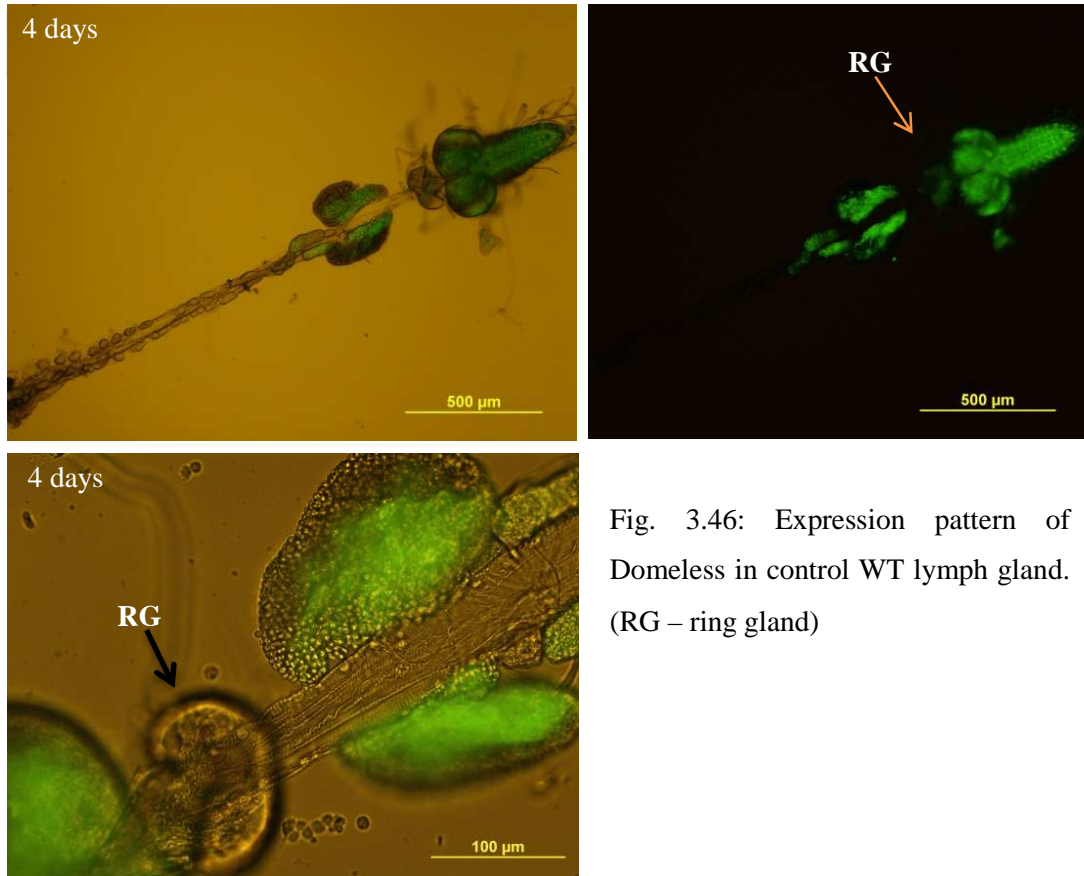


Fig. 3.46: Expression pattern of Domeless in control WT lymph gland. (RG – ring gland)

The illustrative pattern of Domeless expression in the WT LG is in figure 3.46. Domeless is expressed in the inner part of lobes, which corresponds to the medullary zone (MZ). Domeless is also present in secondary lobes and brain. Slight or no expression is detected in the ring gland (RG). Domeless expression in the LG corresponds to the localisation of immature plasmacytes. This Domeless expression pattern is also present in both *dco*^{L39Q S101R} (Fig. 3.48) and *dco*^{L39Q} (Fig. 3.50) heterozygous mutants. However, the domeless expression pattern is totally changed in *dco*^{L39Q S101R} and *dco*^{L39Q} homozygotes and also in *dco null* mutants. In all of these mutants, the Domeless is steadily expressed from late 2nd instar through the 3rd instar in dorsal vessel and greatly in the ring gland. In *dco null* and *dco*^{L39Q S101R} homozygous mutants, Domeless is expressed in the whole primary lobes at the early 3rd instar and this expression disappears from the lobes before the 6th day. Domeless expression is restricted to the inner part of primary lobes, close to the dorsal vessel

in the early 3rd instar in *dco*^{L39Q} homozygous mutants. Later on, the expression spreads throughout the lobes and then disappears around the 6th day similarly to the other mutants. A mix of these patterns is in the *dco*³ mutants (Fig. 3.52). In this particular mutant, Domeless expression is very weak in the RG in the late 2nd/early 3rd instar and expression in primary lobes is alike WT. At the 5th day, there is already no Domeless expression in the RG and it spreads out through the all LG lobes. In the dorsal vessel, there is no or very weak Domeless expression through whole larva life.

DCO NULL (DCO^{DER/LE})

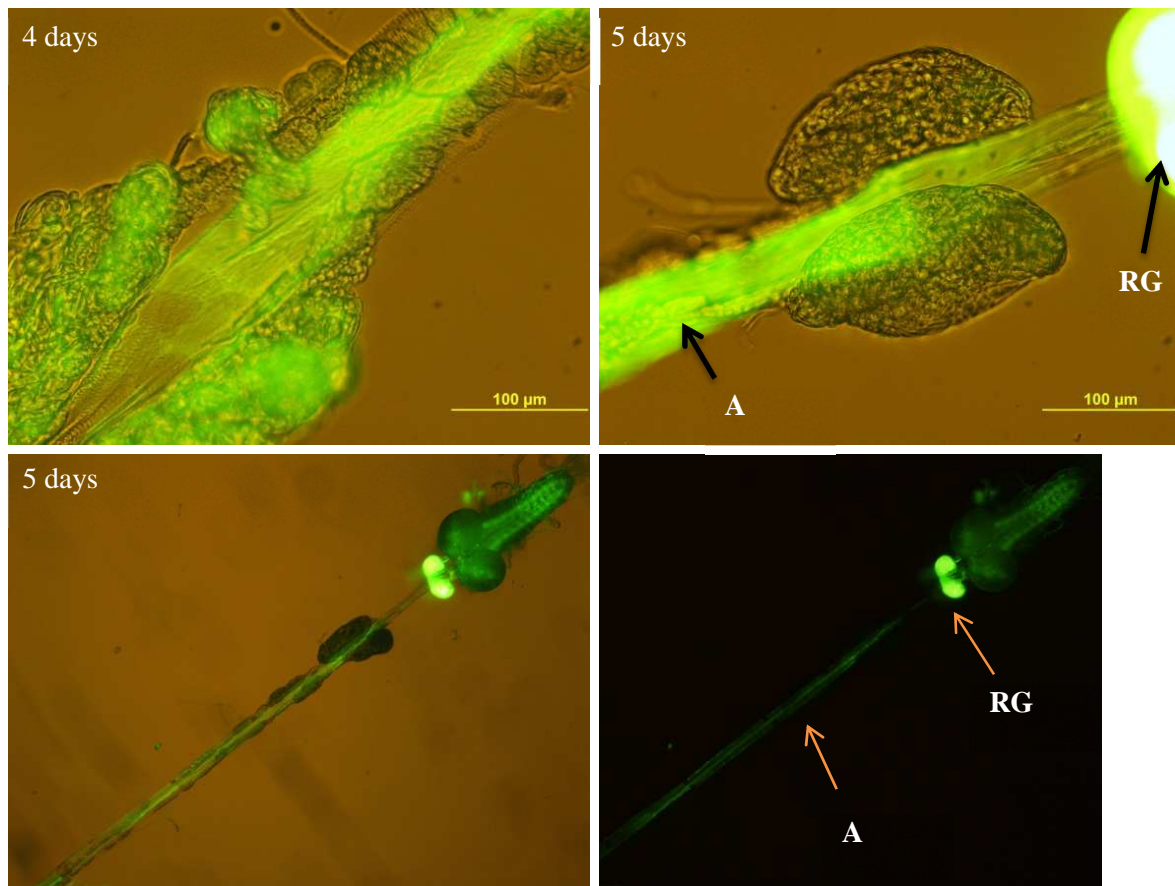


Fig. 3.47: Expression pattern of Domeless in the *dco null* mutants. (RG – ring gland; A – aorta/dorsal vessel)

DCO ^{L39Q S101R}

HETEROZYGOTES

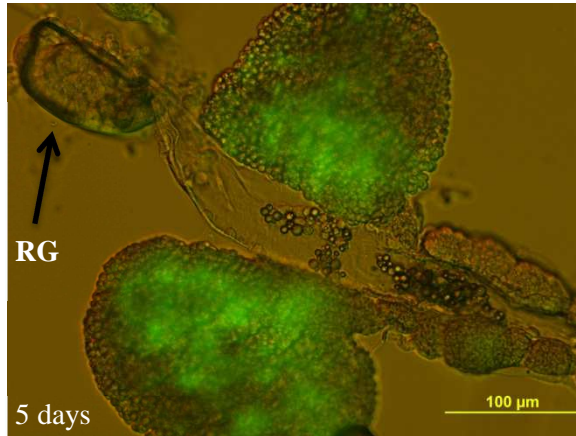


Fig. 3.48: Domeless expression in *dco* ^{L39Q S101R} heterozygous mutants.

HOMOZYGOTES

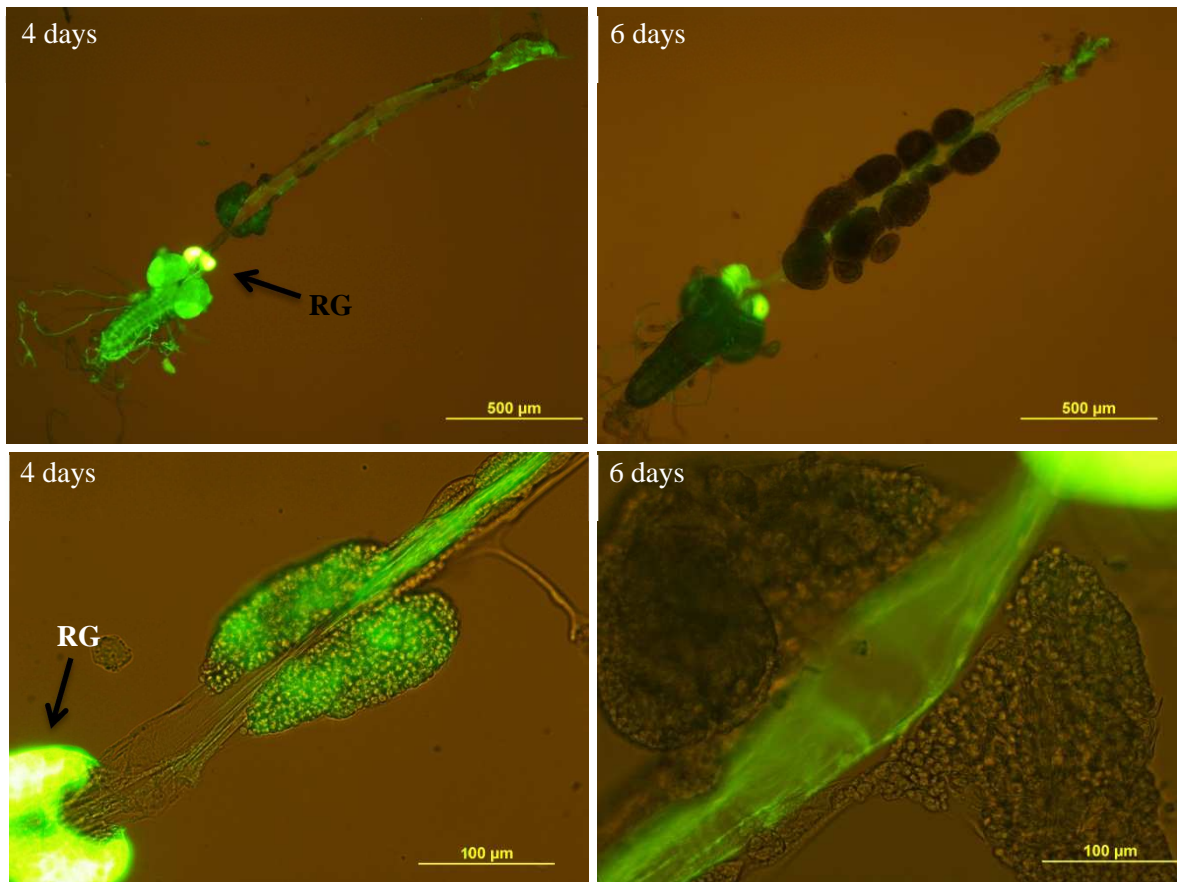


Fig. 3.49: Expression pattern of Domeless in *dco* ^{L39Q S101R} homozygous mutants.

DCO^{L39Q}

HETEROZYGOTES

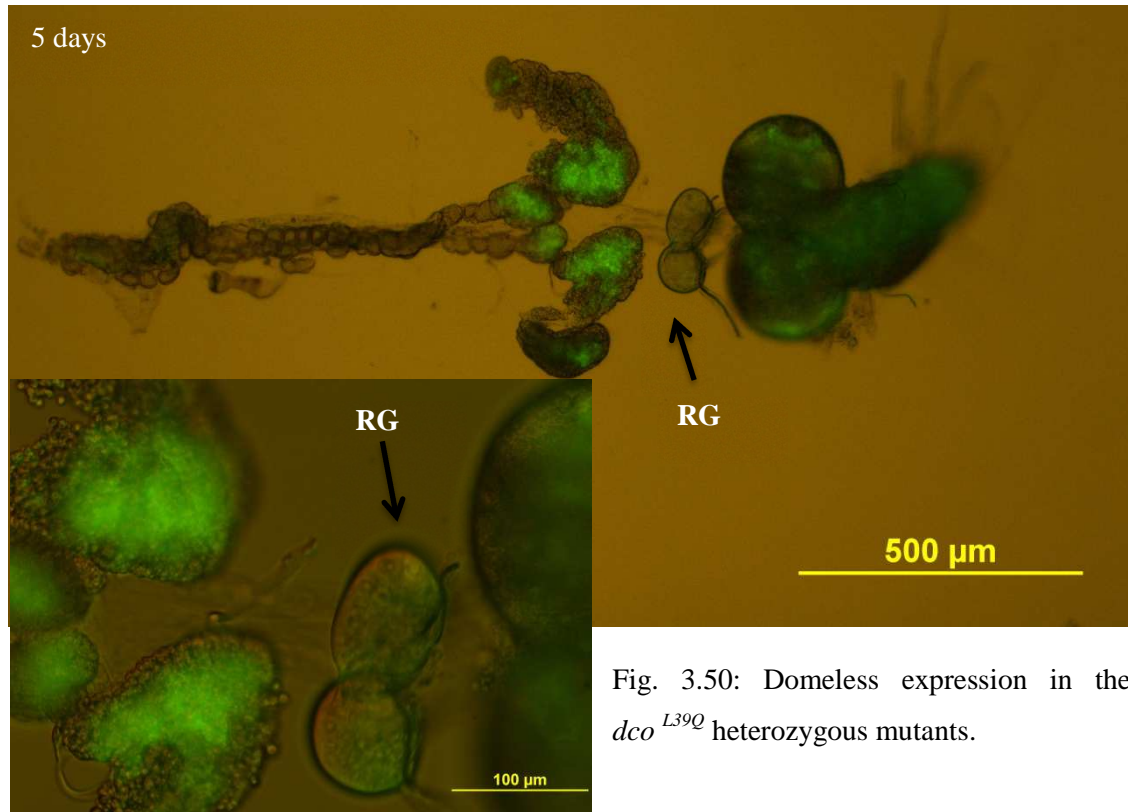


Fig. 3.50: Domeless expression in the *dco*^{L39Q} heterozygous mutants.

HOMOZYGOTES

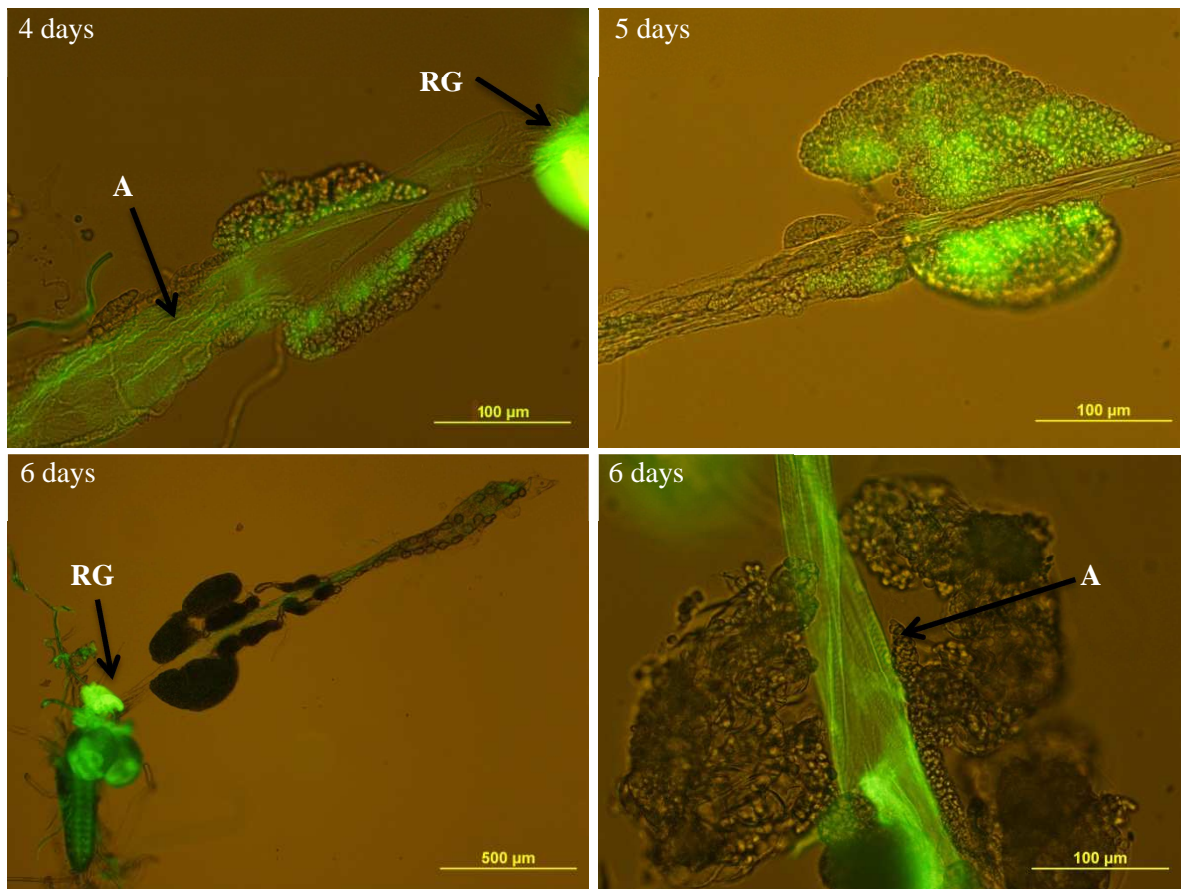


Fig. 3.51: Expression pattern of Domeless in *dco*^{L39Q} homozygous mutants.

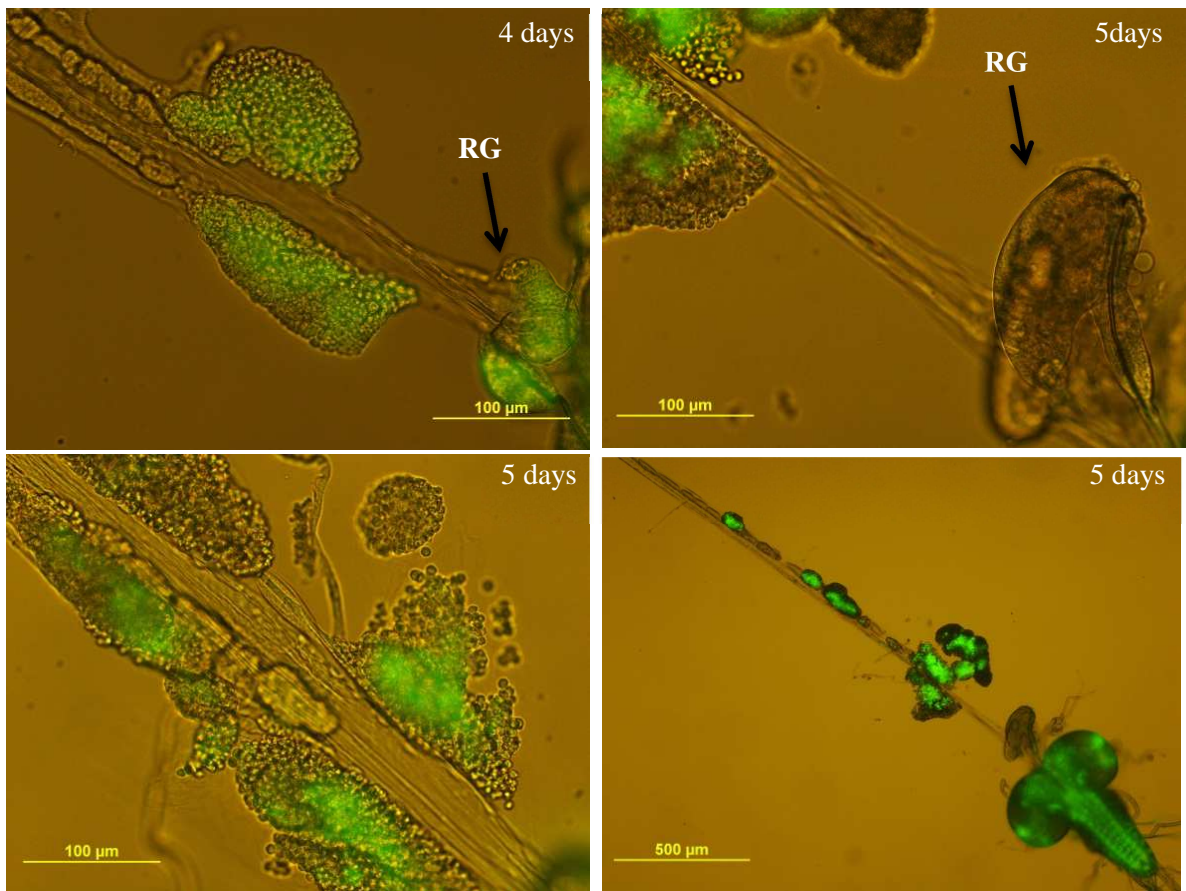
DCO³

Fig. 3.52: Domeless expression in the *dco³* mutants.

WT AFTER THE WASP PARASITIZATION

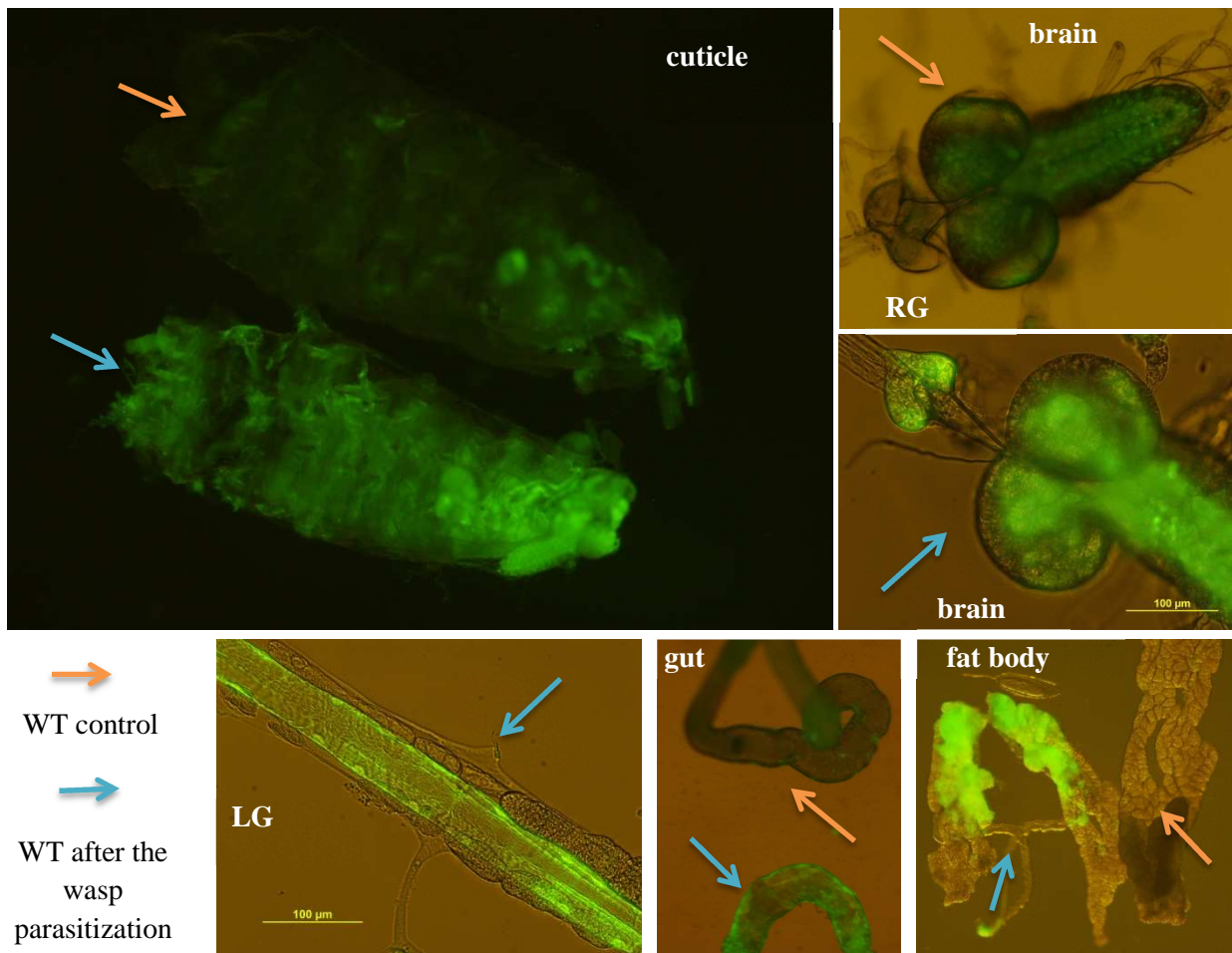


Fig. 3.53: Comparison of Domeless expression in the WT larvae (5 days) and WT larva 2 days after wasp parasitization (5 days in total).

I tested if Domeless expression in the WT changes after the wasp parasitization. As shown in figure 3.53, the Dome expression strikingly increased in cuticle, brain, fat body, gut, LG and also in RG. Domeless expression was changed regarding both intensity and localisation. The Domeless expression pattern in WT larvae after the wasp parasitization is very similar to Dome pattern in the *dco*^{L39Q S101R} and *dco*^{L39Q} homozygous mutants and *dco null* mutants. These results are consistent with the results of Collier expression. Domeless expression in the whole larva body of different mutants is compared in figure 3.54. Noticeably, the *dco* heterozygotes have slightly enhanced Domeless expression and the

Domeless expression is even stronger in the homozygous mutants likewise the WT after the wasp parasitization. Brains with RGs and primary lobes of WT and both *dco*^{L39Q S101R} and *dco*^{L39Q} homozygous mutants to compare the intensity of Domeless expression are in figure 3.55. Both of the *dco* mutants have strikingly increased expression in RG unlike WT control. The Dome expression in mutant brains is weaker than in WT and in the brain of WT larva after the wasp parasitization is the expression even stronger (Fig. 3.53 and 3.55).

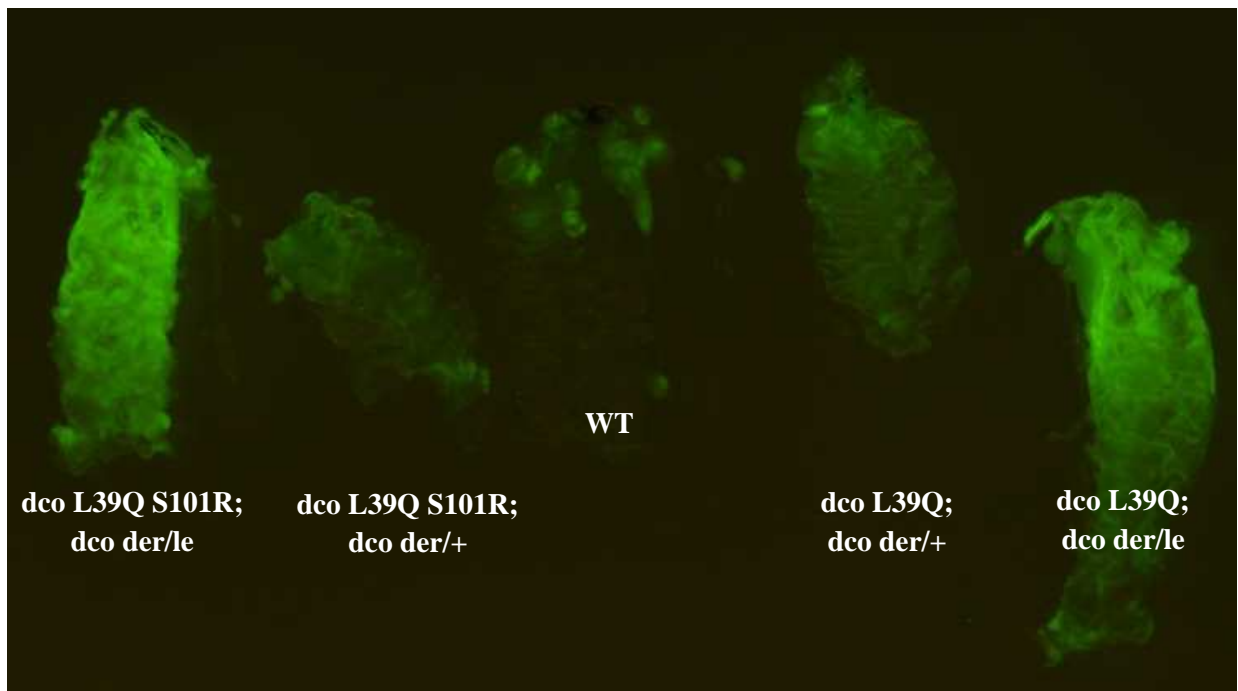


Fig. 3.54: Comparison of Domeless expression intensity in different genetic background.

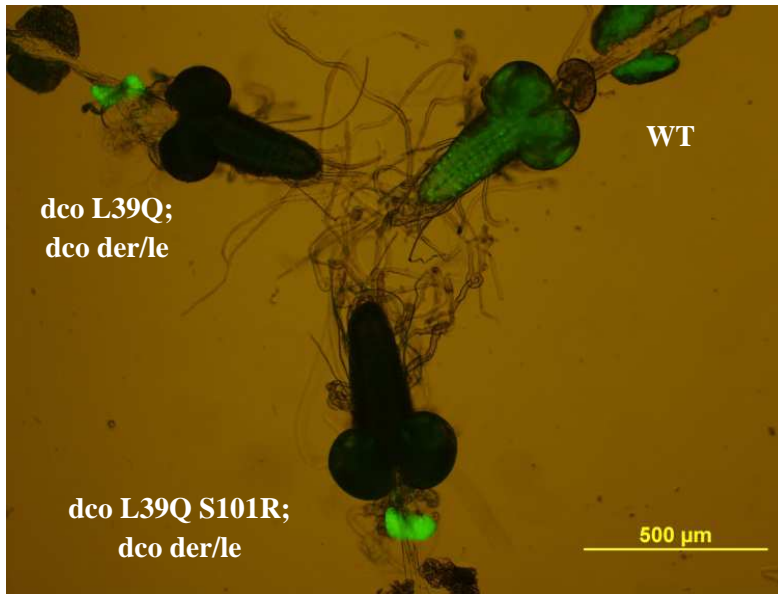


Fig. 3.55: Comparison of Domeless expression in *dco* mutants and WT control.

3.4. EXPRESSION OF DCO

I tested if the *dco* gene conjugated with GFP sequence (hereinafter referred to as FF:*dco*) is fully working. FF:*dco* is a fusion protein, which originate from the construct consisting of a FlyFos vector, GFP reporter tag and a gene of interest (*dco* in this case) with its intact *cis*-regulatory neighbouring regions. Thus, the gene is naturally expressed. After the introduction of this construct into the germ line of flies, it becomes heritable. This enables imaging of gene expression *in vivo* (Muyrers et al., 1999; Bischof et al., 2007; Ejsmont et al., 2009; Fenckova, 2011). The flies with introduced FF:*dco* construct was a kind gift from Michaela Fenckova.

EXPRESSION OF THE FLYFOS CONSTRUCT

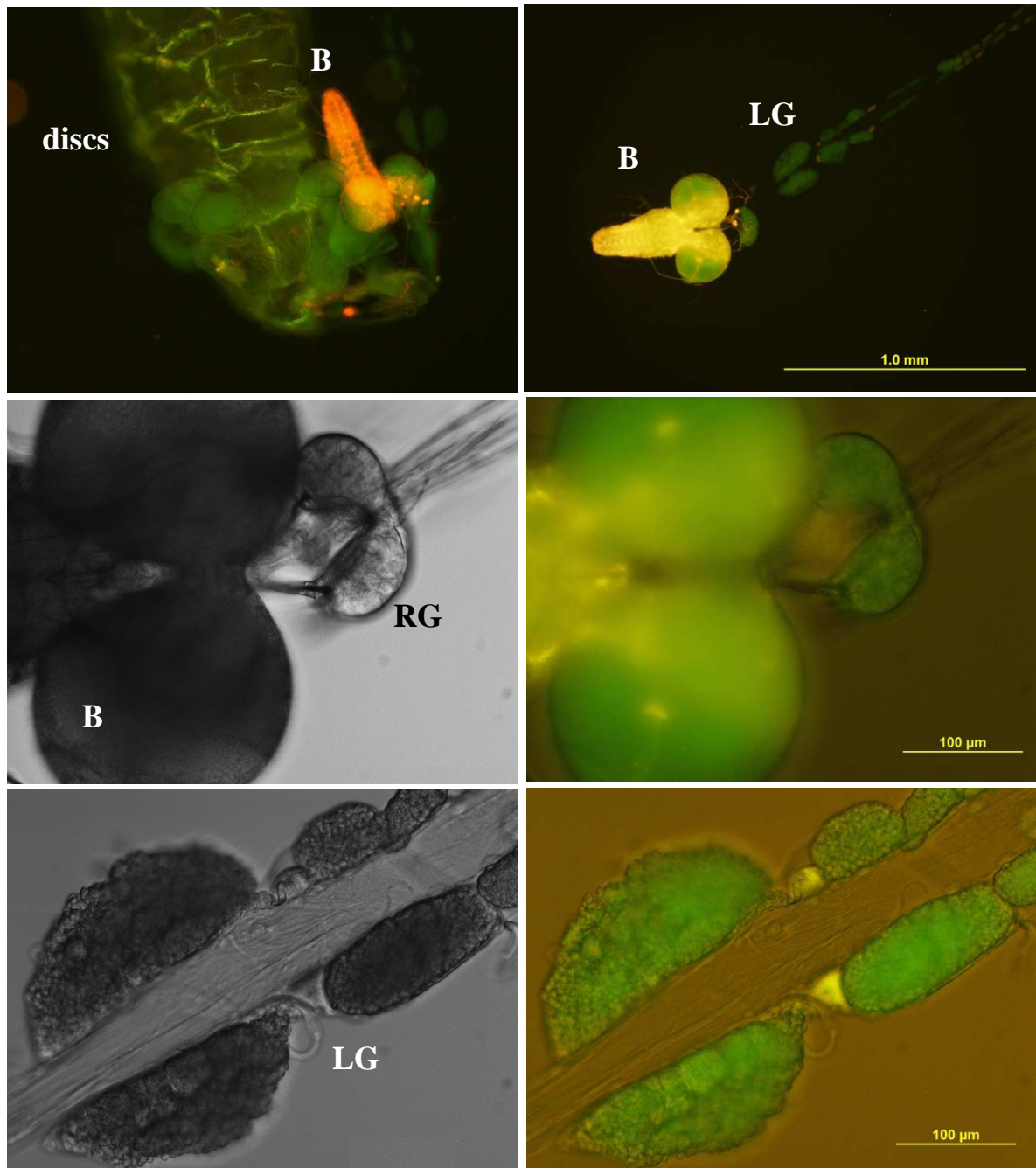


Fig. 3.56: Expression of the FlyFos:*dco* construct in the *dco null* genetic background in a different tissue samples. Red colour corresponds to the dsRed of FlyFos construct. (Continues on the next page)

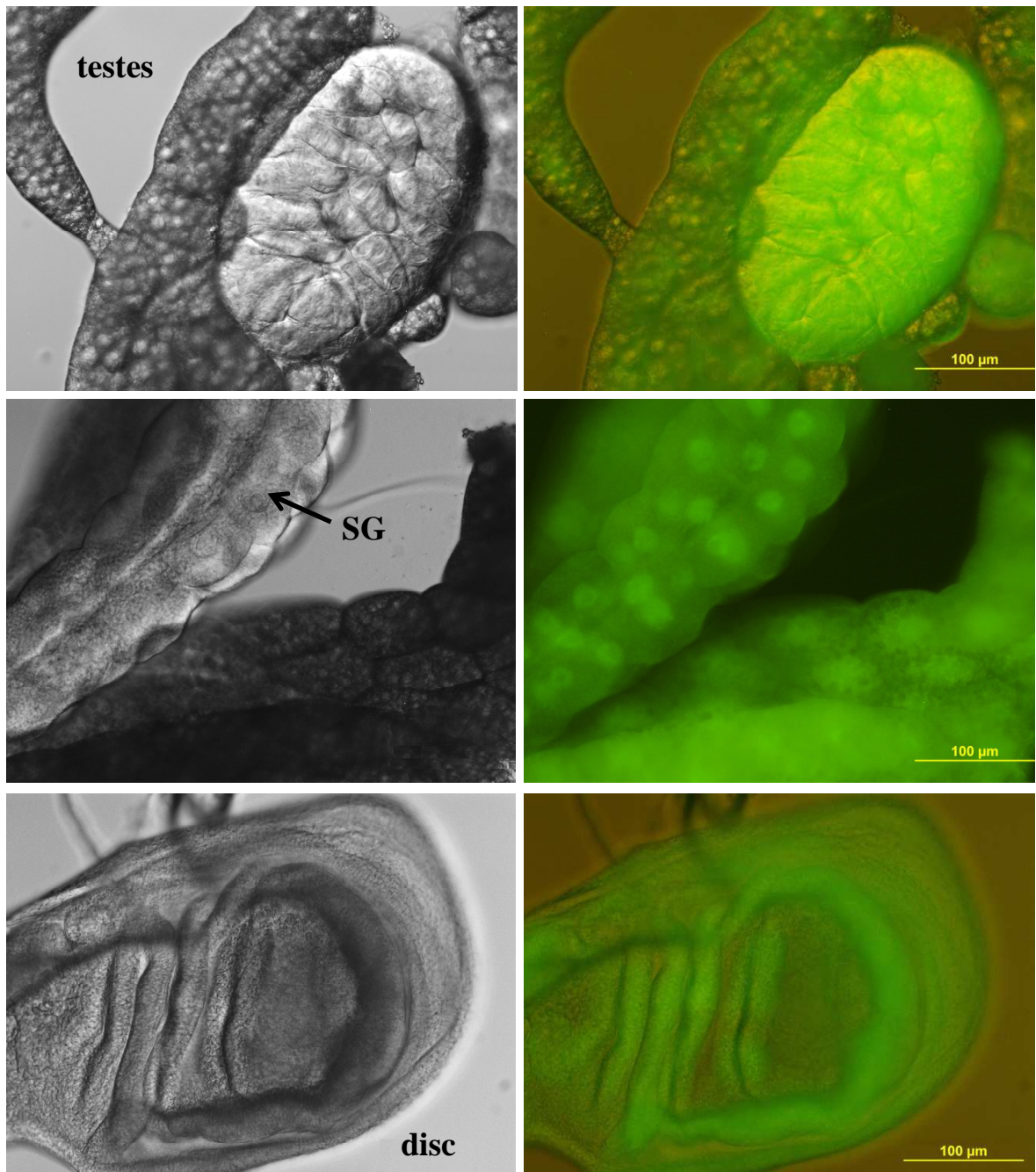


Fig. 3.56 (continuation)

Different larva tissues, where the only functional *dco* allele is the FF:*dco*, are shown in figure 3.56. These flies were obtained after the recombination step, where the FF:*dco* construct was recombined to the *dco*^{le} mutant allele (see more in chapter Methods). These flies are viable in homozygous constitution, where the only Dco protein originates from the FF:*dco* construct. As we can see in figure 3.56, these larvae have normal discs demonstrating that the FF:*dco* is fully functional protein with normal expression. Also the LG has a normal size and morphology. The FF:*dco* is also expressed in other tissues, like fat body, salivary

glands, testes and ring gland. Some of the pictures indicate that the Dco can be localized in the nucleus. By immunostaining, I tested if the Dco is able to move from cytoplasm to nucleus by its own, and that the nuclear localisation is not a consequence of the GFP tag. I used the anti-Dco antibody to visualise the Dco protein in WT larvae and with the use of confocal microscopy analysed the localisation (Figs. 3.57; 3.58 and 3.59). There is a possibility, that the change in Dco nuclear localisation could be a response to for instance immune challenge. Therefore, the fly with this FlyFos:dco construct can be a useful *in vivo* tool for such experiments.

CONFOCAL MICROSCOPY

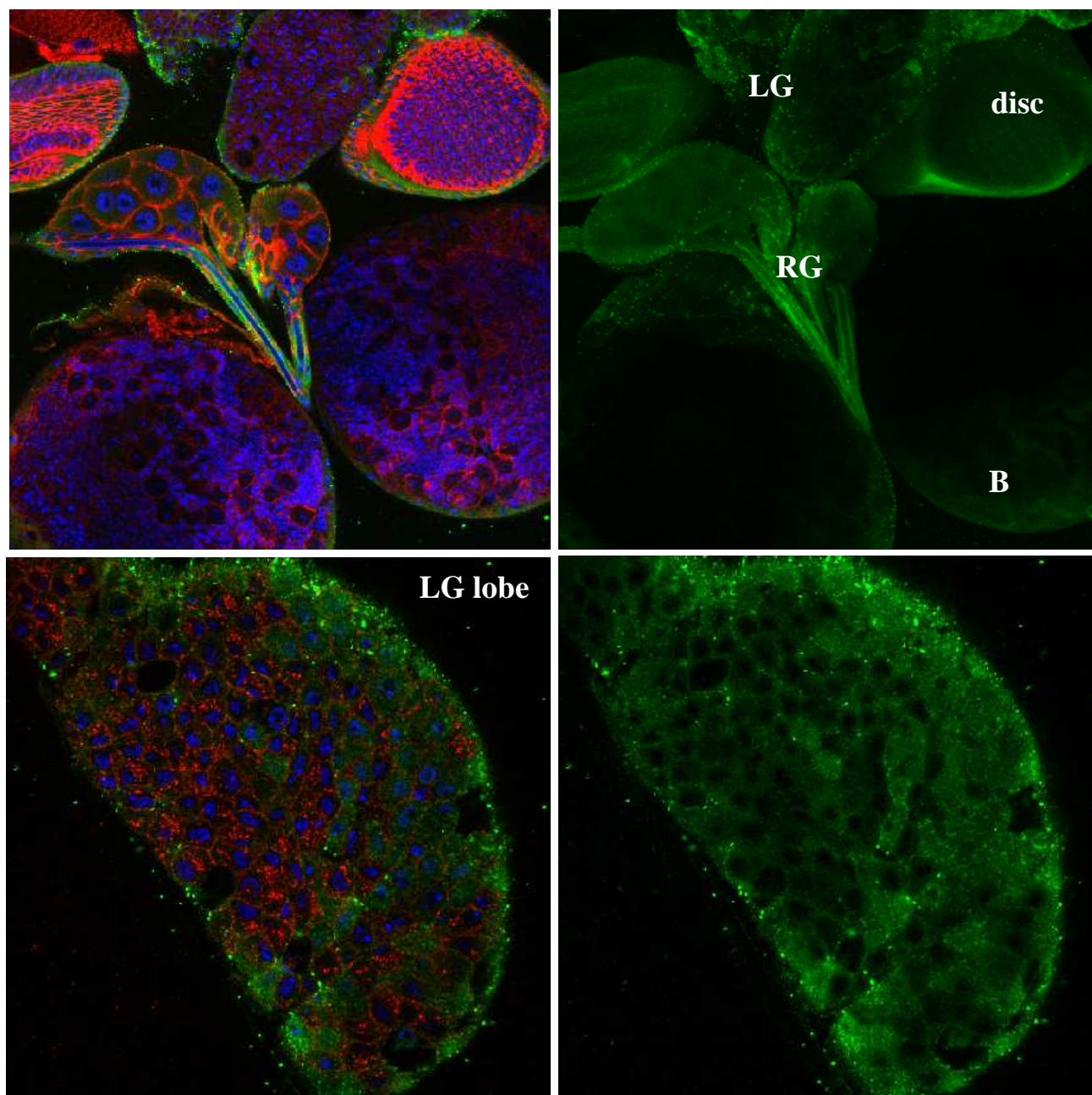


Fig. 3.57: Upper: WT brain (B) with RG (ring gland), part of LG lobe and eye discs. Lower: WT LG lobe. Blue – DAPI labelling nuclei; red – anti discs large antibody; green – anti dco antibody.

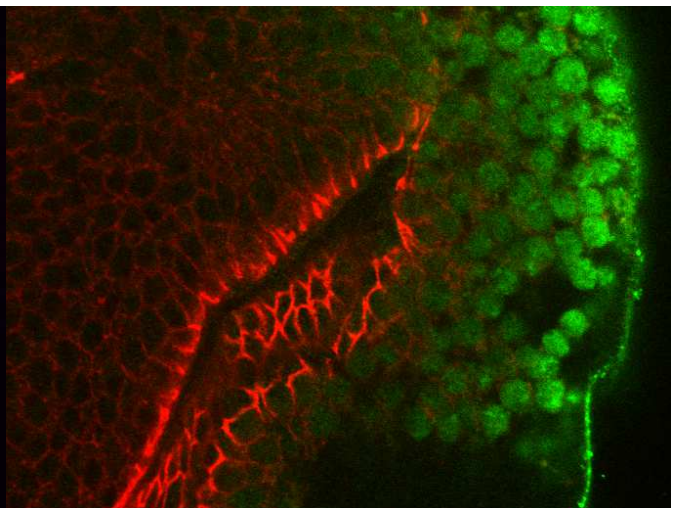
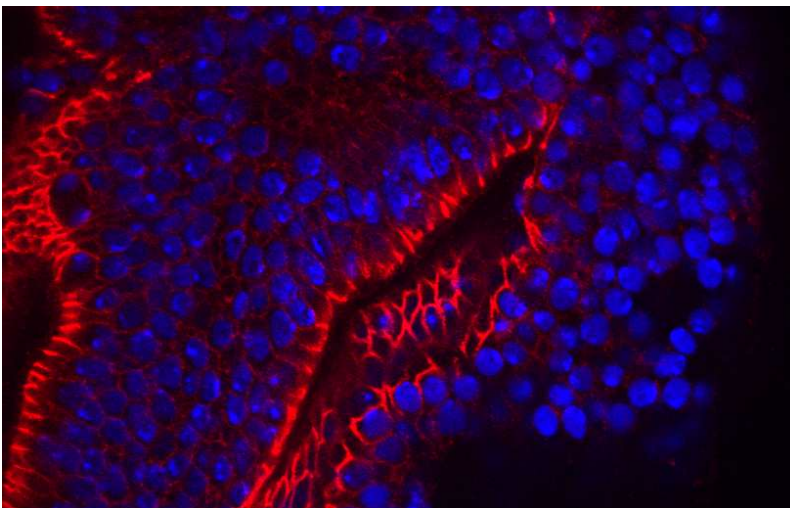
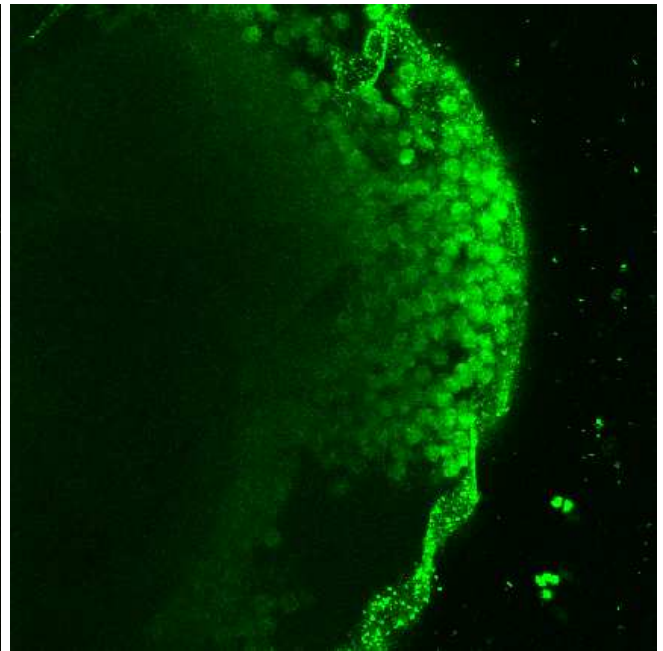
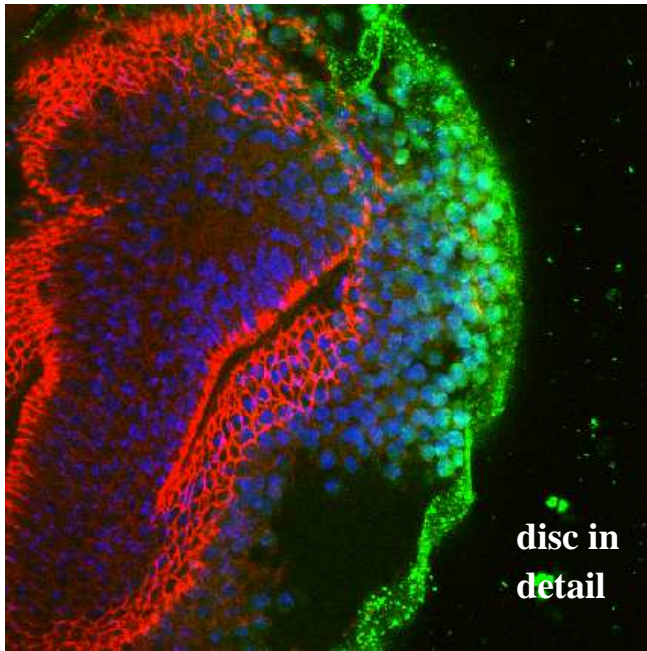
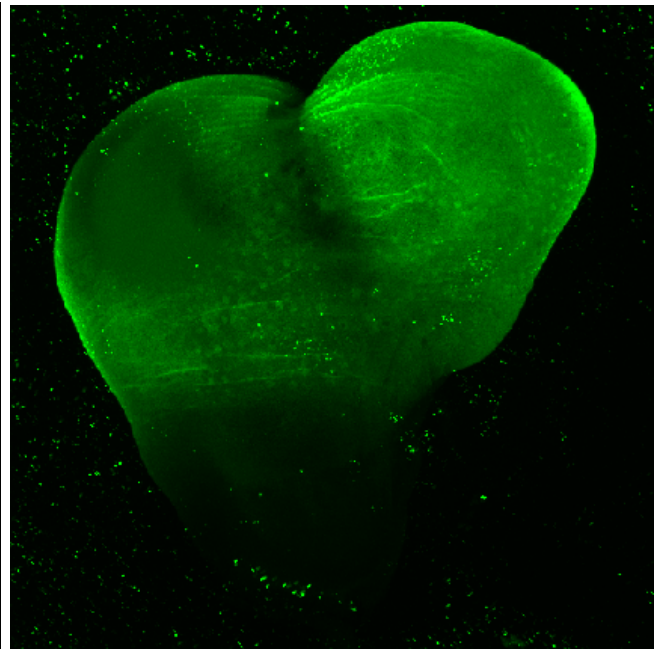
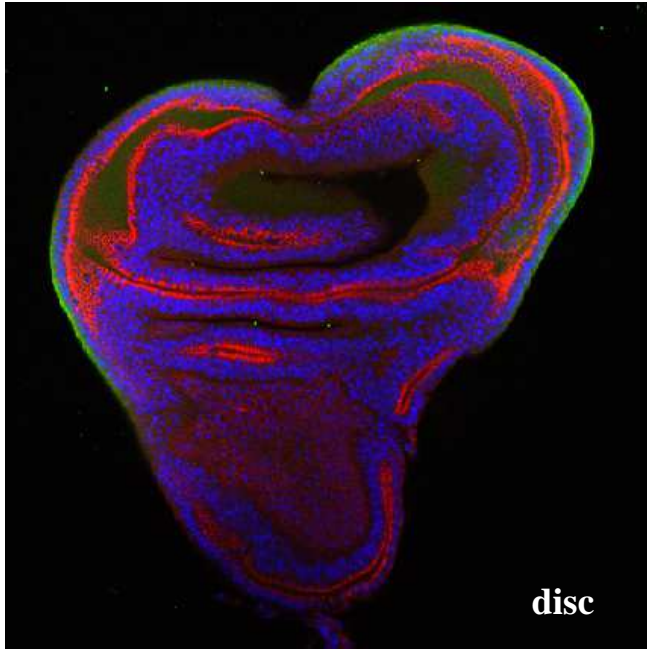


Fig. 3.58 (previous page): WT imaginal wing disc. Upper: the whole disc. Middle: detail of the wing disc. Lower: close-up detail of the wing disc. Blue – DAPI labelling nuclei; red – anti discs large antibody; green – anti dco antibody.

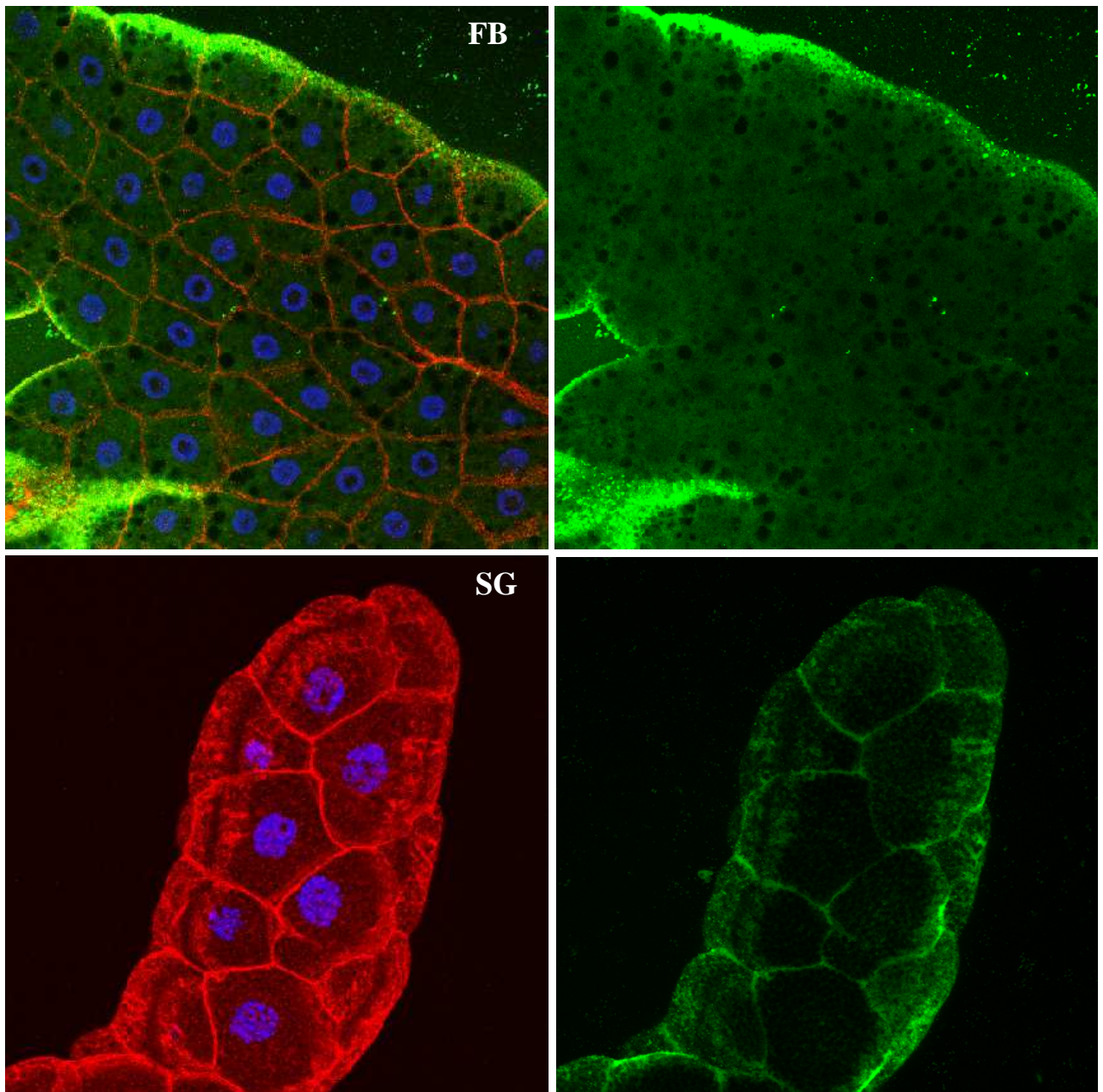


Fig. 3.59: Upper: WT fat body (FB); Lower: WT salivary gland (SG). Blue – DAPI labelling nuclei; red – anti discs large antibody; green – anti dco antibody.

TISSUES EXPRESSING FF:DCO

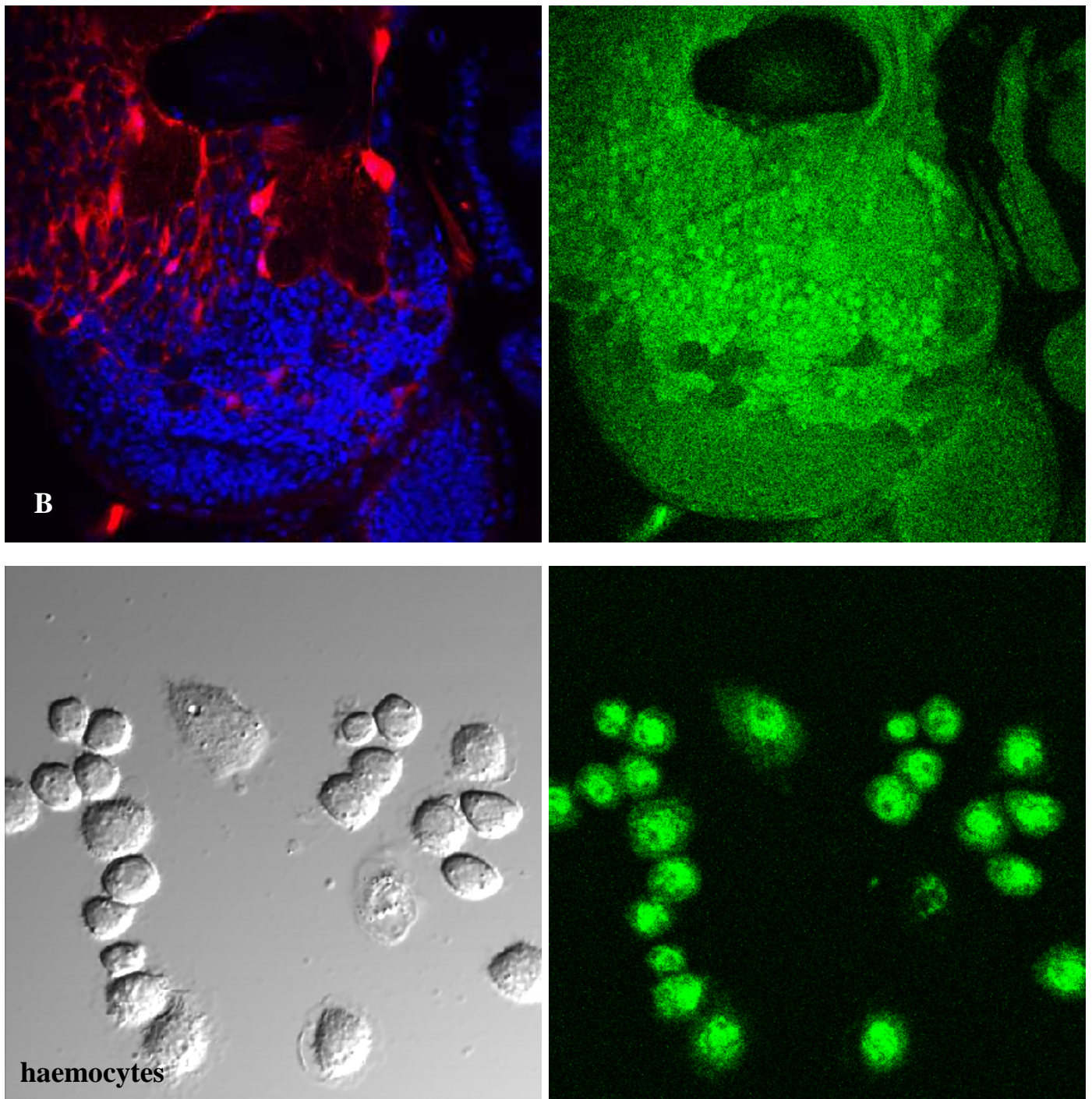


Fig. 3.60: Upper: Brain. Lower: Haemocytes. (FF:dco). Blue – DAPI labelling nuclei; red – anti discs large antibody; green – anti GFP antibody.

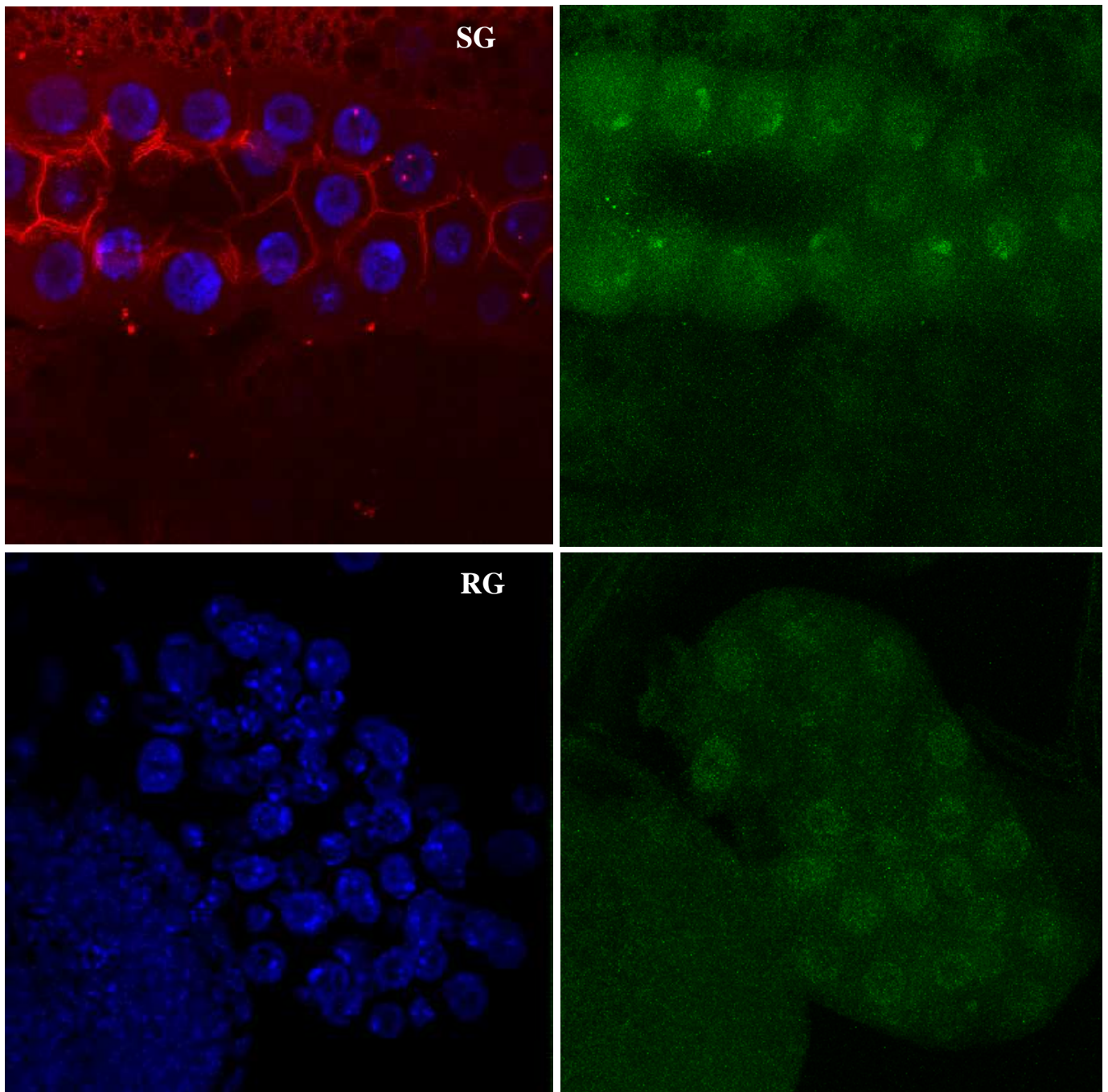


Fig. 3.61: Upper: Salivary gland (SG). Lower: Ring gland (RG). (FF:dco) Blue – DAPI labelling nuclei; red – anti discs large antibody; green – anti GFP antibody.

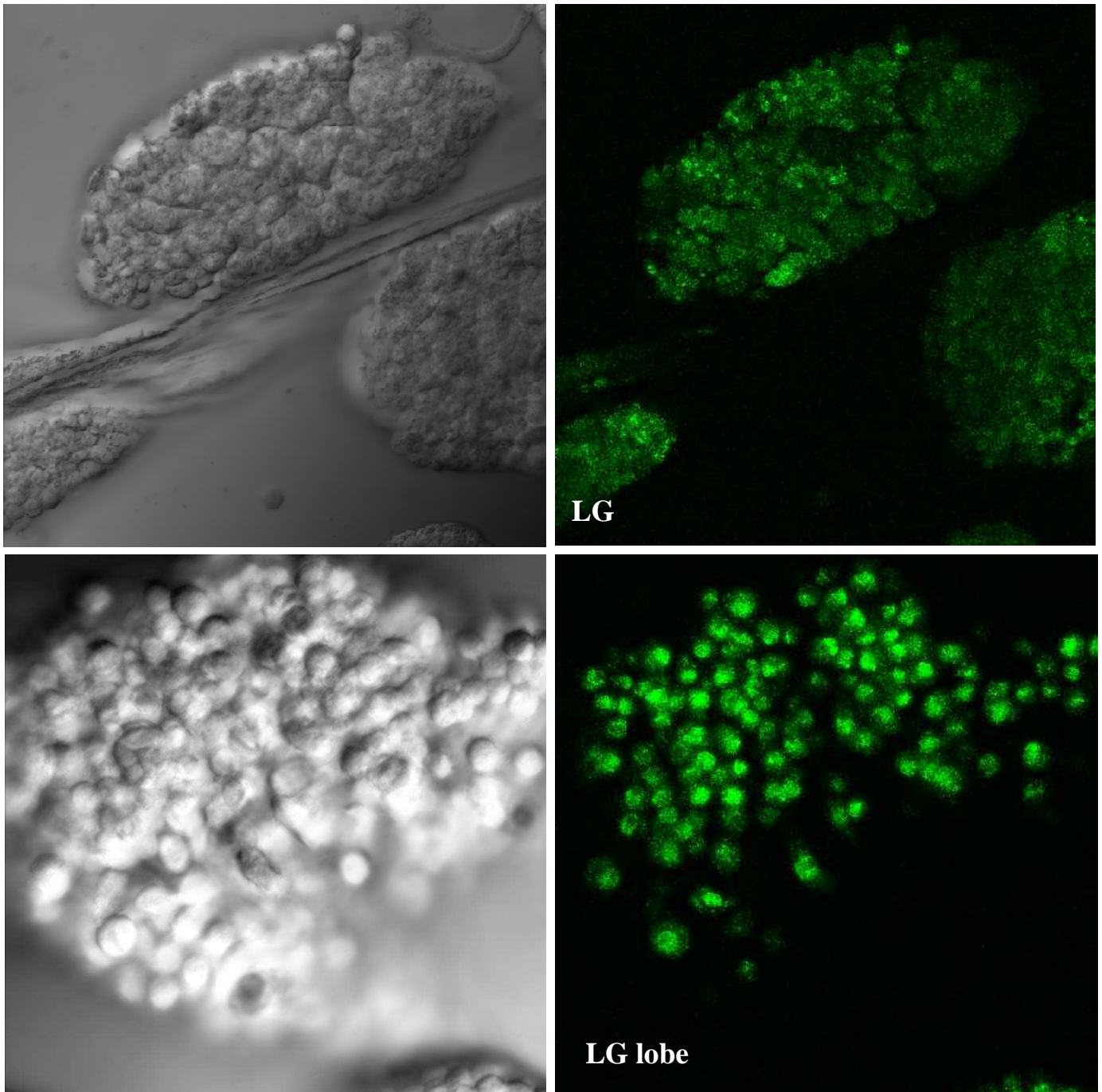


Fig. 3.62: Upper: LG. Lower: Detailed LG lobe. (FF:dco). No antibodies.

I show that the FF:dco protein is both cytoplasmic and nuclear where nuclear localisation has higher intensity. In WT, not all tissues have nuclear Dco. I detected nuclear localisation of WT Dco in LG and disc, but I did not confirm that for RG, fat body or salivary gland.

RT-PCR

I tested the amount of *dco* mRNA in different tissues by use of Q-PCR (Fig. 3.63). These are preliminary results with only one biological replicate. The highest relative amount of *dco* mRNA was detected in gut, fat body and brain. Relatively low amount of *dco* mRNA was detected in haemocytes. Data about the *Dco* expression obtained from the FlyBase database (www.flybase.org) are in figure 3.64. FlyBase is an online database, where the *Drosophila* genome and other data are published.

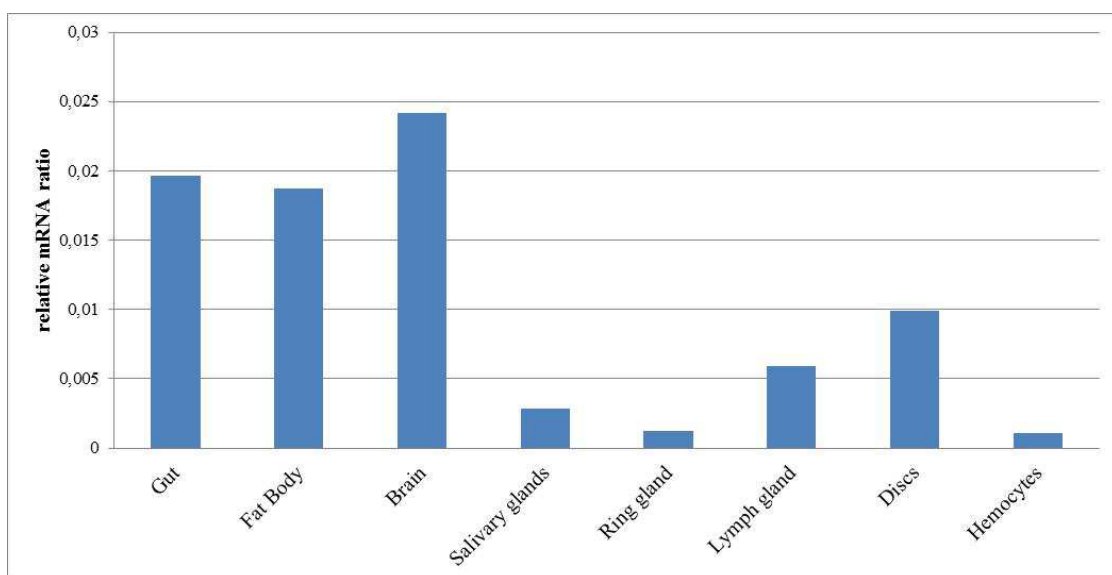


Fig. 3.63: Relative *dco* mRNA ratio in wandering third instar WT (*w*) larval tissues.

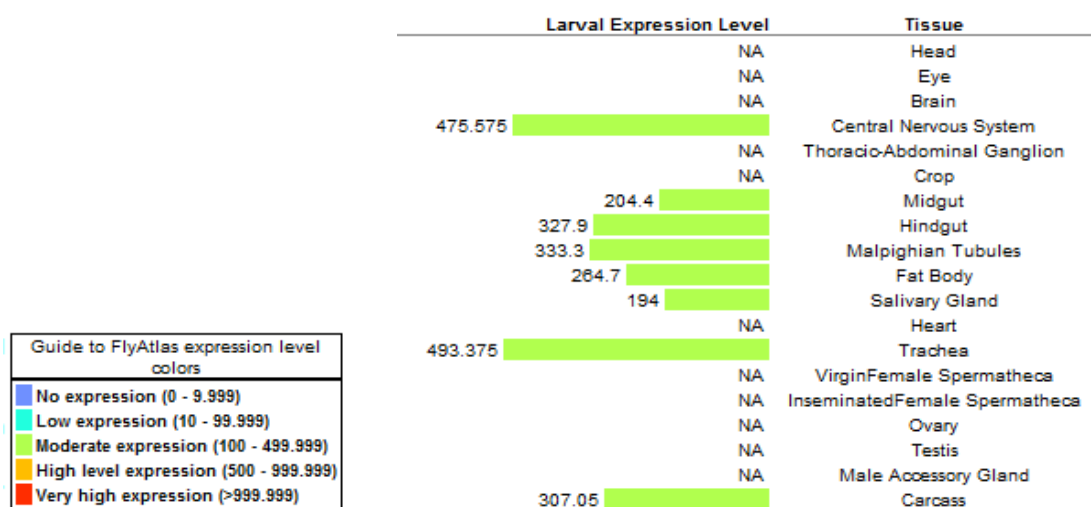


Fig. 3.64: *dco* mRNA data in larval tissues (from FlyBase.org).

4. DISCUSSION

In my thesis, I am dealing with the role of Dco (homologue of human CKIε) in haematopoiesis. It is known that Dco is required for growth of imaginal disc tissues, proliferation of disc cells and also for their survival (Zilian et al., 1999). Furthermore, it is known that abnormal function of Dco protein results in an overgrown phenotype, as it is known for *dco*³ unusual allele (Jursnich et al., 1990; Zilian et al., 1999). I tested the effect of *dco* with introduced point mutations, L39Q and L39Q S101R, found in human breast cancer patients (Fuja et al., 2004) on haematopoiesis in *Drosophila melanogaster*. The role of Dco protein has an ambiguous effect, since abnormal Dco can act as gain-of-function in *dco*^{L39Q} and *dco*^{L39Q S101R} mutants and still has some of the features in common with *dco null* (i.e. loss-of-function) mutants.

The *dco null* mutants have in addition to reduced imaginal disc growth also reduced lymph gland (Fig. 3.2) and circulating haemocyte counts, both mature and immature, as figures 3.12 and 3.13 show. This indicates that Dco is required for haemocyte proliferation. However, Dco is not required for differentiation, since the *dco null* mutants are capable of lamellocyte production after the wasp parasitization (Fig. 3.19) and all the *Drosophila* blood cell types (mature and immature plasmatocytes and also crystal cells) are present in *dco null* mutants. Zilian et al. (1999) detected apoptosis in *dco* mutant imaginal discs. In accordance with this, the Dco protein might be also required for survival of haemocytes. The morphology of *dco null* mutant haemocytes shown in figure 3.20 indicates that apoptosis is in progress. This was also supported by pers. comm. with RNDr. Ladislav Anděra, CSc. Unfortunately; I was not able to verify this by a TUNEL staining due to technical difficulties with this type of staining in *Drosophila* haemocytes. It will be necessary to use other detection principles, such as Annexin V FITC system, to obtain a decisive proof of apoptosis in *dco null* haemocytes.

The *dco*^{L39Q} homozygous mutants have increased counts of both immature haemocytes and lamellocytes, which usually differentiate only after immune challenge. Moreover, even stronger effect can be seen in *dco*^{L39Q S101R} homozygotes, where counts of haemocytes are higher (Figs. 3.11 and 3.18). These overproliferative phenotypes are in conformity with the mutant LG morphology (Fig. 3.3 and 3.4). The LGs in these mutants resemble heterozygous control LGs till the turn of the late 2nd/ early 3rd larval instar. As primary and later also secondary lobes proliferate and produce haemocytes that proceed into

hemolymph during their further development, the LGs become overgrown and their morphology is strikingly changed. The same features can be seen in normal larvae as the response to immune challenge, such as wasp parasitization (Lanot et al., 2001; Sorrentino et al., 2002; Zettervall et al., 2004; Crozatier and Meister, 2007). This indicates that *dco* gene may play a role in immune response. As it was already published, Toll and JAK/STAT signalling pathways play an important role in immune response (Qiu et al., 1998; Agaisse et al., 2003; Zettervall et al., 2004; Jung et al., 2005; Arbouzova and Zeidler, 2006; Matova and Anderson, 2006) and therefore I tested these signalling pathways in mutants of my interest.

Removal of Dorsal, the NF- κ B/Rel-family transcription factor which is activated by Toll signalling, neither reduced the total haemocyte counts (Fig. 3.24) nor suppressed the LG and imaginal disc phenotypes (Figs. 3.28 and 3.29). This result suggests that *dco*^{L39Q} and *dco*^{L39Q S101R} do not act through the Toll signalling pathway, at least not through the Dorsal part of signalling. Interestingly, after removing the *dorsal* gene in *dco* mutants, there are strikingly increased lamellocyte counts. In *dorsal* single mutants, lamellocyte counts are noticeably, but not extremely increased if compared to heterozygous *dco*^{der/+} control and they are also kept at a steady level during the lifetime (Fig. 3.27). This indicates that Dorsal absence increases the differentiation of lamellocytes in the combination with *dco* suggesting that there is a stronger potential of lamellocyte differentiation in the *dco* mutants which is held back by Dorsal and fully released in its absence.

I did not obtain a combination of the *dco* mutation together with the *dorsal Dif* deficiencies, since these combinations have so serious impact on larvae that they cannot handle it. However, the heterozygous *dorsal Dif* deficiency is sufficient to reduce melanotic capsules incidence in *dco*^{L39Q S101R} homozygotes (Figs. 3.21 and 3.31). In some processes only one of them, either Dorsal or Dif, is sufficient for keeping the signal transduction. Therefore, it would be appropriate to test the role of Toll signalling pathway in the combination of *dco* mutation with *dorsal Dif* double mutation. The UAS-GAL4 system could be used for a tissue specific downregulation of Dorsal and Dif transcription factors. This way might be suitable for elimination of side effects of Dorsal Dif removal.

On the other hand, the whole-larva expression pattern of Domeless, the JAK/STAT receptor (Brown et al., 2001; Chen et al., 2002), revealed striking similarities between *dco* mutants and WT larvae parasitized by wasps suggesting that *dco*^{L39Q} and *dco*^{L39Q S101R} may act through the JAK/STAT signalling. This is another aspect, which indicates that the *dco*

mutants mimic the changes in larvae upon the immune challenge. However, the relationship between Dco and the JAK/STAT signalling may be quite complicated and requires further investigation. Interestingly, the expression pattern of Domeless is similar in *dco null* mutant and *dco^{L39Q}* and *dco^{L39Q S101R}* mutants, however only *dco^{L39Q}* and *dco^{L39Q S101R}* mutants show lamellocyte differentiation – a hallmark of response to parasitic wasps.

I also tested Collier expression in mutant LGs. Expression of this protein is specific for PSC (Crozatier et al., 2004) that act in a non-autonomous manner to maintain JAK/STAT signalling activity in prohemocytes to prevent premature differentiation (Krzemień et al., 2007; Mandal et al., 2007). As my results indicate, *dco^{L39Q}* and *dco^{L39Q S101R}* homozygous mutants have the same behaviour regarding Collier expression as the WT after wasp parasitization as well as for Domeless expression.

Immature haemocytes (Hml-) are thickly present in *dco^{L39Q}* and even more in *dco^{L39Q S101R}* homozygous mutants unlike the steady state of mature (Hml+) plasmatocytes in these mutants (Fig. 3.11). It is known that lamellocytes differentiate after the JAK/STAT signalling pathway is downregulated, because the JAK/STAT signalling impedes the premature differentiation (Krzemień et al., 2007; Mandal et al., 2007; Makki et al., 2010). Therefore, the combination of large quantities of immature plasmatocytes and switching off the JAK/STAT signalling pathway in *dco* mutant LGs and haemocytes should result in large quantities of lamellocytes. But there is not such amount of lamellocytes per larva in these mutants, which we could expect on the basis of this theory (Fig. 4.1). These immature haemocytes can be at this point already dedicated to become lamellocytes, but the differentiation was not completed. If this is true, why the lamellocytes already present in hemolymph managed to differentiate and these “dedicated immature haemocytes” did not? To test this possibility, there is a *misshapen* GAL4 driver triggering expression in lamellocytes so in combination with UAS-GFP lamellocytes might be visualized although their morphology is not recognisable.

Immunochallenged larvae launch a complex cellular immune response in which specialised host blood cells, lamellocytes and crystal cells, are activated and they form a capsule around the wasp egg to block its development (Sorrentino et al., 2002). The prophenoloxidase is an enzyme necessary for the immune melanisation process. This enzyme is expressed in both crystal cells and lamellocytes (Sorrentino et al., 2002; Irving et al., 2005). It is still unclear where the lamellocytes come from. One of the theories is that

lamellocytes originate from plasmatocytes (Rizki and Rizki, 1984). Other theory says that lamellocytes can also be derived from plasmatocyte progenitors or at the expense of crystal cells since very few crystal cells or, most often no crystal cells at all, were detected following wasp parasitism (Krzemien et al., 2010).

Since both dco^{L39Q} and $dco^{L39Q S101R}$ mutants have eventually similar size and disintegration of LGs (Figs. 3.35 and 3.37), I am not sure where all the excessive haemocytes (mostly Hml- cells) originate. Both dco^{L39Q} and $dco^{L39Q S101R}$ homozygous mutants have strikingly changed imaginal wing disc morphology and size, but the $dco^{L39Q S101R}$ homozygous imaginal discs are greatly fragile and they easily fall apart. These cells could be mistakable with the haemocytes and therefore partially contribute to the haemocyte counts. This question may be figured out by labelling of haematopoietic cell lineage by UAS-GFP/GAL4 system. Other way how these excessive haemocytes could arise is mitotic division of circulating haemocytes in hemolymph. This might explain why the $dco^{L39Q S101R}$ homozygotes have more than 3 times as much immature plasmatocytes as the dco^{L39Q} homozygotes although their LGs have similar size and degree of disintegration. This question could be sorted out by measuring of mitotic index in these mutants or by a tissue specific expression of mutant *dco* only in haematopoietic cell lineages.

The same approach of tissue specific induction of mutant *dco* can be applied to eliminate the possible side effects of *dco* mutation in the whole larva body. This way may avoid the disc overgrown and/or disintegrating phenotypes, which can exclude the possibility that the abnormal imaginal discs trigger the immune response in the larva body and thus lead to the haematopoietic defects observed in these mutants. However, the dco^3 mutant phenotype goes against this possibility. Imaginal discs are overgrown in the dco^3 mutants; however the haemocyte counts and lamellocytes occurrence is normal. Haemocyte counts are also normal in both dco^{L39Q} and $dco^{L39Q S101R}$ heterozygotes although their imaginal wing discs are to a certain extent overgrown too.

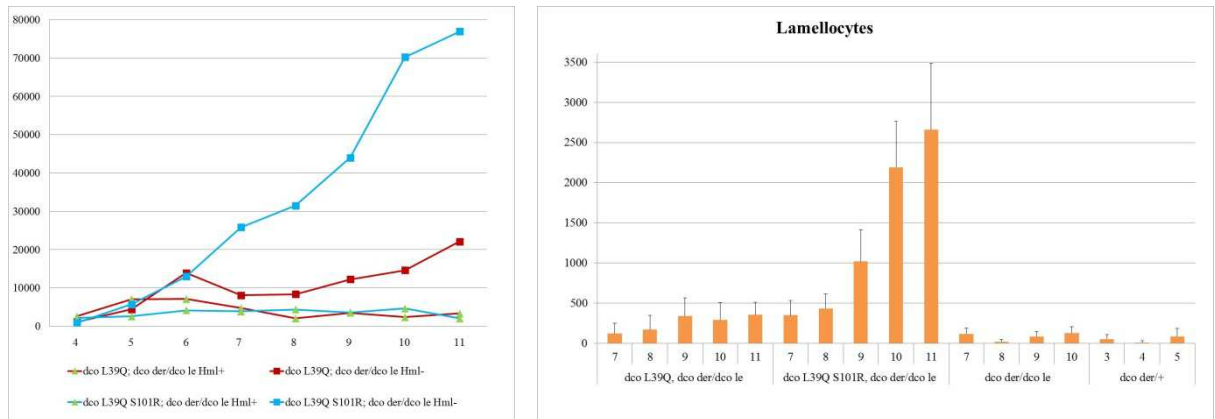
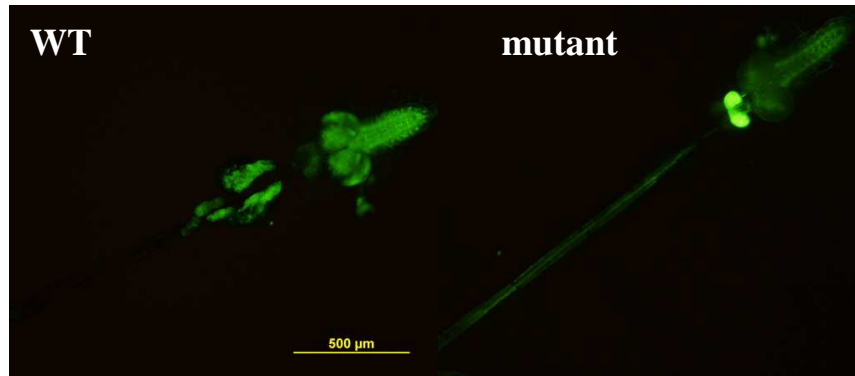


Fig. 4.1: Connection of switching over the Domeless expression not only in the lymph gland, haemocyte overproliferation (Hml-) and lamellocyte differentiation.

The results of Hml-/Hml+ haemocyte ratios (Figs. 3.16 and 3.17) comparison can indicate that the Dco protein can play a role in maintaining the balance between immature and mature haemocytes. Further, the question how the steady state of Hml+ haemocyte counts is maintained in the *dco* mutant, while the immature haemocytes greatly proliferate, remains to be answered. The Hml-/Hml+ haemocyte ratios in the *dco* loss-of-function mutants (*dco* null) are consistent with those in the *dco*^{L39Q} homozygous mutants for the whole larval life and with the *dco*^{L39Q S101R} mutants up to the 8th day ($p < 0,001$). Taken together with Domeless expression, which also does not differ between *dco* null and *dco*^{L39Q} and *dco*^{L39Q S101R} mutants, these results suggest that in some aspects, the *dco*^{L39Q S101R} and *dco*^{L39Q} mutants act rather as loss-of-function mutations. Similar results were observed for human version of these mutations in the Wnt/ β -catenin pathway (Foldynová-Trantírková et al., 2010).

All the homozygous mutants (except *dco*³) have prolonged larval stage duration. Since the increase of haemocyte counts usually comes after the 6th day AEL, there is the question coming out: Is the increase of haemocyte counts an effect of the *dco* mutation, or is it just a result of prolonged larval stage? One of the clues can be that in *dco null* mutant, where the larval stage is prolonged up to 10 days, the haemocyte counts are kept at steady and low level. So if the haemocyte count increase would be the result of prolonged larval stage, there would probably be at least an indication of the increase or kind of fluctuating trend in the *dco null* mutants too. Regardless, haemocytes will need to be counted in larvae that do not have an affected *dco* gene and have simultaneously prolonged larval life. For this purpose, I suggest *ecdysoneless* mutants or for example *smt3* mutants.

It is known that Dco has various roles in various processes. Here I show a novel role of Dco in haematopoiesis bringing its possible role in modulating the immune response. My results suggest that Dco plays in this process through the JAK/STAT signalling pathway. Since Dco is the orthologue of mammalian CKIε, its role could be important also for mammalian immune system. The possibilities that the described effects of *dco* mutations on haematopoiesis are either an immune reaction to the abnormal imaginal disc development or caused by the prolonged larval life will need to be excluded by a tissue-specific manipulation of Dco. However, the expression of Dco in LG and haemocytes as well as the phenotypes of both *dco*³ (going against abnormal disc hypothesis) and *dco null* (going against prolonged development hypothesis) mutants strongly suggest that the Dco plays an important role in haematopoiesis. On one side, Dco is required for haemocytes survival. On the other side, it might be required for modulation during an immune challenge, most likely through the JAK/STAT signalling. Its abnormal functioning could lead to overproliferative phenotypes even without the immune challenge, which would be interesting to study from the haematopietic malignancies point of view.

5. CONCLUSIONS

The Dco, a protein with kinase activity and a homologue of human CKI δ/ϵ , has been shown to be involved in *Drosophila* haematopoiesis. Apart from its requirement for imaginal disc growth, the Dco is also required for a proliferation of the haematopoietic cells and the lymph gland, while it is not needed for the haemocyte differentiation. The Dco seems to be required also for the cell survival, since the haemocyte counts in the *dco null* mutants are rather reduced and haemocyte morphology strikingly resembles to the apoptotic cells. The overproliferative phenotypes of lymph gland and haemocytes in the *dco*^{L39Q S101R} and *dco*^{L39Q} mutants are alike phenotypes known in the Toll and JAK/STAT mutants. I revealed that Dorsal-mediated Toll signalling is not involved in the overproliferative phenotypes of the *dco* mutants. Since the heterozygous dorsal Dif mutation reduced the melanotic capsule incidence in the *dco*^{L39Q S101R} mutant, the Dorsal-Dif-mediated Toll transduction pathway remains to be tested. My results indicate the involvement of the JAK/STAT signalling pathway in orchestrating of the *dco* mutant phenotypes. The overall effects of the Dco mutants on hematopoiesis as well as on JAK/STAT signalling strongly suggest that the Dco is capable to modulate immune response as for example against parasitic wasp eggs.

The phenotypes of different *dco* mutants are summarised in figure 5.1 where symbols express the the strength and direction of the difference between the standard and the particular mutant.

	imaginal disc size and compactness	size of the LG	quantity of plasmatocytes	quantity of lamellocytes	Domeless expression (LG)	Collier expression (LG)	melanotic capsule incidence
<i>dco</i> ^{der/+} (standard)	+	+	+	0/+	+	+	0
WT infected	+	++	X	++	-	++	++
<i>dco</i> ^{der/le}	---	-	-	--	-	+	---
<i>dco</i> ³	++	+	+	0	+	X	0
<i>dco</i> ^{L39Q S101R} ; <i>dco</i> ^{der/+}	+	+	-	0/+	+	+	0
<i>dco</i> ^{L39Q S101R} ; <i>dco</i> ^{der/le}	-	+++	+++	+++	-	++	+++
<i>dco</i> ^{L39Q} ; <i>dco</i> ^{der/+}	++	+	-/+	0/+	+	+	0
<i>dco</i> ^{L39Q} ; <i>dco</i> ^{der/le}	+++	+++	++	+	-	++	+
Dl-	X	++	++	++	X	X	++
<i>dco</i> ^{der/le} ; Dl	---	X	-	--	X	X	---
<i>dco</i> ^{L39Q S101R} ; Dl-; <i>dco</i> ^{der/le}	-	+++	+++	++++	X	X	++
<i>dco</i> ^{L39Q} ; Dl-; <i>dco</i> ^{der/le}	++	+++	+++	++++	X	X	++

Tab. 5.1: Summary of the phenotypes. The *dco*^{der/+} is used as standard value. (X was not examined; 0 was not observed, but can be present; + present; - absent or disrupted; quantity of (+) or (-) represents the strength of variation in comparison to the standard.

REFERENCES:

- Agaisse, H., and Perrimon, N. (2004). The roles of JAK/STAT signaling in *Drosophila* immune responses. *Immunological Reviews* **198**, 72–82.
- Agaisse, H., Petersen, U.M., Boutros, M., Mathey-Prevot, B., and Perrimon, N. (2003). Signaling Role of Hemocytes in *Drosophila* JAK/STAT-Dependent Response to Septic Injury. *Developmental Cell* **5**, 441–450.
- Arbouzova, N.I., and Zeidler, M.P. (2006). JAK/STAT signalling in *Drosophila*: insights into conserved regulatory and cellular functions. *Development* **133**, 2605–2616.
- Asha, H., Nagy, I., Kovacs, G., Stetson, D., Ando, I., and Dearolf, C.R. (2003). Analysis of Ras-induced overproliferation in *Drosophila* hemocytes. *Genetics* **163**, 203–215.
- Belvin, M.P., and Anderson, K.V. (1996). A conserved signaling pathway: the *Drosophila* Toll-Dorsal pathway. *Annual Review of Cell and Developmental Biology* **12**, 393–416.
- Binari, R., and Perrimon, N. (1994). Stripe-specific regulation of pair-rule genes by *hopscotch*, a putative Jak family tyrosine kinase in *Drosophila*. *Genes & Development* **8**, 300–312.
- Bischof, J., Maeda, R.K., Hediger, M., Karch, F., and Basler, K. (2007). An optimized transgenesis system for *Drosophila* using germ-line-specific Φ C31 integrases. *Proceedings of the National Academy of Sciences* **104** (9), 3312–3317.
- Bourbon, H.M., Gonzy-Treboul, G., Peronnet, F., Alin, M.F., Ardourel, C., Benassayag, C., Cribbs, D., Deutsch, J., Ferrer, P., and Haenlin, M. (2002). A P-insertion screen identifying novel X-linked essential genes in *Drosophila*. *Mechanisms of Development* **110**, 71–83.
- Brown, S., Hu, N., and Hombría, J.C.G. (2001). Identification of the first invertebrate interleukin JAK/STAT receptor, the *Drosophila* gene *domeless*. *Current Biology* **11**, 1700–1705.
- Carton, Y., and Nappi, A.J. (2001). Immunogenetic aspects of the cellular immune response of *Drosophila* against parasitoids. *Immunogenetics* **52**, 157–164.

- Chen, H.W., Chen, X., Oh, S.W., Marinissen, M.J., Gutkind, J.S., and Hou, S.X. (2002). mom identifies a receptor for the *Drosophila* JAK/STAT signal transduction pathway and encodes a protein distantly related to the mammalian cytokine receptor family. *Genes & Development* **16**, 388-398.
- Crozatier, M., and Meister, M. (2007). *Drosophila* haematopoiesis. *Cellular Microbiology* **9**, 1117–1126.
- Crozatier, M., Ubeda, J.-M., Vincent, A., and Meister, M. (2004). Cellular Immune Response to Parasitization in *Drosophila* Requires the EBF Orthologue Collier. *PLoS Biology* **2** (8), e196.
- Crozatier, M., Valle, D., Dubois, L., Ibensouda, S., and Vincent, A. (1996). Collier, a novel regulator of *Drosophila* head development, is expressed in a single mitotic domain. *Current Biology* **6**, 707–718.
- Defaye, A., Evans, I., Crozatier, M., Wood, W., Lemaitre, B., and Leulier, F. (2009). Genetic Ablation of *Drosophila* Phagocytes Reveals Their Contribution to Both Development and Resistance to Bacterial Infection. *Journal of Innate Immunity* **1**, 322–334.
- Dimarcq, J.L., Imler, J.L., Lanot, R., Ezekowitz, R.A.B., Hoffmann, J.A., Janeway, C.A., and Lagueux, M. (1997). Treatment of l(2)mbn *Drosophila* tumorous blood cells with the steroid hormone ecdysone amplifies the inducibility of antimicrobial peptide gene expression. *Insect Biochemistry and Molecular Biology* **27** (10), 877–886.
- Dolezal, T., Kucerova, K., Neuhold, J., and Bryant, P.J. (2010). Casein kinase I epsilon somatic mutations found in breast cancer cause overgrowth in *Drosophila*. *The International Journal of Developmental Biology* **54**, 1419–1424.
- Ejsmont, R.K., Sarov, M., Winkler, S., Lipinski, K.A., and Tomancak, P. (2009). A toolkit for high-throughput, cross-species gene engineering in *Drosophila*. *Nature Methods* **6**, 435–437.
- Evans, C.J., Hartenstein, V., and Banerjee, U. (2003). Thicker than blood: conserved mechanisms in *Drosophila* and vertebrate hematopoiesis. *Developmental Cell* **5**, 673–690.

- Fencková M, (2011) Role of extracellular adenosine in *Drosophila*. Ph.D. Thesis. University of South Bohemia, Faculty of Science, School of Doctoral Studies in Biological Sciences, České Budějovice, Czech Republic.
- Foldynová-Trantírková, S., Sekyrová, P., Tmejová, K., Brumovská, E., Bernatík, O., Blankenfeldt, W., Krejčí, P., Kozubík, A., Doležal, T., Trantírek, L. and Vítězslav Bryja (2010). Breast cancer-specific mutations in CK1 ϵ inhibit Wnt/ β -catenin and activate the Wnt/Rac1/JNK and NFAT pathways to decrease cell adhesion and promote cell migration. *Breast Cancer Research* **12**, R30.
 - Franc, N.C., Dimarcq, J.L., Lagueux, M., Hoffmann, J., and Ezekowitz, R.A.B. (1996). Croquemort, a novel *Drosophila* hemocyte/macrophage receptor that recognizes apoptotic cells. *Immunity* **4**, 431–443.
 - Fuja, T.J., Lin, F., Osann, K.E., and Bryant, P.J. (2004). Somatic mutations and altered expression of the candidate tumor suppressors CSNK1 ϵ , DLG1, and EDD/hHYD in mammary ductal carcinoma. *Cancer Research* **64**, 942–951.
 - Gateff, E. (1994). Tumor suppressor and overgrowth suppressor genes of *Drosophila melanogaster*: Developmental aspects. *The International Journal of Developmental Biology* **38**, 565–590.
 - Goto, A., Kadowaki, T., and Kitagawa, Y. (2003). *Drosophila* hemolectin gene is expressed in embryonic and larval hemocytes and its knock down causes bleeding defects. *Developmental Biology* **264**, 582–591.
 - Govind, S. (1999). Control of development and immunity by Rel transcription factors in *Drosophila*. *Oncogene* **18**, 6875–6887.
 - Govind, S., Brennan, L., and Steward, R. (1993). Homeostatic balance between dorsal and cactus proteins in the *Drosophila* embryo. *Development* **117**, 135–148.
 - De Gregorio, E., Han, S.J., Lee, W.J., Baek, M.J., Osaki, T., Kawabata, S.I., Lee, B.L., Iwanaga, S., Lemaitre, B., and Brey, P.T. (2002). An Immune-Responsive Serpin Regulates the Melanization Cascade in *Drosophila*. *Developmental Cell* **3**, 581–592.

- Hanratty, W.P., and Dearolf, C.R. (1993). The *Drosophila Tumorous lethal* hematopoietic oncogene is a dominant mutation in the hopscotch locus. *Molecular and General Genetics MGG* **238**, 33–37.

- Harrison, D.A., Binari, R., Nahreini, T.S., Gilman, M., and Perrimon, N. (1995). Activation of a *Drosophila* Janus kinase (JAK) causes hematopoietic neoplasia and developmental defects. *The EMBO Journal* **14** (12), 2857-2865.

- Hombria, J.C.G., and Brown, S. (2002). The fertile field of *Drosophila* Jak/STAT signalling. *Current Biology* **12**, 569–575.

- Hou, S.X., Zheng, Z., Chen, X., and Perrimon, N. (2002). The JAK/STAT pathway in model organisms: emerging roles in cell movement. *Dev. Cell* **3**, 765–778.

- Hou, X.S., Melnick, M.B., and Perrimon, N. (1996). *marelle* Acts Downstream of the *Drosophila* HOP/JAK Kinase and Encodes a Protein Similar to the Mammalian STATs. *Cell* **84**, 411–419.

- Hultmark, D. (2003). *Drosophila* immunity: paths and patterns. *Current Opinion in Immunology* **15**, 12–19.

- Irving, P., Ubeda, J.-M., Doucet, D., Troxler, L., Lagueux, M., Zachary, D., Hoffmann, J.A., Hetru, C., and Meister, M. (2005). New insights into *Drosophila* larval haemocyte functions through genome-wide analysis. *Cellular Microbiology* **7** (3), 335–350.

- Jung, S.H., Evans, C.J., Uemura, C., and Banerjee, U. (2005). The *Drosophila* lymph gland as a developmental model of hematopoiesis. *Development* **132**, 2521–2533.

- Jursnich, V.A., Fraser, S.E., Held, L.I., Ryerse, J., and Bryant, P.J. (1990). Defective gap-junctional communication associated with imaginal disc overgrowth and degeneration caused by mutations of the *dco* gene in *Drosophila*. *Developmental Biology* **140**, 413–429.

- Kloss, B., Price, J.L., Saez, L., Blau, J., Rothenfluh, A., Wesley, C.S., and Young, M.W. (1998). The *Drosophila* Clock Gene *double-time* Encodes a Protein Closely Related to Human Casein Kinase I ϵ . *Cell* **94**, 97–107.

- Krzemiń, J., Dubois, L., Makki, R., Meister, M., Vincent, A., and Crozatier, M. (2007). Control of blood cell homeostasis in *Drosophila* larvae by the posterior signalling centre. *Nature* **446**, 325–328.

- Krzemien, J., Oyallon, J., Crozatier, M., and Vincent, A. (2010). Hematopoietic progenitors and hemocyte lineages in the *Drosophila* lymph gland. *Developmental Biology* **346**, 310–319.
- Lanot, R., Zachary, D., Holder, F., and Meister, M. (2001). Postembryonic Hematopoiesis in *Drosophila*. *Developmental Biology* **230**, 243–257.
- Lebestky, T., Chang, T., Hartenstein, V., and Banerjee, U. (2000). Specification of *Drosophila* hematopoietic Lineage by Conserved Transcription Factors. *Science* **288**, 146–149.
- Lebestky, T., Jung, S.H., and Banerjee, U. (2003). A Serrate-expressing signaling center controls *Drosophila* hematopoiesis. *Genes & Development* **17**, 348–353.
- Lemaitre, B. (2004). The road to Toll. *Nature Reviews Immunology* **4**, 521–527.
- Lemaitre, B., Meister, M., Govind, S., Georgel, P., Steward, R., Reichhart, J.M., and Hoffmann, J.A. (1995). Functional analysis and regulation of nuclear import of dorsal during the immune response in *Drosophila*. *The EMBO Journal* **14** (3), 536-545.
- Luo, H., and Dearolf, C.R. (2001). The JAK/STAT pathway and *Drosophila* development. *BioEssays* **23**, 1138–1147.
- Luo, H., Hanratty, W.P., and Dearolf, C.R. (1995). An amino acid substitution in the *Drosophila hopTum-1* Jak kinase causes leukemia-like hematopoietic defects. *The EMBO Journal* **14** (7), 1412-1420.
- Makki, R., Meister, M., Pennetier, D., Ubeda, J.-M., Braun, A., Daburon, V., Krzemień, J., Bourbon, H.-M., Zhou, R., Vincent, A., Crozatier M.. (2010). A Short Receptor Downregulates JAK/STAT Signalling to Control the *Drosophila* Cellular Immune Response. *PLoS Biology* **8**, e1000441.
- Mandal, L., Martinez-Agosto, J.A., Evans, C.J., Hartenstein, V., and Banerjee, U. (2007). A Hedgehog- and Antennapedia-dependent niche maintains *Drosophila* haematopoietic precursors. *Nature* **446** (7133), 320–324.
- Matova, N., and Anderson, K.V. (2006). Rel/NF-κB double mutants reveal that cellular immunity is central to *Drosophila* host defense. *Proceedings of the National Academy of Sciences* **103** (44), 16424–16429.

- Matova, N., and Anderson, K.V. (2010). *Drosophila* Rel proteins are central regulators of a robust, multi-organ immune network. *Journal of Cell Science* **123**, 627–633.
- Muyrers, J.P.P., Zhang, Y., Testa, G., and Stewart, A.F. (1999). Rapid modification of bacterial chromosomes by ET-recombination. *Nucleic Acids Research* **27** (6), 1555–1557.
- Okamura, A., Iwata, N., Nagata, A., Tamekane, A., Shimoyama, M., Gomyo, H., Yakushijin, K., Urahama, N., Hamaguchi, M., and Fukui, C. (2004). Involvement of casein kinase I ϵ in cytokine-induced granulocytic differentiation. *Blood* **103** (8), 2997–3004.
- Okamura, A., Iwata, N., Tamekane, A., Yakushijin, K., Nishikawa, S., Hamaguchi, M., Fukui, C., Yamamoto, K., and Matsui, T. (2006). Casein kinase I ϵ down-regulates phospho-Akt via PTEN, following genotoxic stress-induced apoptosis in hematopoietic cells. *Life Sciences* **78**, 1624–1629.
- Peter McQuilton, Susan E. St. Pierre, Jim Thurmond, and the FlyBase Consortium (2012). FlyBase 101 – the basics of navigating FlyBase. *Nucleic Acids Res.* 40(Database issue):D706-14. [PMID: 22127867] [NAR40D1D706]
- Qiu, P., Pan, P.C., and Govind, S. (1998). A role for the *Drosophila* Toll/Cactus pathway in larval hematopoiesis. *Development* **125**, 1909–1920.
- Rizki, R.M., and Rizki, T.M. (1984). Selective destruction of a host blood cell type by a parasitoid wasp. *Proceedings of the National Academy of Sciences* **81**, 6154–6158.
- Roth, S., Hiromi, Y., Godt, D., and Nusslein-Volhard, C. (1991). *cactus*, a maternal gene required for proper formation of the dorsoventral morphogen gradient in *Drosophila* embryos. *Development* **112**, 371–388.
- Sorrentino, R.P., Carton, Y., and Govind, S. (2002). Cellular Immune Response to Parasite Infection in the *Drosophila* Lymph Gland Is Developmentally Regulated. *Developmental Biology* **243**, 65–80.
- Tepass, U., Fessler, L.I., Aziz, A., and Hartenstein, V. (1994). Embryonic origin of hemocytes and their relationship to cell death in *Drosophila*. *Development* **120**, 1829–1837.
- Utz, A.C., Hirner, H., Blatz, A., Hillenbrand, A., Schmidt, B., Deppert, W., Hennebruns, D., Fischer, D., Thal, D.R., and Leithäuser, F. (2010). Analysis of cell type-specific

expression of CK1 ϵ in various tissues of young adult BALB/c mice and in mammary tumors of SV40 T-Ag-transgenic mice. *Journal of Histochemistry & Cytochemistry* **58** (1), 1–15.

▪ Valanne, S., Wang, J.H., and Rämét, M. (2011). The *Drosophila* toll signaling pathway. *The Journal of Immunology* **186**, 649–656.

• Zettervall, C.J., Anderl, I., Williams, M.J., Palmer, R., Kurucz, E., Ando, I., and Hultmark, D. (2004). A directed screen for genes involved in *Drosophila* blood cell activation. *Proceedings of the National Academy of Sciences of the United States of America* **101** (39), 14192–14197.

▪ Zilian, O., Frei, E., Burke, R., Brentrup, D., Gutjahr, T., Bryant, P.J., and Noll, M. (1999). *double-time* is identical to *discs overgrown*, which is required for cell survival, proliferation and growth arrest in *Drosophila* imaginal discs. *Development* **126**, 5409–5420.